APPLICATION OF NOVEL TECHNIQUES FOR CHARACTERIZATION OF SUB-VISIBLE AND SUB-MICRON PARTICLES IN BIOPHARMACEUTICAL PREPARATIONS

Inauguraldissertation

zur

Erlangung der Würde eines Doktors der Philosophie

vorgelegt der

Philosophisch-Naturwissenschaftlichen Fakultät

der Universität Basel

von

Anacelia Ríos Quiroz

aus Mexiko

Basel, 2017

Genehmigt von der Philosophisch-Naturwissenschaftlichen Fakultät

auf Antrag von

Prof. Dr. Jörg Huwyler, Dr. Atanas Koulov and Prof. Dr. Wolfgang Friess

Basel, 10th November 2015

<div align="right">

Prof. Dr. Jörg Schibler
The Dean of Faculty

</div>

Dedicated to all the kind mothers in my life,

Especially Laura, Lau, Erika, Mar and Khandro

CONTENT

APPLICATION OF NOVEL TECHNIQUES FOR CHARACTERIZATION OF SUB-VISIBLE AND SUB-MICRON PARTICLES IN BIOPHARMACEUTICAL PREPARATIONS

LIST OF ABBREVIATIONS

CC	Coulter Counter
CV	Coefficient of variance
ECD	Equivalent circular diameter
FC	Flow Cam
FI	Flow imaging
MFI	Micro Flow Imaging
LO	Light Obscuration
NTA	Nanoparticle Tracking Analysis
PFS	Pre-Filled Syringe
r.h.	Relative humidity
RMM	Resonant Mass Measurement
RMM (+)	Positively buoyant particles detected by RMM
RMM (-)	Negatively buoyant particles detected by RMM
SLO	Standard Light obscuration method
TEM	Transmission electron microscopy
TLO	Time resolved light obscuration method

SUMMARY

A large number of protein-based medicines have successfully improved the treatment and quality life of patients in diverse therapeutic areas (1). Due to the typically chronic and frequent administration regimens, in many cases the subcutaneous route of administration is preferred. This modality facilitates self-administration and prevents the necessity of professional health assistance. However, as the maximum volume that the area between skin and muscle can support is < 2 mL, highly concentrated formulations have to be developed in order to reach the required large doses of several mg/mL/Kg-bodyweight (2). From a pharmaceutical technology perspective, the main associated implications are high viscosity (3, 4) and increased protein aggregation tendency (5, 6) that typically characterize protein formulations.

Both aspects represent new challenges to the pharmaceutical development field (7, 8). For example, despite the proven safety and efficacy of biotechnological products, some publications have suggested that the particulate matter present in liquid formulations has immunogenic properties (9-11). Thus, there is an increasing interest to research and characterize protein particles beyond the limits of current USP applications of Chapter <787> (12) had appeared in the recent years. A number of analytical techniques have emerged for the characterization of particles size between the upper size limit of chromatography techniques and the lower size limit of the compendial light obscuration method (6, 13-16). Although this represents an instrumentation achievement, the analytical performance of such tools is unknown.

This present Doctoral research aims to evaluate the applicability of the new techniques in the analysis of biotechnological products including deeper understanding of their principles as well as the comparative evaluation with the compendial light obscuration method.

As a starting point, stability study was performed using a representative Biotech product (**Chapter 1**). Particle numbers were followed using a broad analytical toolbox that covered particle sizes from nano to micrometers. This research revealed a series of inconsistencies not only between the different instruments but also between the different time points. Whereas some instruments showed no significant changes over the 13 week duration of the study, other methods reported a decrease in the number of particles even when a stress condition was applied. These results clearly exemplified the

complexity of particle characterization. Whether these trends were meaningful or not, or if they were just artefacts resulting from sample unsuitability, becomes a main concern for results interpretation. Hence, a detailed study on the analytical performance of the instruments was undertaken. Although certain information was available from vendor suppliers, no information was found about precision and accuracy assessment in the frame of Biotherapeutics. It was also clear that different factors might be involved as the results from the stability study did not reproduce vendor information.

The first part related to precision is studied in **Chapter 1,** where repeatability and intermediate precision experiments are presented. The use of both, protein particle suspension and polystyrene beads – the later typically used as calibration standard material, - revealed interesting differences inherent to the nature of the sample. Whereas measurements of standard solutions representing a size-monodisperse system showed good precision, the performance of the instrument when measuring protein polydisperse samples showed deficiencies for particle sizes that were underrepresented in the sample. More importantly, the amount of sample measured was determined to be a critical factor for the precision performance of the methods. The smaller the sample volume to analyse, the less precise the measurement was. This important extrapolation factor effect appeared to influence mainly the submicrometer methods, thus limiting their applicability.

The second part of the instrument performance evaluation was investigated in **Chapter 2**. It included accuracy and linearity studies. In this part of the work, not only the standards and protein particles were included, but also different morphologies of such protein particles. This approach succeed in showing that besides sample composition, sample morphology can influence method accuracy. Interestingly, as well as in the precision study, the relative size composition of the samples was found to impact the counting accuracy. Three categories were identified: i) good accuracy irrespectively of particle size, ii) better accuracy for those particles sizes that were mainly represented and iii) poor accuracy. In terms of accuracy sizing, a general overestimation in the lower size limit of the instruments was found. In contrast, an underestimation occurred towards the upper size limit. Similarly to precision, the linearity assessment of submicrometer methods had greater difficulty in providing accurate measurements as compared to the micrometer ones. **Chapter 2** also provides a detailed analysis on the instrument-to-instrument correlation in those cases on which a size overlap

exist. The particle morphology and concentration variables were found to be the most important factors for obtaining consistent particle numbers among different methods at a given size. An extra value of this experimental approach is that it proved to be effective in defining practical limits for particle quantification in a product and instrument specific mode.

Together, **Chapter 1** and **Chapter 2** provide a highly integrative understanding of the strengths and weaknesses of the available techniques for protein particle characterization in Biotechnological products. The results presented in these chapters suggest that the newer methodologies still require more development in order to be considered reliable analytical techniques. This knowledge was then applied to generate tools that could improve the actual status of the analytical instruments. Instrumental, operational and data analysis approaches are described in Chapters 3 to 4.

Light obscuration method is the focus of **Chapter 3**. This particle counting method has been part of the US Pharmacopeia since 1985 (USP XXI) and together with the membrane method is the only one stipulated and harmonized in all parenteral-related legislation. However, with the emergence of Biotechnological products, some shortcomings of the technique had been exposed. For example, protein particles are in general highly translucency and irregular in shape. For the light blockage principle, this represents potential misleading sizing assessments, especially for particles in the lower size range of the technique (1-2 µm). In order to overcome this scenario, an innovative instrumental modification was evaluated in **Chapter 3.** Whereas the standard principle is based on the measurement of the height of the voltage signal; this instrumental approach examines on the benefits of measuring the width of the peak instead. The new method was named Time Resolved Light Obscuration and it demonstrated improvements in the accuracy of the technique when measuring highly translucent protein particles around 1-2 µm.

In **Chapter 4** an empirical approach was applied to the study of the performance of the Nano Tracking Analysis technique. From Chapters 1 and 2, this technique appeared to be the least robust and the most affected by user-defined settings. Hence a detailed study on the variables that can impact the measurements was conducted. Both, sample- and instrument-related aspects were considered. For some samples the measurement was not possible due to the high presence of scattering oligomeric species. The effect of dilution, a common practice to reduce that noise signal, together with the study

of various combinations of camera levels showed the broadness of the possible results. Such high variability was worse in the case of the concentration assessments. This suggested that the Nano Tracking Technology is more suited for size distribution assessments.

Altogether through the findings outlined in the present Doctoral thesis a better understanding of the particle characterization techniques can be obtained. An additional value of the research is that it considers realistic (sample types and concentration burdens) and highly integrative (complete and broad set of analytical tools included) scenarios in the frame of Pharmaceutical Industry. This allowed for the detection of inherent instrument-to-sample incompatibilities that constrain the applicability of the techniques to rather narrow size and concentration ranges. In some cases such ranges were not relevant considering the likely particle burden of Biotherapeutic products. Sampling efficiency was found to be the most important factor affecting instrument performance. In terms of precision, this was reflected mainly in the case of submicron methods due to the tiny samples volumes that are measured. In terms of accuracy, the same effect was encountered for the least represented sizes within the sample. Furthermore, the collected research findings pointed to the necessity of sample-specific method development and, in most cases, the severe immaturity of the techniques as demonstrated by the high variability of the results. Whereas research tasks can profoundly benefit from these new methodologies due to their high flexibility and new capabilities, apart from the compendial Light Obscuration technique any other should remain as supportive tool. Nevertheless, their performance can be improved by applying the concepts here described.

References (Summary)

1.   G. Walsh. Biopharmaceutical benchmarks 2014. Nature Biotechnology. 32:992-1000 (2014).

2.   N.W. Warne. Development of high concentration protein biopharmaceuticals: The use of platform approaches in formulation development. European Journal of Pharmaceutics and Biopharmaceutics. 78:208-212 (2011).

3.   M.S. Neergaard, D.S. Kalonia, H. Parshad, A.D. Nielsen, E.H. Møller, and M. van de Weert. Viscosity of high concentration protein formulations of monoclonal antibodies of the IgG1 and IgG4

subclass – Prediction of viscosity through protein–protein interaction measurements. European Journal of Pharmaceutical Sciences. 49:400-410 (2013).

4.   A. Allmendinger, S. Fischer, J. Huwyler, H.-C. Mahler, E. Schwarb, I.E. Zarraga, and R. Mueller. Rheological characterization and injection forces of concentrated protein formulations: An alternative predictive model for non-Newtonian solutions. European Journal of Pharmaceutics and Biopharmaceutics. 87:318-328 (2014).

5.   W. Wang. Protein aggregation and its inhibition in biopharmaceutics. International Journal of Pharmaceutics. 289:1-30 (2005).

6.   H.C. Mahler, Friess, W., Grauschopf, U., Kiese, S. Protein aggregation: pathways, induction factors and analysis. Journal of Pharmaceutical Sciences. 98:2909-2934 (2009).

7.   S.J. Shire, Shahrokh, Z., Liu, J. Challenges in the development of high protein concentration formulations. Journal of Pharmaceutical Sciences. 93:1390-1402 (2004).

8.   M. Adler. Challenges in the development of pre-filled syringes for biologics from a formulation's scientist point of view. American Pharmaceutical Review 15: (2012).

9.   A.S. Rosenberg. Immunogenicity of biological therapeutics: a hierarchy of concerns. Developments in biologicals. 112:15-21 (2003).

10.   J.F. Carpenter, Randolph, Theodore W., Jiskoot, Wim, Crommelin, Daan J. A., Middaugh, C. Russell, Winter, Gerhard, Fan, Ying-Xin, Kirshner, Susan, Verthelyi, Daniela, Kozlowski, Steven, Clouse, Kathleen A., Swann, Patrick G., Rosenberg, Amy, Cherney, Barry. Overlooking Subvisible Particles in Therapeutic Protein Products: Gaps That May Compromise Product Quality. Journal of Pharmaceutical Sciences. 98:1201-1205 (2009).

11.   S.K. Singh, N. Afonina, M. Awwad, K. Bechtold-Peters, J.T. Blue, D. Chou, M. Cromwell, H.-J. Krause, H.-C. Mahler, B.K. Meyer, L. Narhi, D.P. Nesta, and T. Spitznagel. An industry perspective on the monitoring of subvisible particles as a quality attribute for protein therapeutics. Journal of Pharmaceutical Sciences. 99:3302-3321 (2010).

12.   USP. General Chapters: <787> Subvisible particulate matter in therapeutic protein injections, Pharmacopeial Forum: Volume No. 28, pp. USP32-NF27.

13.   L.O. Narhi, Jiang, Yijia, Cao, Shawn, Benedek, Kalman, Shnek, Deborah. A Critical Review of Analytical Methods for Subvisible and Visible Particles. Current Pharmaceutical Biotechnology. 10:373-381 (2009).

14.   B. Demeule, Messick, S., Shire, S. J., Liu, J. Characterization of Particles in Protein Solutions: Reaching the Limits of Current Technologies. AAPS Journal. 12:708-715 (2010).

15.   S. Zölls, Tantipolphan, R., Wiggenhorn, M., Winter, G., Jiskoot, W., Friess, W., Hawe, A. Particles in therapeutic protein formulations, Part 1: Overview of analytical methods. Journal of Pharmaceutical Sciences. 101:914-935 (2012).

16.   V. Filipe, Hawe, A., Carpenter, J. F., Jiskoot, W. Analytical approaches to assess the degradation of therapeutic proteins. Trendsin Analytical Chemistry. 49:118-125 (2013).

I INTRODUCTION

"Biotherapeutic" is a term that encompasses therapeutic proteins (medicinal products, therapeutics, prophylactics and in vivo diagnostics) with active agents inherently biological in nature and manufactured using biotechnology (1). The emergence of this type of medicinal products dates to 1970's when the increasing demand of insulin for the treatment of diabetes urged scientists to look for other sources of production rather than animal models (2). As a result, DNA recombinant technologies emerged, allowing the successful expression of human insulin in bacteria models in laboratory conditions followed by commercial scale and industry production (3, 4). Nowadays not only the treatment of diabetes and other endocrine diseases benefit from this technology but also inflammatory, immune, cardiovascular, infectious and respiratory diseases as well as oncology (5-7) (see Table I.a).

The polymeric nature and highly ordered structure that are characteristic properties of proteins make their formulation much more challenging than that of (small) chemically synthetized molecules. Several strategies can be applied to improve protein chemical stability *e.g.* use of additives like salts,

Table I.a Examples of Biopharmaceuticals approved during 2013-2014 in Europe and United States of America. *Extracted from reference (1)*

Category	Product	Company	Therapeutic indication
Recombinant blood factors	Nuwiq	Octapharma AB	Hemophilia A
	Alprolix	Biogen Idec	Hemophilia B
	Jetrea	ThromboGenics	Symptomatic vitreomacular adhesion
Recombinant hormones	Afrezza	MannKind	Diabetes mellitus
	Tresiba	Novo Nordisk	Diabetes
	Somatropin	BioPartners	Growth hormone deficiency
	Ovaleap	Teva Pharma	Infertility/subfertility
	Elonva	Merck Sharp Dohme	Controlled ovarian stimulation
	Myalept	AstraZeneca	Some forms of lipodystrophy
	Grastofil	Apotex	Neutropenia
	Lonquex	Teva Pharmaceuticals	Neutropenia
	Plegridy	Biogen Idec	Multiple sclerosis
Recombinant vaccines	Bexsero	Novartis	Against invasive meningococcal disease
	Flublok	Protein Sciences	Against influenza
	Provenge	Dendreon	Prostate cancer
Monoclonal antibody based products	Sylvant	Janssen Biotech	Multicentric Castleman's disease
	Cyramza	Eli Lilly	Gastric cancer
	Gazyva	Roche (Genentech)/ Roche	Chronic lymphocytic leukemia
	Kadcyla	Roche (Genentech)/ Roche	Breast cancer
	Perjeta	Roche (Genentech)/ Roche	Breast cancer
	Simponi Aria	Janssen Biotech	Rheumatoid arthritis
Recombinant enzymes	Vimizim	BioMarin	Morquio A síndrome
	Krystexxa	Savient	Gout
Gene therapy	Kynamro	Sanofi/Isis	Familial hypercholesterolemia

polyalcohol compounds or detergents; the replacement of specific residues of the primary protein sequence to remove reactive sites or chemical modifications to prevent their reactivity (8-11). On the other hand, the physical stability can be enhanced by stabilizing the native conformation of the protein *e.g.* using certain sugars (12-14) or by reducing the molecular collisions and limiting protein mobility through the lyophilisation process (15, 16). However, both, chemical (17) and physical (18) denaturation pathways (see Table I.b) can take place at different stages of the production procedure starting from cell culture up to final container filling or even upon storage conditions (19). Additionally, the poor bioavailability due to the many degradation pathways that proteins can undertake (20, 21) triggers the necessity of intravenous or subcutaneous administration routes as well

Table I.b Examples of instabilities that can take place in biotherapeutics. *Extracted from reference (2)*

	Definition	Causes	Type	Description	Examples of consequences
Chemical instability	Modification or alteration of the aminoacid residues	Protein intrinsic reactivity	Deamidation	Hydrolysis of the side chain amide linkage of Gnl or Asn to form a free carboxylic acid	Loss of biological activity (3) possible participation in immunogenicity (4)
			Oxidation	Side chains of aromatic aminoacids to radiolysis in the presence of oxygen.	Generation of micron-sized aggregates, secondary structure changes and immune resistivity breakage (5, 6)
			Proteolisys	Intramolecular catalysis by a carboxyl group of the Asp residue	Loss of enzymatic activity (7)
			Disulfide scrambling	Formation of sulfhydril groups and disulfide bons using Cys residues	Covalent aggregation via cross linking (8)
			Racemization / Beta elimination	Deprotonation of the hydrogen of the alfa carbon	Aggregation susceptibility upon freezing (9)
Physical instability	Modification or alteration of the native spatial arrangement of the protein	Environmental factors like *e.g.*temperature; pH; ionic strength; air exposure; surface interactions	Adsorption	Adhesion to biomaterials of primary containers	Fogging phenomena after lyophilization (10)
			Aggregation	Accumulation of proteins in a non-native state forming agglomerates	Possible participation in immunogenicity (11)

as high concentrated formulations (*e.g.* Cimzia, Pharma/UCB is formulated at 200 mg/mL). This represents another possible cause of instability as protein-protein interactions are enhanced, likely triggering the formation of protein aggregates and particles (22).

On the other hand, in cases where sub cutaneous administration is preferred, a pre-filled syringe primary container is typically used (23, 24). The silicon oil layer in the internal face of the glass barrel can migrate into solution adding a second particulate population (25-27). Furthermore, it has been proposed those oil droplets likely serve as nucleation template and initiate protein aggregation processes (28-31). For the device development area, this is an active topic of research and some efforts have been made to produce silicon-oil free prefillable syringe systems demonstrating lower particle counts in solutions (32).

Table I.c Classification of protein aggregates *Summarized/modified from reference (12)*

Category	Classification	Description
Size	Monomer	Smallest existent and/or functional unit
	Aggregate	> 100 μm 1-100 μm 100 - 1000 nm < 100 nm
	Oligomer	Any aggregate that contains more than one monomeric unit in a non-native state
Reversibility	Reversible	Aggregates that exist in equilibrium with the native monomeric subunit. Might be accompanied with the time scale of the observation
	Dissociable	Recovery of the monomeric specie is possible applying certain conditions
	Irreversible	Aggregation state is not dissociable
Conformation	Native	Conformation of non-aggregated active protein in which the protein originates
	Partially unfolded	Changes can be detected but native structure still remains
	Misfolded	Different three dimensional conformation as the native protein
	Unfolded	Protein condition after strong denaturation procedure *e.g.* guanidine 6M
	Inherently disordered	No defined three dimensional is associated with the functionality of the protein
	Amyloid	Cross- β diffraction pattern is exhibit
Chemical modification	Cross linked	Formation of covalent non-reducible new bonds intra o intermolecularly
	Site directed	Modification of specific residues on the primary sequence
Morphology	Physical	Aspect ratio, diameter, perimeter, surface roughness etc.
	Optical	Refractive index and transparency/intensity

Protein particles can be classified as intrinsic or extrinsic. Intrinsic if their source can be explained as naturally formed through any mechanism related with the nature of the formulated protein itself and described in Table I.b. Extrinsic when it is non-related with the product or its production process. A more detailed classification of particles considers aspects like size; reversibility; conformation; chemical modification and morphology (see Table I.c). The previously described possible causes and sources of protein instability and particles explain why the presence of particulate matter in parenteral pharmaceutical formulations can be considered a common finding (33). This represents an important quality control attribute. Thus, not only the formulation strategies had to be adapted as already mentioned but the compendial and regulatory aspects around parenteral products as well.

The historical development of the topic can be appreciated by following the evolution of the USP editions (see Table I.d). Starting in 1936, edition 11th established the concept of *clearness* for parenteral formulations. Later, edition 14th in 1946 changed from clearness to a *substantially free* definition. More specificity was included in 1984 when instrumentation developments helped to establish quantitative limits for those particles that could not be detected by the naked eyes. In that edition light obscuration and membrane methods were defined as compendial for the evaluation of particulate matter of sizes > 10 µm (limit 6000 particles/mL) and > 25 µm (limit 600 particles/mL). At

Table I.d Historical development of particle-related regulations in parenteral formulations
Extracted from reference (13)

Period	Events
Cognitive	1905 Parenteral solutions are included as compendial drug
	1936 Parenterals must have clearness and be "substantially free" of precipitates; cloudiness or turbidity
Latent	1946 Frist medical events related to particles are reported
	1949 Individual visual inspection is established
	1965 Development of the first type of particulate standard in Austria
Definitive	1966 First symposium on safety of large volume parenterals
	1975 Membrane test is stablished for large volume injections
	1984 Membrane microscopic and light obscuration methods are defined for large and small volume parenterals, respectively
	1985 A method for small volume parenterals is added
Evaluative	1995 Light obscuration is the preferred method over membrane microscopy
	2004 Ophthalmic solutions are included in a special chapter
Harmonization	2007 USP, EP and JP agreement on method definitions and limits
	2014 Particulate matter in therapeutic protein injections is included in a special chapter.

present (mostly triggered by technical developments), the status of this topic is facing a new era. The USP chapter <788> for Particulate Matter in Injections establishes the quality control criteria that parenteral products should meet. Given the special characteristics of biotechnological products, this chapter had to be adjusted and special recommendations for sample preparation are established in Chapter <787>. Furthermore, discussions about the necessity of monitoring sub visible particles ≤ 10µm over the already well standardized control of particles >10 and >25 µm (USP <788>) are taking place (34, 33). Such motivation is based on the alleged immunogenic properties of small particulate matter. As consequence, in addition to the traditionally used and compendial light obscuration method, many other techniques have been emerged or been re-adapted. The aim is to fulfil the necessity of a more complete size-wise particle characterization of biotechnological products. It is then of the highest importance to build a sound base knowledge of such analytical tools.

This area of instrumentation development has become very active and in a relatively short period of time, new instruments and/or several new versions of them have appeared on the market. Instruments can be grouped in submicron and micron categories depending on the particle size range on which they can be used for characterization. For the assessment of particles between 100-1000 nm size (submicron range), Nanoparticle Tracking Analysis, (NTA) and Resonant Mass Measurement (RMM) instruments can be used. For the assessment of particles between 1-100 µm size (micron range), Coulter Counter (CC); Flow Microscopy (Micro Flow imaging (MFI) and Flow Cam (FC)) and the compendial Light Obscuration (HIAC) are available. In the following paragraphs, each methodology is described together with some pharmaceutical applications.

NTA is a technique which combines laser light scattering microscopy and a video imaging system for real time sizing of particles suspended in liquids. This technique is based on the video recording of the light scattered by particles under Brownian motion as they interact with a laser beam that illuminates a sample area of approximately $8x10^{-8}$ cm^3. Such movement is possible to track using the charged couple device principle connected to a microscope (20x amplification) and a high speed camera (30 frames per second) combination. This allows for individual and simultaneous visualization of particles that can be analysed using the instrument software. Some user defined parameters are needed as follows: i) threshold value for a particle to be differentiated from the background signal ii) pixel area

to be sum around a particle centre iii) probabilistic distance that a particle can travel from one frame to another and iv) number of continuous frames on which a given particle can be encountered. The two dimensional distance that each particle moves allows for the calculation of the diffusion coefficient of the particles. Finally the hydrodynamic diameter is calculated by the Stokes-Einstein equation. NTA has general size capabilities from 30 to 1000 nm, but refractive index properties can tighten this range. In terms of concentration, 10^7 to 10^9 particles per mL is recommended by the vendor. In comparison with similar methodologies, also based on light scattering NTA offers some advantages. For example, NTA has less interference of larger particles than can possible obscure the intensity fluctuations of smaller particles. Hence, the image analysis offers better determinations when z-axis collocation occurs as compared with the analysis of time-dependent fluctuations. However, other factors related with inter-particle distance and to two dimensional dynamics become important in avoiding erroneous particle sizing (35).

In the RMM instrument, particles move in their native suspensions through a Micro Electro Mechanical Systems fabricated microfluidic channel that resonates mechanically. The presence of a particle adds to the total mass and shifts the sensor resonant frequency. The shifts are measured as each individual particle passes through the sensor. The RMM device offers an excellent tool for differentiation between protein and silicon population. This instrument is based on the differential vibration frequency that a resonator will present due the different densities of silicon oil and protein particles with respect to the liquid in which they are immersed.

The CC instrument relies on the Electrical Sensing Zone principle. The device is equipped with a glass tube with a known diameter aperture which is then immersed in the conductive sample. A current is applied using electrodes placed inside and outside of the tube. A particle passing through the aperture causes a short-term increase in resistance. The magnitude of the resistance change depends on the volume of the particle. The particle size (calculated by volume) and particle counts are obtained based on the change in the electrical resistance.

In the FI techniques bright-field images are captured in successive frames as a continuous sample stream passes through a flow cell positioned in the field of view of a microscopic system. The digital images of the particles present in the sample are processed by image morphology analysis software

that allows their quantification in size and count. Micro flow imaging allows not only enumerating the subvisible particles present in the sample, but also a visual examination of the images of all the captured particles as well as identification of contaminants like silicone oil droplets, for example. Finally, LO bases the determination of particle size and counts on the blockage of a constant source of light and the measurement of the consequent drop in voltage. Such response is caused by particles suspended in liquids as they go through a channel of defined diameter at a constant flow rate. Data analysis implies the comparison of the registered drop with a preloaded calibration curve built with particles of certified size. Interpolation allows the translation of voltage changes into particle size. The number of signals recorded is related to the user-defined analysed volume to determine the cumulative particle concentration per millilitre.

The previously described analytical tool box is a complex one with a rather new set of technologies that can support the characterization of subvisible and submicron particles. Partial and limited attempts have been made to characterize and understand the number of factors governing the analytical performance of all those techniques (36-58). Some interesting findings and exciting applications as well as some limitations and shortcomings have been already reported (59-61). However, some aspects require further research, especially in terms of basic analytical evaluation and guidelines for method development. Thus, the study and thorough understanding of how they work and the factors that affect their functionality constitutes the main objective of this dissertation.

References (Introduction)

1.   R.A. Rader. (Re)defining biopharmaceutical. Nature Biotechnology. 26:743-751 (2008).

2.   I. Johnson. Human insulin from recombinant DNA technology. Science. 219:632-637 (1983).

3.   G. Kohlerand C. Milstein. Continuous cultures of fused cells secreting antibody of predefined specificity. Nature. 256:495-497 (1975).

4.   R.E. Chanceand B.H. Frank. Research, development, production, and safety of biosynthetic human insulin. Diabetes Care. 16:133-142 (1993).

5.   O.H. Brekkeand I. Sandlie. Therapeutic antibodies for human diseases at the dawn of the twenty-first century. Nature Reviews Drug Discovery. 2:52-62 (2003).

6.   A.K. Pavlou, Belsey, M. J. The therapeutic antibodies market to 2008. European Journal of Pharmaceutics and Biopharmaceutics. 59:389-396 (2005).

7.   G. Walsh. Biopharmaceutical benchmarks 2014. Nature Biotechnology. 32:992-1000 (2014).

8.   M. Manning, K. Patel, and R. Borchardt. Stability of Protein Pharmaceuticals. Pharmaceutical Research. 6:903-918 (1989).

9.   R.J. Harris, S.J. Shire, and C. Winter. Commercial manufacturing scale formulation and analytical characterization of therapeutic recombinant antibodies. Drug development research. 61:137-154 (2004).

10.   M.C. Manning, D.K. Chou, B.M. Murphy, R.W. Payne, and D.S. Katayama. Stability of protein pharmaceuticals: an update. Pharmaceutical Research. 27:544-575 (2010).

11.   N.W. Warne. Development of high concentration protein biopharmaceuticals: The use of platform approaches in formulation development. European Journal of Pharmaceutics and Biopharmaceutics. 78:208-212 (2011).

12.   T. Arakawaand S.N. Timasheff. Stabilization of protein structure by sugars. Biochemistry. 21:6536-6544 (1982).

13.   J.F. Carpenter, B.S. Kendrick, B.S. Chang, M.C. Manning, and T.W. Randolph. [16] Inhibition of stress-induced aggregation of protein therapeutics. Methods in Enzymology. Volume 309, Academic Press, 1999, pp. 236-255.

14.   L. Nicoud, N. Cohrs, P. Arosio, E. Norrant, and M. Morbidelli. Effect of polyol sugars on the stabilization of monoclonal antibodies. Biophysical Chemistry. 197:40-46 (2015).

15.   M.T. Cicerone, M.J. Pikal, and K.K. Qian. Stabilization of proteins in solid form. Advanced Drug Delivery Reviews. Volume 93, 1 October 2015, Pages 14–24.

16.   X. Tangand M. Pikal. Design of Freeze-Drying Processes for Pharmaceuticals: Practical Advice. Pharmaceutical Research. 21:191-200 (2004).

17.   J.L.E. Reubsaet, J.H. Beijnen, A. Bult, R.J. van Maanen, J.A.D. Marchal, and W.J.M. Underberg. Analytical techniques used to study the degradation of proteins and peptides: chemical instability. Journal of Pharmaceutical and Biomedical Analysis. 17:955-978 (1998).

18.   E. Chi, S. Krishnan, T. Randolph, and J. Carpenter. Physical Stability of Proteins in Aqueous Solution: Mechanism and Driving Forces in Nonnative Protein Aggregation. Pharmaceutical Research. 20:1325-1336 (2003).

19.   M.E. Cromwell, E. Hilario, and F. Jacobson. Protein aggregation and bioprocessing. The AAPS Journal. 8:E572-E579 (2006).

20.   S.J. Shire, Shahrokh, Z., Liu, J. Challenges in the development of high protein concentration formulations. Journal of Pharmaceutical Sciences. 93:1390-1402 (2004).

21.   W. Wang, E.Q. Wang, and J.P. Balthasar. Monoclonal Antibody Pharmacokinetics and Pharmacodynamics. Clinical Pharmacology & Therapeutics. 84:548-558 (2008).

22.   H.C. Mahler, Friess, W., Grauschopf, U., Kiese, S. Protein aggregation: pathways, induction factors and analysis. Journal of Pharmaceutical Sciences. 98:2909-2934 (2009).

23.   A. Badkar, Wolf, Amanda, Bohack, Leigh, Kolhe, Parag. Development of Biotechnology Products in Pre-filled Syringes: Technical Considerations and Approaches. AAPS PharmSciTech. 12:564-572 (2011).

24.   M. Adler. Challenges in the development of pre-filled syringes for biologics from a formulation's scientist point of view. American Pharmaceutical Review. 15: (2012).

25.   E. Chantelau, Berger, M., Bohlken, B. Silicone oil released from disposable insulin syringes. Diabetes Care. 9:672-673 (1986).

26.   K.B. Auge, Blake-Haskins, A. W., Devine, S., Rizvi, S., Li, Y. M., Hesselberg, M., Orvisky, E., Affleck, R. P., Spitznagel, T. M., Perkins, M. D. Demonstrating the stability of albinterferon alfa-2b in the presence of silicone oil. Journal of Pharmaceutical Sciences. 100:5100-5114 (2011).

27.   F. Felsovalyi, Janvier, S., Jouffray, S., Soukiassian, H., Mangiagalli, P. Silicone-oil-based subvisible particles: Their detection, interactions, and regulation in prefilled container closure systems for biopharmaceuticals. Journal of Pharmaceutical Sciences. 101:4569-4583 (2012).

28.   L.S. Jones, Kaufmann, A., Middaugh, C. R. Silicone oil induced aggregation of proteins. Journal of Pharmaceutical Sciences. 94:918-927 (2005).

29.   L. Liu, Ammar, D. A., Ross, L. A., Mandava, N., Kahook, M. Y., Carpenter, J. F. Silicone Oil Microdroplets and Protein Aggregates in Repackaged Bevacizumab and Ranibizumab: Effects of

Long-term Storage and Product Mishandling. Investigative Ophthalmology & Visual Science. 52:1023-1034 (2011).

30.   K.A. Britt, Schwartz, D. K., Wurth, C., Mahler, H. C., Carpenter, J. F., Randolph, T. W. Excipient effects on humanized monoclonal antibody interactions with silicone oil emulsions. Journal of Pharmaceutical Sciences. 101:4419-4432 (2012).

31.   P. Basu, Krishnan, S., Thirumangalathu, R., Randolph, T. W., Carpenter, J. F. IgG1 aggregation and particle formation induced by silicone-water interfaces on siliconized borosilicate glass beads: A model for siliconized primary containers. Journal of Pharmaceutical Sciences. 102:852-865 (2013).

32.   K. Yoshino, K. Nakamura, A. Yamashita, Y. Abe, K. Iwasaki, Y. Kanazawa, K. Funatsu, T. Yoshimoto, and S. Suzuki. Functional Evaluation and Characterization of a Newly Developed Silicone Oil-Free Prefillable Syringe System. Journal of Pharmaceutical Sciences. 103:1520-1528 (2014).

33.   S.K. Singh, N. Afonina, M. Awwad, K. Bechtold-Peters, J.T. Blue, D. Chou, M. Cromwell, H.-J. Krause, H.-C. Mahler, B.K. Meyer, L. Narhi, D.P. Nesta, and T. Spitznagel. An industry perspective on the monitoring of subvisible particles as a quality attribute for protein therapeutics. Journal of Pharmaceutical Sciences. 99:3302-3321 (2010).

34.   J.F. Carpenter, Randolph, Theodore W., Jiskoot, Wim, Crommelin, Daan J. A., Middaugh, C. Russell, Winter, Gerhard, Fan, Ying-Xin, Kirshner, Susan, Verthelyi, Daniela, Kozlowski, Steven, Clouse, Kathleen A., Swann, Patrick G., Rosenberg, Amy, Cherney, Barry. Overlooking Subvisible Particles in Therapeutic Protein Products: Gaps That May Compromise Product Quality. Journal of Pharmaceutical Sciences. 98:1201-1205 (2009).

35.   P. Van der Meeren, Kasinos, Marios, Saveyn, Hans. Relevance of two-dimensional Brownian motion dynamics in applying nanoparticle tracking analysis. Methods in Molecular Biology (Clifton, NJ). 906:525-534 (2012).

36.   J.S. Philo. Is any measurement method optimal for all aggregate sizes and types? AAPS Journal. 8:E564-E571 (2006).

37.   B. Demeule, Lawrence, M. J., Drake, A. F., Gurny, R., Arvinte, T. Characterization of protein aggregation: The case of a therapeutic immunoglobulin. Biochimica Et Biophysica Acta-Proteins and Proteomics. 1774:146-153 (2007).

38.   B. Demeule, C. Palais, G. Machaidze, R. Gurny, and T. Arvinte. New methods allowing the detection of protein aggregates: A case study on trastuzumab. MAbs Journal. 1:142-150 (2009).

39.   L.O. Narhi, Jiang, Yijia, Cao, Shawn, Benedek, Kalman, Shnek, Deborah. A Critical Review of Analytical Methods for Subvisible and Visible Particles. Current Pharmaceutical Biotechnology. 10:373-381 (2009).

40.   V. Filipe, Hawe, Andrea, Jiskoot, Wim. Critical Evaluation of Nanoparticle Tracking Analysis (NTA) by NanoSight for the Measurement of Nanoparticles and Protein Aggregates. Pharmaceutical Research. 27:796-810 (2010).

41.   K. Wuchner, Buchler, J., Spycher, R., Dalmonte, P., Volkin, D. B. Development of a microflow digital imaging assay to characterize protein particulates during storage of a high concentration IgG1 monoclonal antibody formulation. Journal of Pharmaceutical Sciences. 99:3343-3361 (2010).

42.   M.N. Rhyner. The Coulter Principle for Analysis of Subvisible Particles in Protein Formulations. AAPS Journal. 13:54-58 (2011).

43.   J.G. Barnard, Rhyner, M. N., Carpenter, J. F. Critical evaluation and guidance for using the Coulter method for counting subvisible particles in protein solutions. Journal of Pharmaceutical Sciences. 101:140-153 (2012).

44.   V. Filipe, Poole, R., Oladunjoye, O., Braeckmans, K., Jiskoot, W. Detection and Characterization of Subvisible Aggregates of Monoclonal IgG in Serum. Pharmaceutical Research. 29:2202-2212 (2012).

45.   D.C. Ripple, Dimitrova, M. N. Protein particles: What we know and what we do not know. Journal of Pharmaceutical Sciences. 101:3568-3579 (2012).

46.   M. Wright. Nanoparticle tracking analysis for the multiparameter characterization and counting of nanoparticle suspensions. Methods in Molecular Biology (Clifton, NJ). 906:511-524 (2012).

47.   H. Zhao, M. Diez, A. Koulov, M. Bozova, M. Bluemel, and K. Forrer. Characterization of aggregates and particles using emerging techniques. In H.-C. Mahlerand W. Jiskoot (eds.), Analysis of aggregates and particles in protein pharmaceuticals, Wiley & Sons, Inc., 2012, pp. 133-167.

48.   S. Zölls, Tantipolphan, R., Wiggenhorn, M., Winter, G., Jiskoot, W., Friess, W., Hawe, A. Particles in therapeutic protein formulations, Part 1: Overview of analytical methods. Journal of Pharmaceutical Sciences. 101:914-935 (2012).

49.   Z. Hamrang, N.J.W. Rattray, and A. Pluen. Proteins behaving badly: emerging technologies in profiling biopharmaceutical aggregation. Trends in Biotechnology. 31:448-458 (2013).

50.   A. Hawe, Schaubhut, F., Geidobler, R., Wiggenhorn, M., Friess, W., Rast, M., de Muynck, C., Winter, G. Pharmaceutical feasibility of sub-visible particle analysis in parenterals with reduced volume light obscuration methods. European Journal of Pharmaceutics and Biopharmaceutics. 85:1084-1087 (2013).

51.   G.A. Wilsonand M.C. Manning. Flow imaging: Moving toward best practices for subvisible particle quantitation in protein products. Journal of Pharmaceutical Sciences. 102:1133-1134 (2013).

52.   S. Zölls, Weinbuch, D., Wiggenhorn, M., Winter, G., Friess, W., Jiskoot, W., Hawe, A. Flow Imaging Microscopy for Protein Particle Analysis-A Comparative Evaluation of Four Different Analytical Instruments. AAPS Journal. 15:1200-1211 (2013).

53.   S. Zölls, Gregoritza, M., Tantipolphan, R., Wiggenhorn, M., Winter, G., Friess, W., Hawe, A. How subvisible particles become invisible-relevance of the refractive index for protein particle analysis. Journal of Pharmaceutical Sciences. 102:1434-1446 (2013).

54.   J. Panchal, J. Kotarek, E. Marszal, and E.M. Topp. Analyzing Subvisible Particles in Protein Drug Products: a Comparison of Dynamic Light Scattering (DLS) and Resonant Mass Measurement (RMM). AAPS Journal. 16:440-451 (2014).

55.   D. Weinbuch, W. Jiskoot, and A. Hawe. Light obscuration measurements of highly viscous solutions: sample pressurization overcomes underestimation of subvisible particle counts. The AAPS Journal. 16:1128-1131 (2014).

56.   T. Werk, Volkin, D. B., Mahler, H. C. Effect of solution properties on the counting and sizing of subvisible particle standards as measured by light obscuration and digital imaging methods. European Journal of Pharmaceutical Sciences. 53:95-108 (2014).

57.   R. Vasudev, S. Mathew, and N. Afonina. Characterization of Submicron (0.1-1 mum) Particles in Therapeutic Proteins by Nanoparticle Tracking Analysis. Journal of Pharmaceutical Sciences. 104:1622-1631 (2015).

58.   C. Zhou, A.B. Krueger, J.G. Barnard, W. Qi, and J.F. Carpenter. Characterization of Nanoparticle Tracking Analysis for Quantification and Sizing of Submicron Particles of Therapeutic Proteins. Journal of Pharmaceutical Sciences. (2015).

59.   B. Demeule, Messick, S., Shire, S. J., Liu, J. Characterization of Particles in Protein Solutions: Reaching the Limits of Current Technologies. AAPS Journal. 12:708-715 (2010).

60.   H. Mach, Arvinte, T. Addressing new analytical challenges in protein formulation development. European Journal of Pharmaceutics and Biopharmaceutics. 78:196-207 (2011).

61.   T.K. Das. Protein Particulate Detection Issues in Biotherapeutics Development-Current Status. AAPS PharmSciTech. 13:732-746 (2012).

62.   Y.D. Liu, J.Z. van Enk, and G.C. Flynn. Human antibody Fc deamidation in vivo. Biologicals. 37:313-322 (2009).

63.   H.A. Doyle, R.J. Gee, and M.J. Mamula. Altered immunogenicity of isoaspartate containing proteins. Autoimmunity. 40:131-137 (2007).

64.   V. Filipe, Jiskoot, W., Basmeleh, A. H., Halim, A., Schellekens, H., Brinks, V. Immunogenicity of different stressed IgG monoclonal antibody formulations in immune tolerant transgenic mice. mAbs Journal. 4:740-752 (2012).

65.   R. Torosantucci, C. Schöneich, and W. Jiskoot. Oxidation of Therapeutic Proteins and Peptides: Structural and Biological Consequences. Pharmaceutical Research. 31:541-553 (2014).

66.   T.J. Ahern, J.I. Casal, G.A. Petsko, and A.M. Klibanov. Control of oligomeric enzyme thermostability by protein engineering. Proceedings of the National Academy of Sciences of the United States of America. 84:675-679 (1987).

67.   B.S. Chang, B.S. Kendrick, and J.F. Carpenter. Surface-induced denaturation of proteins during freezing and its inhibition by surfactants. Journal of Pharmaceutical Sciences. 85:1325-1330 (1996).

68.   A.M. Abdul-Fattah, R. Oeschger, H. Roehl, I. Bauer Dauphin, M. Worgull, G. Kallmeyer, and H.-C. Mahler. Investigating factors leading to fogging of glass vials in lyophilized drug products. European Journal of Pharmaceutics and Biopharmaceutics. 85:314-326 (2013).

69.   J.G. Barnard, Babcock, K., Carpenter, J. F. Characterization and quantitation of aggregates and particles in interferon- products: Potential links between product quality attributes and immunogenicity. Journal of Pharmaceutical Sciences. 102:915-928 (2013).

70.   L.O. Narhi, Schmit, J., Bechtold-Peters, K., Sharma, D. Classification of protein aggregates. Journal of Pharmaceutical Sciences. 101:493-498 (2012).

71.   S. Aldrich. USP Workshop on particle size, particle detection and measurement. Historical perspective and current chapter review. 2010.

II SCOPE

The present Doctoral thesis was motivated by the increasing interest in subvisible and submicron protein particles present in biotechnological products. In view of the potential biological consequences of such particulate matter, especial attention was given to the analytical instrumentation used to characterize protein particles. More specifically, this dissertation was focused on those that measure particles suspended in liquids. Four main groups were included: light obscuration (HIAC and SYRINGE); flow imaging (Micro Flow Imaging and Flow Cam); electro zone sensing (Coulter Counter) and nano-range technologies (Nano Tracking Analysis and Resonant Mass Measurement).

Aiming to increase our knowledge about those new analytical tools the present dissertation was divided in 4 chapters. Broadly, in the first two chapters the aim was to present and identify general factors that govern instrument performance. In the last 2 chapters and using that experience, the focus was on the areas of opportunity in order to offer analytical tools that improve the current status of the subvisible particle analysis.

It was the goal of **Chapter 1** to expose the unclear aspects and main questions about the analytical toolbox performance. To achieve that objective an integrative and realistic stability study with a low concentrated biopharmaceutical product was conducted. Such a highly challenging configuration was chosen to illustrate a worst case scenario and hence allowed the identification of general instrumental-related factors.

The results of that stability study triggered the interest in a more profound research on the basics of instruments analytical operation. **Chapter 1** focused on the precision and **Chapter 2** on the accuracy and linearity performance. In each case, the fundament of each method was challenged using particle models in concentration, size, morphology and nature of interest for the Pharmaceutical Industry.

Due to the fact that each sample might develop its own experimental method guidelines, to provide exact numbers for quantitation limits was not in the scope of this dissertation. However, despite the individual instruments' differences, it was the aim of **Chapter 1** and **Chapter 2** to establish some generalities to rationalize the strengths and weaknesses of the techniques.

Once the specific effects that directly impact the analytical performance were identified, the goal of **Chapter 3** and **Chapter 4** was to propose instrument and method improvements.

Since light obscuration technique is the most established one as indicated in the Pharmacopoeia, it was the aim of **Chapter 3** to improve the applicability of the technique to the exigencies of Biotechnological samples. More precisely, by means of changing the measuring mode of the light obscuration sensor, the aims were to lower the detection limit to particles < 1 µm and to improve the detection of highly translucent particles.

Finally, in **Chapter 4** the aim was to identify and rationalize the artefacts that can affect the Nano Tracking-based technique and provide guidance for the development of product-specific analytical methods and for the proper results interpretation.

CHAPTER 1

Factors Governing The Precision Of Subvisible Particle Measurement Methods – A Case Study With A Low-Concentration Therapeutic Protein Product In A Prefilled Syringe

Anacelia Ríos Quiroz
Jens Lamerz
Thierry Da Cunha
Adeline Boillon
Michael Adler
Christof Finkler
Joerg Huwyler
Roland Schmidt
Hanns-Christian Mahler
Atanas V. Koulov

1.1 ABSTRACT

The current study was performed to assess the precision of the principal subvisible particle measurement methods available today. Special attention was given to identifying the sources of error and the factors governing analytical performance. The performance of individual techniques was evaluated using a commercial biologic drug product in a prefilled syringe container. In control experiments, latex spheres were used as standards and instrument calibration suspensions. The results reported in this manuscript clearly demonstrated that the particle measurement techniques operating in the submicrometer range have much lower precision than the micrometer size-range methods. It was established that the main factor governing the relatively poor precision of submicrometer methods in general and inherently, is their low sampling volume and the corresponding large extrapolation factors for calculating final results. The variety of new methods for submicrometer particle analysis may in the future support product characterization; however, the performance of the existing methods does not yet allow for their use in routine practice and quality control

1.2 INTRODUCTION

Due to concerns related to the hypothesis that proteinaceous particles may act as potential immune activators, significant attention has been focused on the protein particles sized between ca. 1 μm and 100 μm, the "subvisible particles" (1-4). The high interest triggered by this topic has resulted in a number of scientific publications (5-9). As a result from the intense focus on subvisible particles over the last decade, several new analytical methods were developed and introduced in industry. At present, the "gold standard" for subvisible particle analysis is the light obscuration method. This method is often combined with additional characterization methods utilizing a different measurement principle, offering the possibility to extend the size range of analysed particles from 10 μm down to 30 nm. Thus, the apparent gap of measurable particle sizes (i.e. the "submicron gap") can be closed (10, 11).

The different measurement principles of the newly emerged methods can be summarized as follows (see Table 1.1): Nanoparticle Tracking Analysis (NTA) is a technique, which combines laser light scattering microscopy and a video imaging system for sizing and counting of particles. After recording a video of the sample, the NTA software identifies and tracks the particles which are moving under Brownian motion. The rate of diffusion of each individual particle captured on film is related to its size according to a modified 2-dimensional Stokes–Einstein equation. In the Resonant Mass Measurement (RMM) technique, particles in suspensions are pumped through a microfluidic channel that resonates mechanically. The presence of a particle in the resonator channel adds to the total mass and therefore shifts the sensor resonant frequency. These shifts are recorded as each individual particle passes through the sensor. Density differences between the particles and the fluid matrix, allows for particle categorization in positive or negative buoyant populations. The Coulter Counter (CC) instrument relies on the Electrical Sensing Zone principle. The device is equipped with a glass tube with an aperture of given diameter, which is immersed in the conductive sample. A current is applied between electrodes placed inside and outside of the tube. A particle passing through the aperture causes a short-term increase in resistance. The magnitude of the resistance change depends on the volume of the particle. Thus, the particle size (calculated by volume) and particle counts are derived based on a change in electrical resistance. In the micro flow imaging technique (MFI), bright-field images are captured in successive frames as a continuous sample stream passes through a flow cell positioned in the field of

Table 1.1 Instruments in scope

	Principle	Data processing	Size [µm]*												Sample concentration [particles/mL]**
			0.03	0.05	0.2	0.3	0.6	0.5	0.8	1	2	5	18	25	
Nano track analysis. NTA	Tracking of Brownian motion of individual particles using a microscope and a video camera	Hypothetical hard spheres that diffuse at the same speed of the tracked particles are assumed. The hydrodynamic diameter is obtained according to the 2D-modified Stokes-Einstein equation. For count determinations the averaged particle abundance (average number of particles per frame) is divided by the estimated volume of the sample chamber	▓	▓	▓	▓	▓	▓	▓						3×10^8 - 1×10^9 , ~20-70 centers per frame
Resonant mass measurements. RMM	Changes in frequency due to added mass as particles go through a micro resonator channel	Shifts in frequency with respect to sensor baseline resonance are converted into buoyant mass using the sensor-specific sensitivity. Sensitivity is obtained using size standards as calibrators. Knowing the fluid and particle density, buoyant mass is converted into dry mass. Finally, assuming a sphere shape, particle diameter is calculated. Concentration is obtained relating the number of events (particles) registered with the volume of sample dispensed		▓	▓	▓	▓	▓	▓	▓	▓				$< 8\times10^6$
Coulter counter. CC	Changes in resistance due to volume displacement as particles immersed in conductive solutions cross an aperture in a glass tube	The impedance pulses generated as particles are pumped through an orifice in a glass tube are individually analyzed by the instrument electronic components. As the electrical current is constrained in the aperture orifice each pulse is directly proportional to the volume that the particle displaced and its size. Concentration is obtained relating the number of events (particles) registered with the volume of sample dispensed			▓	▓	▓	▓	▓	▓	▓	▓	▓		$\sim 2\times10^5$, coincidence $< 5\%$
Flow imaging microscopy. MFI	Viewing of single particles passing through a flow cell and are photographed with a high speed camera	Digital images are analyzed by the instrument software. Following background comparison, intensity values are assigned to each activated pixel. Adjoining pixels below 96% of the maximum brightness is grouped as particles. Internal algorithms are used to generate morphological descriptors per each particle. Concentration is obtained relating the number of events (particles) registered with the volume of sample dispensed								▓	▓	▓	▓	▓	$< 9\times10^4$
Light obscuration. HIAC	Drop in current due to the amount of light blocked as particles cross the light source	A calibration curve size-voltage is prebuild using calibration size standards. Particle size is obtained by direct interpolation in the calibration curve of the voltage recorded when a particle blocks the sensor. Concentration is obtained relating the number of events (particles) registered with the volume of sample dispensed								▓	▓	▓	▓	▓	$< 1.8\times10^4$

* Size bins used in this study are presented in a discontinuous scale. Instrument actual measuring size ranges might be broader.

** Maximum values as recommended for the supplier.

view of an optical system with a 5x magnification objective. The digital images of the particles present in the sample are processed based on image morphology and yields information on particle size and count. It should be noted that microscopic imaging supports morphological characterization of particles. Thus, silicone oil droplets and other particulate contaminants can be identified and excluded from protein analysis. Finally, the Light Obscuration (LO) method measures the drop in voltage consequence of the blockage of a constant source of light illuminating as particles pass through the flow-cell.

Each individual method from the diverse collection described above utilizes a different measuring principle and therefore – presents its unique challenges. Although the recent literature provides a good overview of the latest analytical developments in the field of particle analysis (12-19), a systematic critical assessment and comparison of the individual methods is still missing. In particular, a detailed comparative evaluation of the analytical performance of the individual methods and most importantly – a qualitative understanding of the sources of error (both random and systematic) of these methods are not yet available.

The aim of the present study was to conduct detailed assessment of analytical performance of particle measurement techniques currently available with respect to one of the main analytical performance attributes – method precision (including repeatability and intermediate precision). The most widely used analytical tools (Table 1.1) for subvisible particle measurements in liquids were evaluated in terms of precision and limitations leading to deviations between typically used (and NIST certified) polystyrene standard calibration samples and actual drug product samples. Microscopy techniques other than flow imaging microscopy (e.g. TEM or membrane microscopy) which include additional sample preparation steps like for example filtration, were out of the scope of this study. Furthermore, this study was focused on particle counting rather than on characterizing morphological attributes or particle identity. In this study, performance of instruments was verified using a commercial biologic drug product. In control experiments, latex spheres were used as standards and instrument calibration suspensions.

1.3 MATERIALS AND METHODS

Polystyrene beads in a Count standard configuration (3000 particles/mL, COUNT CAL, Thermo Fisher

Scientific) of 2; 5; 10 and 25 µm and RI of 1.59 were used for the precision assessment of micrometer methods (HIAC; MFI and CC).

A therapeutic protein product with a molecular weight in the range of 50 kDa and concentration of 0.36 mg/mL were stored in stacked-in-needle Pre-Filled Syringes (PFS), (1mL syringe with 0.5 mL filled in volume) and type 1 glass vials (6 mL vial with 5 mL filled in volume), respectively. The study employed recommended storage conditions (2-8 °C), accelerated storage conditions (25 °C/60% r.h.), and a stress condition (40 °C/75% r.h.). Samples were analysed at selected time points (T) 0; 4; 8 and 13 weeks (w). Protein formulation as well as placebo samples (*i.e.* formulation without protein) were included in the accelerated stability study. All samples were prepared in a particle-free environment, utilizing material extensively rinsed with particle free water. Water was treated by several filtration and degassing steps (Liqui-cel Membrane Contactors, Membrana Germany). Air used for drying was filtered (0.22 µm pore size Millex PES filter membranes, Millipore Ltd, Cork, Ireland). Sample pooling was done as follows: the content of syringes was homogenized by gently inverting them 20 times in a vertical position. Solution was manually ejected into the glass vials within 20 to 25 seconds (s). Finally, before measurements, pooled solutions were manually homogenized by repeated inversions of the vials. The pool size was defined accordingly to instrument minimum sample requirements and experiment intent as described in following sections.

Syringes containing protein formulation stored for 2 months at 2-8 °C were used for precision assessment (repeatability and intermediate precision) and container to container variability (pool size and pump speed) experiments. Repeatability was defined as the variability of the values of triplicate consecutive measurements of the same sample performed by the same analyst and was assessed by the magnitude of the associated standard deviation and coefficient of variance. Intermediate precision was defined as the variability of the values of triplicate consecutive measurements of identically prepared and independent samples performed by different analysts on different days and was assessed by the magnitude of the associated standard deviation and coefficient of variance.

Particle counts were reported per mL of sample and in the typically used cumulative size bins. Plots were constructed as the ratio of the standard deviation to the mean values (CV %) versus particle size using Origin 9.1 software.

Light obscuration (HIAC)

The light obscuration measurements were performed using a HIAC Royco counting System 9703 equipped with an HRLD400HC sensor. Analyses were made with a flushing volume of 1 mL followed with a small volume method of 4 runs of 1 mL each. The first run was rejected and remaining runs were averaged to get particle counts per mL in the following size categories: ≥ 1, ≥ 2, ≥ 5, 10 and ≥ 25 µm. Blank runs were performed before each sample allowing no more than 20, 5 and 1 particles/mL for sizes ≥ 2 µm; ≥ 5 µm and ≥ 10 µm, respectively. Suitability test per day of measurements involved the measurement of 2, 5, 10 and 25 µm count standards (Count-cal, Thermo Fisher Scientific, Fremont, USA) accordingly to supplier specifications. Intermediate precision and stability samples were prepared by pooling the contents of either 40 syringes or 4 vials (total sample volume of 20 mL) from which 3 aliquots of 5 mL were measured. Pool-to-pool variability was assessed by single measurements of six independent and identically prepared solutions, each obtained by pooling the contents of 10 syringes.

Micro flow imaging (MFI)

Flow microscopy analysis was performed using a DPA4200 MFI Flow Microscope System (ProteinSimple, Toronto, Canada). Method parameters were set to 1 mL sample volume as termination type, 0.2 mL as purge volume (analysed volume ~0.59 mL) and "edge particle rejection" as well as "fill particle" options activated. Light optimization step was performed with the correspondent filtrated sample matrix. Either single or 3 independent runs of the same dilution were performed for blanks and particle samples, respectively. Cumulative particle counts per mL were obtained in the following bins: ≥ 1, ≥ 2, ≥ 5, ≥ 10, and ≥ 25 µm using the software MVSS version 2 (ProteinSimple, Canada). Acceptance criteria for blanks was less than 100 particles per mL > 1µm. Suitability test per day of experiment involved 1) measurement of 5 µm count standards (Thermo Fisher Scientific) with acceptance limits of ± 10 % the reported concentration for particles > 3 µm and 2) measurement of 5 µm size standard with acceptance limits of Equivalent Circular Diameter ECD mean of ± 25 % the

reported size and standard deviation <0.4. Intermediate precision and stability samples were manually prepared by pooling the content of 10 syringes for a total sample volume of 5 mL from which 3 aliquots of 1 mL were measured. Bulk solutions were used directly from the initial vial container. Pool-to-pool variability was assessed by single measurements of six independent and identically prepared solutions, each obtained by pooling the contents of 1, 3, 6 and 10 syringes using an automated syringe pump (Harvard PHD Apparatus, 2000 infusion) at a rate of 1.5 mL/min (dispensing time 20 s) and collecting samples in individual glass vials. A modified method of 0.5 mL sample volume as termination type and 0.2 mL as purge volume was used (analysed volume was ~0.17 mL).

Coulter counter (CC)

A CC4 model of Beckman Coulter with a 20 μm aperture tube was used. Protein sample conductivity was ~17 mS hence used without further adjustments. For any other sample isotone (Beckman Coulter, Monheim, Germany) was used as matrix (~18 mS). Electrolyte jar was filled with the same buffer solution as that of sample matrix. Method parameters were set to: volume analysed 50 μl, runs 3, current 600 μA and gain 4. Aperture tube's cleanness was verified in between every sample with blank (isotone or buffer) measurements allowing less than 1000 particles/mL. Instrument was daily calibrated using 3 μm size standards in the correspondent sample matrix. As sample container a small volume cuvette of 5 mL capacity (Beckman Coulter, Monheim, Germany) was used with especial attention into full electrode coverage. Intermediate precision and stability samples for T0 w, T4 w, and T13 w were prepared by pooling the content of 10 syringes. For T8 w, 24 syringes were pooled. From the respective final volumes, aliquots of 5 mL were measured. Bulk solutions were used directly from the initial vial container. Pool-to-pool variability was assessed by single measurements of six independent and identically prepared solutions, each obtained by pooling the content of 10 syringes manually.

Resonant Mass Measurements (Archimedes)

Resonant mass measurements were performed using Archimedes system (Affinity Biosensors, Santa Barbara, USA) equipped with a Hi-Q micro sensor. Prior to each sample, system was rinsed as follows: matrix sample solution for 2 minutes, PCC54 detergent solution (ThermoScientific, Illinois, USA) for 2 minutes and particle-free water for 10 minutes. A threshold of 0.04 Hz and 0.03 Hz for

protein and polystyrene standards was applied, respectively. The density of the fluid was 1.004 g/mL. The density of proteinaceous particles and silicon oil droplets was defined as 1.32 and 0.9 (vendor recommendation), respectively. Hence, positively buoyant particles (RMM (+)) were assigned as silicon oil like particles and negatively buoyant particles (RMM (-)) were assigned as protein like particles. Run time of 8 hours or 10000 collected particles was defined as termination type point to ensure sufficient volume sampled, high number of detected particles and hence sound statistics. Such long measurement time allowed for single runs only instead of triplicates. The frequency vs time chart obtained in real time as the measurement is running was used to monitor possible sensor clogging. When such trend showed strange gaps and/or irregularities in the points distribution, the run was disregarded, the sensor cleaned (or replaced) and the run repeated. The data was collected and analysed using software ParticleLab version 1.8.570 (Affinity Biosensors, USA). Intermediate precision and stability samples T3 w; T8 w and T13 w were prepared by pooling the content of 10 syringes. From the final sample volume of 5 mL, single aliquots of 1 mL were prepared for the measurements. The actual measured volume varied among samples and was obtained from the *.csv* file (in general 7 – 10 µL). Bulk solutions were used directly from the initial vial container.

Nanoparticle Tracking Analysis (NTA)

The NTA measurements were performed with the Nanosight NS200, LM20 equipped with a 405 nm laser. Before measurements, the chamber was cleaned with 0.02 µm filtered (Anotop 25, Whatman, Glattbrugg, Switzerland) water and analysed to confirm the absence of particles. Samples were injected using 1 mL sterile syringes (Norm-Ject, HSW, Tuttlingen, Germany). First volume was used to rinse out the flushing water and with the remaining volume 3 videos of 90 s were recorded using replenished sample each time. Video recording settings were set so that clear and sharp particle images were obtained. During the measurement, the temperature was controlled and recorded by a temperature sensor contained in the viewing unit. The software used for capturing and analysing the samples was the NTA 2.2. In order to get statistically reliable results, a minimum of 300 completed tracks was required. Intermediate precision and stability samples were prepared by pooling the content of 6 syringes. From the final sample volume of 3 mL, aliquots of 1 mL were prepared for the measurements. Information from the supplier reports chamber sample dimensions of approximately

10x120x80 μm. Hence the measuring volume can be estimated as 9.6×10^{-8} mL. Bulk solutions were used directly from the initial vial container.

Poisson distribution statistical simulations

All simulations were performed using R 3.2.2 (R Foundation for Statistical Computing, Vienna, Austria). To estimate the distribution and magnitude of CV based on simulation alone, 1000 simulations runs were performed based on the expected number of particles λ. Three (for repeatability) or six (for intermediate precision) random values of the Poisson distribution were generated and their respective CV computed

1.4 RESULTS

In the present study, a number of particle measurement methods (Table 1.1) were compared in the context of an accelerated stability study. For the assessment of particles between 100-1000 nm size, Nanoparticle Tracking Analysis, (NTA), Resonant Mass Measurement (RMM) and the Coulter Counter (CC) instruments were included. These methods will be hereafter referred to as *submicrometer* methods. For the assessment of particles between 1-100 μm size, Flow Microscopy (Micro Flow imaging (MFI)), Coulter Counter (CC) and the compendial Light Obscuration (HIAC) were included. These methods will hereafter be referred to as *micrometer* methods. The methods were used to analyse a commercial protein, which was stored under accelerated stability conditions. Samples were analysed at T0 and 4, 8 and 13 weeks and protein particles in cumulative counts per mL were reported as presented in Table 1.2. Significant discrepancies between the different measurement methods were observed as well as inconsistent trends within different time points. For example: a) HIAC light obscuration method reported very similar quantities of particle of the samples stored at 5 ºC and 25 ºC, while in the samples stored at 40 ºC there was an apparent increase in the particle count over time. An apparent increase in the spread between individual results for different replicates with the time of storage was also observed. b) The results from the RMM measurements showed an apparent increase of the overall counts with temperature, but an apparent decrease of counts with time within each condition. These inconsistent results and the large and unexpected deviations between the

Table 1.2 Number of particle per mL measured in a low-concentration therapeutic product in a prefilled syringe container at 5°C; 25°C and 40°C over the course of 4, 8 and 13 weeks. Instruments are described in Table 1.1

	Size [um]	5°C			25°C			40°C		
		4	8	13	4	8	13	4	8	13
HIAC	>1	19055 ± 133	13446 ± 481	14929 ± 4291	19584 ± 849	12370 ± 415	15933 ± 7673	12107 ± 400	19019 ± 657	20704 ± 7390
	>2	12352 ± 186	8119 ± 324	10701 ± 2213	10247 ± 406	6664 ± 214	8448 ± 4448	6257 ± 166	10503 ± 279	12620 ± 4967
	>5	6466 ± 94	3821 ± 167	5939 ± 849	2845 ± 282	2514 ± 58	2276 ± 1149	1933 ± 11	3425 ± 50	3961 ± 1210
	>10	1179 ± 50	691 ± 36	819 ± 449	310 ± 66	452 ± 25	254 ± 123	231 ± 4	573 ± 11	552 ± 69
	>25	6 ± 3	6 ± 0	1 ± 2	3 ± 2	2 ± 2	2 ± 2	2 ± 3	7 ± 2	10 ± 3
MFI	>1	19205 ± 699	40437 ± 215	16612 ± 8276	33813 ± 554	28067 ± 108	30830 ± 3996	32140 ± 692	62658 ± 847	41138 ± 1223
	>2	7547.8 ± 226	18054 ± 170	6872 ± 3520	9743 ± 170	9324 ± 107	9569 ± 275	9527 ± 82	22972 ± 228	14444 ± 782
	>5	2092 ± 185	5627 ± 235	1727 ± 496	1241 ± 46	1473 ± 28	793 ± 171	1269 ± 29	3989 ± 77	1763 ± 203
	>10	792 ± 154	1382 ± 101	427 ± 110	222 ± 22	224 ± 17	67 ± 27	139 ± 9	519 ± 52	182 ± 33
	>25	12 ± 5	12 ± 6	1 ± 1	4 ± 3	6 ± 6	1 ± 0	4 ± 2	7 ± 4	3 ± 4
CC	>0.4	740667 ±18595	434133 ± 16754	457167 ± 16292	815600 ± 14152	553933 ± 23150	625400 ± 37013	782800 ± 16008	899333 ± 36875	2014667 ± 42336
	>0.5	464967 ± 11918	297100 ± 10872	283400 ± 11663	525233 ± 9347	383667 ± 15292	405233 ± 26508	515767 ± 13639	559333 ± 22396	703500 ± 10835
	>0.8	137033 ± 2631	106300 ± 3851	91700 ± 4506	170700 ± 4949	141433 ± 4200	139533 ± 10995	179233 ± 4409	203000 ± 7234	214033 ± 4802
	>1	73200 ± 1837	59890 ± 2923	50887 ± 2728	88110 ± 3637	81990 ± 2330	75410 ± 7123	96063 ± 3403	113767 ± 4661	108433 ± 2150
	>2	14587 ± 500	13050 ± 920	10773 ± 670	13523 ± 613	16547 ± 304	12313 ± 705	13820 ± 512	19893 ± 935	12030 ± 318
	>5	1719 ± 159	1969 ± 44	1099 ± 26	1336 ± 115	1931 ± 123	895 ± 33	1014 ± 103	2760 ± 243	1256 ± 181
	>10	175 ± 34	229 ± 58	74 ± 42	107 ± 24	95 ± 30	65 ± 40	75 ± 34	147 ± 64	52 ± 20

Table 1.2 C*ontinuation*

RMM (+) >0.3	236000	140000	99200	672000	202000	185000	1120000	322000	201000
>0.4	236000	140000	10	672000	202000	185000	1120000	322000	201000
>0.5	231000	138000	10	656000	198000	185000	1050000	317000	200000
>0.8	15400	21000	13300	76300	28300	24100	122000	46000	32100
>1	2130	6600	3010	18100	8420	7420	26900	9750	72400
>2	0	309	0	0	213	102	106	0	0
>5	0	0	0	0	0	0	0	0	0
RMM (-) >0.3	138000	28100	7880	107000	24800	40700	197000	13600	62100
>0.4	78000	13900	3010	58300	11100	31200	43100	5910	43100
>0.5	28900	3090	726	23800	2240	22000	9350	1560	16900
>0.8	2740	206	0 ± 0	1770	0	508	0	0	210
>1	913	103	0 ± 0	417	0	0	0	0	0
>2	0 ± 0	0 ± 0	0 ± 0	0	0	0	0	0	0
>5	0 ± 0	0 ± 0	0 ± 0	0	0	0	0	0	0
NTA[a] >0.05	221 ± 34	279 ± 36	267 ± 24	250 ± 20	161 ± 33	183 ± 31	75 ± 4	63 ± 9	43 ± 6
>0.2	61 ± 12	65 ± 8	75 ± 24	82 ± 5	37 ± 21	51 ±11	31 ± 5	27 ± 8	19 ± 12
>0.3	18 ±13	16 ± 4	25 ± 7	24 ± 9	11 ± 7	14 ± 6	8 ± 3	11 ± 7	7 ± 9
>0.4	9 ± 12	4 ± 1	13 ± 6	14 ± 6	5 ± 4	6 ± 4	3 ± 2	4 ± 5	2 ± 2
>0.5	5 ± 8	1 ± 0	8 ± 8	10 ± 5	1 ± 0	4 ± 3	1 ± 1	3 ± 5	1 ± 1
>0.8	2 ± 3	0 ± 0	1 ± 2	3 ± 2	0 ± 0	1 ± 1	0 ± 0	2 ± 3	0 ± 0
>1	0 ± 0	0 ± 0	1 ± 1	1 ± 1	0 ± 0	0 ± 0	0 ± 0	1 ± 2	0 ± 0

[a] E8 particles/mL

different instruments were indicative of analytical artefacts. In order to address this problem, the precision of the methods, the repeatability and intermediate precision were determined.

Repeatability assessment

The repeatability of all methods was assessed by measuring an identical sample repeatedly within a short interval of time (< 1 h) on the same instrument by the same analyst. The results from this assessment are summarized in Table 1.3A (See also Table S1.1 the complete dataset). In these experiments the micrometer methods HIAC; MFI and CC demonstrated very good repeatability (CV % in the range of 4 ± 3) except for the larger particle sizes of >10 µm and >25 µm (CV % 50 ± 69). In contrast, the submicrometer methods RMM and NTA exhibited relatively poor repeatability (CV % 84 ± 51) in all particle sizes except for 0.05 µm particles, where NTA measurements showed CV % of 7. Interestingly, the results for the positively buoyant particles (presumably silicone oil droplets originating from the lubricant layer of the syringes) were much more precise than the measurements of the negatively buoyant particles (presumably protein particles) with CV % 37 ± 10 for the former and CV % 136 ± 21 for the latter.

In all methods, the precision of measurement for the larger particles within the same sample was

Table 1.3 Precision assessments of subvisible particle measurements using a low-concentration protein therapeutic product in PFS. Data expressed as coefficient of variation % (CV%). Values bigger than 10% are marked in italics

A) Repeatability							
Size µm	HIAC	MFI	CC	Size µm	RMM(+)	RMM(-)	NTA
>0.4	nd	nd	6	>0.05	nd	nd	7
>0.5	nd	nd	1	>0.2	nd	nd	*33*
>0.8	nd	nd	3	>0.3	*29*	*128*	*34*
>1	nd	2	5	>0.4	*29*	*127*	*67*
>2	3	5	1	>0.5	*30*	*132*	*122*
>5	3	*12*	5	>0.8	*49*	*120*	*92*
>10	7	*29*	*173*	>1	*47*	*173*	*134*
>25	*17*	*25*	nd				
B) Intermediate precision							
Size µm	HIAC	MFI	CC	Size µm	RMM(+)	RMM(-)	NTA
>0.4	nd	nd	6	>0.05	nd	nd	*20*
>0.5	nd	nd	*23*	>0.2	nd	nd	*47*
>0.8	nd	nd	*39*	>0.3	*39*	*99*	*82*
>1	nd	*51*	*44*	>0.4	*39*	*100*	*114*
>2	*48*	*58*	*49*	>0.5	*39*	*107*	*101*
>5	*51*	*61*	*56*	>0.8	*50*	*122*	*77*
>10	*38*	*55*	*104*	>1	*48*	*127*	*118*
>25	*27*	*46*	*nd*				

significantly poorer, compared to that of the small particles. This is a known phenomenon which is usually attributed to the very small number of particles from the larger sizes present in the sample, which results in very poor sampling. In order to assess this apparent discrepancy of the precision of measuring smaller and larger particles, an experiment using latex bead count standards of different nominal sizes (2 μm, 5 μm, 10 μm and 25 μm) was carried out. The used standard suspensions contained a known concentration of particles (3000 beads/mL). As expected, in all bead sizes the repeatability was nearly identical from size to size and very low in magnitude ~CV % 5 ± 4, (Table 1.4A).

Intermediate precision assessment

The intermediate precision of all techniques was evaluated by measuring samples prepared and measured independently in different days by different analysts. The results of this assessment are presented in Table 1.3B. Contrary to the relatively high precision demonstrated in the repeatability study, the micrometer methods showed poor intermediate precision (CV% 50±18, except for 0.4 μm particles in CC with CV% of 6). On the other hand, the submicrometer methods, showed also poor performance with even larger variance (CV % 78 ± 35) as compared to the micrometer methods, which was expected considering the poor repeatability of the submicrometer techniques described above. This overall larger variance (all methods) in the intermediate precision experiments suggests the likely contribution of additional factors besides the ones influencing the repeatability of these measurements (typically, instrument-related). Such additional factors usually reflect the contribution of the analyst, i.e. factors related to sample preparation, as well as real differences from sample to sample. Similarly to the repeatability experiments, the intermediate precision also improved when

Table 1.4 Precision assessment of subvisible particle measurements using count standards. Data expressed as coefficient of variation % (CV%). Values bigger than 10% are marked in italics

Size um	A) Repeatability			B) Intermediate precision		
	HIAC	MFI	CC	HIAC	MFI	CC
>2	1	4	10	2	3	*23*
>5	1	1	10	2	*12*	7
>10	3	4	10	4	*13*	7
>25	5	2	*11*	4	7	*11*

standard suspension of known size and concentration was used ([Table 1.4B](#)).

1.5 DISCUSSION

At present due to concerns related to the immunogenic potential of subvisible protein particles, a growing number of new analytical tools for their characterization were introduced during the last years.

They are often combined to characterize particles over the entire sub-visible size-range. Unfortunately, one difficulty associated with this approach is major discrepancies between analytical results from different methods. In particular, information on particle concentrations of identical samples may deviate considerably (this study and (1)). Such differences may originate from the different physical principles that some of the methods use, thus presenting inherent difficulties. Additional challenges may be posed by sample composition and the properties of the different types of particles present in the sample (for example, particles with refractive index values close to that of the medium may be difficult to detect accurately by either light obscuration or flow microscopy measurements (2-4)). As we develop comprehensive understanding of the analytical performance of the various techniques for particle characterization available today, it is essential that we strive to grasp the complex factors governing their operation.

In this study we present the results of a short term stability study using a low-concentration therapeutic protein product in a prefilled syringe. Despite the low protein particle burden that our model product depicted as compared to the amount of intrinsic silicon oil droplets; this model represents a worst case that clearly exposed the strengths and weaknesses of the instruments in scope.

Factors governing method repeatability

One striking outcome from the evaluation of method precision was the very poor repeatability of the submicrometer methods NTA and RMM. This observation is intriguing as it hints to a phenomenon that seemingly affects both methods, although they are based on completely different measurement principles. One such common feature is the very low measurement volumes that both methods utilize. In some cases, the volume measured is as low as 0.08 nL, which requires extrapolation of more than 12 million fold in order to represent particle concentration in "particles per mL" units, as required for parenteral formulations. This is a serious problem, especially if the particle count in a given sample is

relatively low. This effect can be illustrated using the concept of statistical probabilities. In a 1 mL hypothetical sample containing a single particle, measurement of 0.1 mL portion of this sample will decrease the probability of detection of the single particle to 10 %, as compared to measuring the entire sample volume. In cases when measurement volumes as low as 1 nL are used (e.g. RMM measurements), the probability of detection of a single particle will be drastically reduced to just 0.0001 %.

As mentioned above, the sampling efficiency (the portion of 1 mL sample which is measured in each method) varies extensively from technique to technique and in some cases can be as low as 0.08×10^{-6} %, (see Table 1.5). Interestingly, many submicrometer methods nevertheless seem to focus on low sampling volume, resulting in very large extrapolation factors used to calculate final particle concentrations and in turn poor precision. Thus, the sampling efficiency is perhaps the main factor governing the precision of particle submicrometer counting instruments. Figure 1.1 illustrates the correlation of high variability with the large extrapolation factor (due to the low sampling efficiency). Methods with extrapolation factors smaller than 20 fold (*e.g.* HIAC, MFI and CC) demonstrated far better repeatability as indicated by the CV % as compared to the methods with larger extrapolation factors (*e.g.* RMM and NTA).

To further elaborate in this phenomenon, the CV experimental values were compared to simulated ones using a Poisson distribution model. That model describes the occurrence of successful events when the associated probability is low. For each combination of instrument and particle size bin, 1000 simulation runs were performed to estimate the CV distribution. Based on the respective instrument

Table 1.5 Sample volume and extrapolation factors of the different instruments. To report final protein concentrations normalized to 1 mL of sample volume, the indicated extrapolation factors are needed

Instrument	Measurement volume, V (mL)	Extrapolation factor, 1/V (mL^{-1})
HIAC	> 1	1.0x
MFI	0.6	1.6x
CC	0.05	20x
RMM	0.01	100x
NTA	0.00000008	12500000x
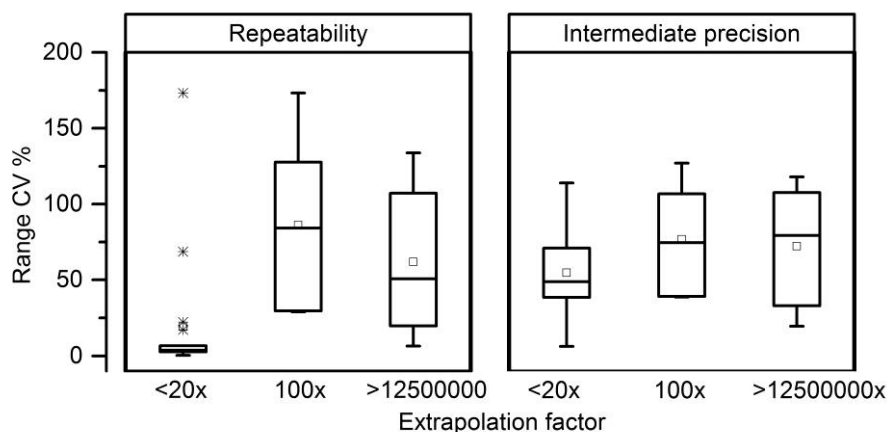
Figure 1.1 Precision of subvisible particle methods in relation to the applied extrapolation factors. Syringes containing protein formulation stored for 2 months at 2-8 °C were used for precision assessment. Results, reported as CV% were plotted against the corresponding extrapolation factors. Factors used were <20x for HIAC, MFI and CC. 100x for RMM. 12500000x for NTA

specific measured volume as λ (*e.g.* for MFI λ is the actual number of particles found in the 0.6 mL volume sampled), three (for repeatability) or six (for intermediate precision) random values of the Poisson distribution were generated and their respective CV computed. The distribution of simulated and observed CV is compared in Figure 1.2 by means of boxplots, separated by type of instrument and precision assessment. It can be observed that the computational estimates of repeatability CV% for all of the methods which we evaluated show similar or lower values as compared to the ones measured experimentally (see Figure 1.2). As the simulation process considers exclusively the effect of sampling volume, this result supports the conclusion that sampling efficiency is likely the major factor governing precision of submicroscopic methods. As expected, these results also demonstrate that in some cases additional experimental factors likely contribute as well. The corresponding statistical simulations for intermediate precision show values that are generally lower than the experimentally measured ones, which is also an expected result, considering the fact that additional experimental factors surely contribute to intermediate precision. In a second simulation, the impact of the encountered particles in such small volumes was studied. In very small volumes, the number of particles n becomes very low too. For example, let us compare the volume under investigation in a given Instrument$_1$ with V$_1$ = 1 mL with the volume of another Instrument$_2$ with V$_2$ = 0.08 nL. In this
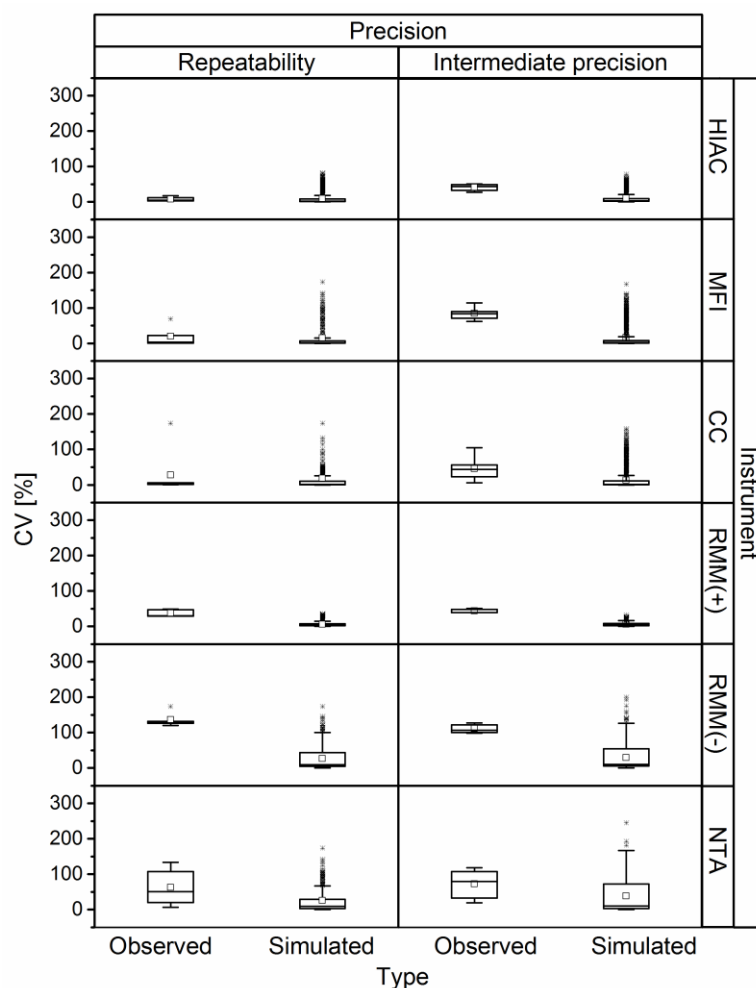
Figure 1.2 Comparison of the experimentally measured and simulated (using Poisson distribution) CV% values per instrument and type of precision analysis. For additional details, please refer to Materials and Methods Section 1.3

hypothetical situation, V_1 is about 10^8 larger than V_2. Let us assume that in the sample $n_1 = 100'000$ particles were found. Then the expected was numbers of particles n_2 in the investigated Volume V_2 of Instrument$_2$ would be $\lambda = n_2 = n_1 * V_2/V_1$. Using the Poisson distribution, we have simulated this situation with different numbers of originating particles n_1 and ratios of V_2/V_1 resulting in different expected numbers of particle, λ. Each setting simulated 1000 times, and the CV was estimated for 3 random numbers. Figure S1.1 demonstrates, that the CV is highest for $\lambda = 1$. Here a median CV of approximately 100 % is found. With $\lambda = 10$ it already reduces down to a median CV of 25 %, and at $\lambda = 100'000$ this CV is already negligible. Figure S1.1 also demonstrates that the CV is not dependent on the total number of particles in the sample, n1. It is simply dependent on the number of expected particles in the volume under investigation. Moreover, it shows that the contribution of counting small

numbers to the overall loss of precision is highly considerable. The same phenomenon of poor precision due to very low number of particles is also reflected in the measurements of the larger particle sizes in both the micrometer and submicrometer ranges. The precision for these larger sizes was considerably decreased as compared to smaller size ranges. As can be seen in Table 1.3A, the CV % decreased from 173 to 6 for <10 µm and <0.04 µm particles, respectively, using the CC method. Thus, the precision of a given method is a function of particle number. To confirm this hypothesis, an additional experiment was performed using different polystyrene bead count-standards with identical and defined concentration in individual size-bins (*i.e.* 3000 particles/mL for particles sizes from 2 µm up to 25 µm). It is important to note that in contrast to polystyrene beads, protein particles are typically heterogeneous in shape, optically uneven, exhibit higher pliability and perhaps different refractive indexes along the entire size distribution. Such characteristics pose much higher challenge for particle detection and quantification as compared to polystyrene beads. The impact of these differences on the measurements has been studied and efforts to generate standard material that resembles better the characteristics of protein particles are also published. (25, 26) However, polystyrene standards are broadly used for the calibration and verification of particle counting instruments due to the easy handling and good stability of the particles. As expected the results from these measurements demonstrated that the precision in a given size-range was (at least partially) dependent on the number of particles present (Table 1.4). Good repeatability was confirmed for particles up to 5 µm, and notably, good repeatability was also found for particles >10 µm and >25 µm. This finding confirms that precision is independent of particle size but strongly influenced by particle number. An analysis of the size distribution of data corroborates these findings. For example, particles >25 µm in the HIAC represent in average less than 3 % of the total size distribution and therefore have a poor CV % of > 17. Particles between 0.05 and 0.2 µm in the NTA represent in average more than 70 % of all particles and have a much better CV % of 6.5. Finally, additional support for the fundamental importance of sampling efficiency was provided by the apparent difference between the precision of measurement of the positively buoyant and negatively buoyant particles counted by RMM. The results for the former appear more precise than the results for the latter, which corresponds well to their

relative abundance (the more abundant positively buoyant particles were measured more precisely than the less abundant negatively buoyant particles).

Our results suggest that the large discrepancies in repeatability from technique to technique are mainly due to the large differences in the measured volumes (sampling efficiency). Thus, one potential direction for future instrument development is improving sampling efficiency, particularly in the techniques which currently allow for measuring very low effective volumes only.

Factors governing method intermediate precision

The measured intermediate precision of all different subvisible measurement methods used in this study was relatively poor. As expected, the CV % values measured for each individual method were larger than the values for repeatability, likely indicating that additional factors may play a role. These potential factors include instrument-related (*e.g.* day-to-day instrument performance differences not reflected by routine suitability test runs) and sample-related effects (*e.g.* sample preparation, container-to-container variability, etc.). To gain further insight into the relative contribution of these two types of factors, a set of experiments using different sample preparation procedures was carried out. Samples were prepared by pooling a different number of containers. These different pools were measured and the corresponding precision values were correlated to the size of each pool. Measurements of uniform samples (certified bead concentration standards) demonstrated very high intermediate precision in all size categories (in general CV % < 11, Table 1.4). Interestingly, the results from the pooling experiments (MFI measurements) indicate that the larger the pool size, the better the precision (Figure 1.3). Similarly low variability for larger pools (N=10) was confirmed for HIAC and CC methods (Figure S1.1). These results indicate that the measured variance is likely sample-related – e.g. possible small differences in the siliconization level of individual syringes or minor variation in the sample preparation procedure (manual ejection of the syringe content is difficult to control). As the pool size increases such container-to-container differences presumably are averaged out. Contribution from the instrument day-to-day variability was excluded, because the system suitability tests performed on each measurement day remained within acceptance limits (data not shown).

The repeatability and intermediate precision data presented in this study highlight general principles
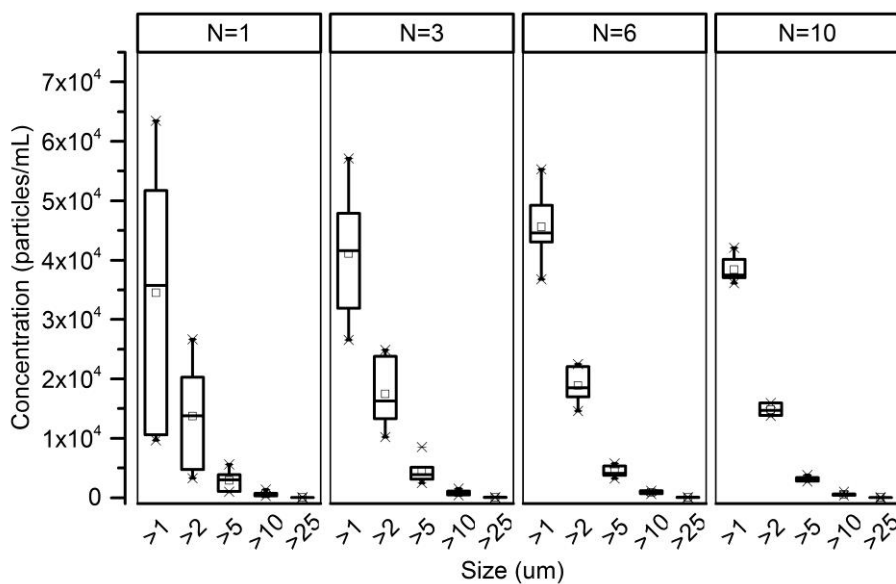
Figure 1.3 Protein particle concentration variability as a function of pool size Comparison of the variability of 6 independently prepared samples of commercial proteins. The content of a number N of prefilled syringes was pooled and analysed by MFI

and factors influencing the performance of a new generation of particle counting methods. It should be emphasized, that the used analytical methods are not yet generic methods but need to be adapted to address specific needs of users. For example, assay parameters and instrument configurations need to be optimized to account for differences in sample properties (*e.g.* viscosity, turbidity, refractive index contaminants, buffer systems etc. As a final remark, it needs to be pointed out that the specific values of the method attributes measured in this study should not be taken outside of the context of these experimental conditions. These measured values should serve as examples/guides only in order to demonstrate the general factors in play. In other test systems the values of the method attributes will likely be different as these are dependent on the specific test system used. Surely, further case studies from different laboratories using other model systems will be valuable in shedding more light on the methods' variability and the factors that affect it. However, the current study is meant to provide a systematic evaluation of the analytical performance of subvisible particle methods with the main goal to identify the principal factors controlling the precision of the methods assessed.

1.6 CONCLUSIONS

To our knowledge, the current report is the first detailed and systematic comparative assessment of the precision of a broad array of subvisible particle measurement methods. A commercial pharmaceutical protein product was used as representative and realistic test system. In this specific frame, our study revealed serious shortcomings of all tested subvisible particle measurement methods with the exception of the compendial light obscuration method and other micrometer methods. Despite the fact that the exact precision numbers (CV % values) might vary for different drug products, intriguingly, the submicrometer particle measurement methods demonstrated particularly poor precision. This finding could be explained by the extremely small samples volumes utilized by these methods limiting the probability for particle detection and necessitating large extrapolation factors to calculate the measurement results. We conclude that the very low precision of the submicrometer particle measurement techniques is an inherent instrument problem which for the moment excludes them from use in routine or quality control setting.

1.7 REFERENCES

1.   J.F. Carpenter, Randolph, Theodore W., Jiskoot, Wim, Crommelin, Daan J. A., Middaugh, C. Russell, Winter, Gerhard, Fan, Ying-Xin, Kirshner, Susan, Verthelyi, Daniela, Kozlowski, Steven, Clouse, Kathleen A., Swann, Patrick G., Rosenberg, Amy, Cherney, Barry. Overlooking Subvisible Particles in Therapeutic Protein Products: Gaps That May Compromise Product Quality. Journal of Pharmaceutical Sciences. 98:1201-1205 (2009).

2.   S.K. Singh, N. Afonina, M. Awwad, K. Bechtold-Peters, J.T. Blue, D. Chou, M. Cromwell, H.-J. Krause, H.-C. Mahler, B.K. Meyer, L. Narhi, D.P. Nesta, and T. Spitznagel. An industry perspective on the monitoring of subvisible particles as a quality attribute for protein therapeutics. Journal of Pharmaceutical Sciences. 99:3302-3321 (2010).

3.   A.S. Rosenberg, D. Verthelyi, and B.W. Cherney. Managing uncertainty: A perspective on risk pertaining to product quality attributes as they bear on immunogenicity of therapeutic proteins. Journal of Pharmaceutical Sciences. 101:3560-3567 (2012).

4.   A. Ríos Quiroz, G. Québatte, F. Stump, C. Finkler, J. Huwyler, R. Schmidt, H.-C. Mahler, A.V. Koulov, and M. Adler. Measuring Subvisible Particles in Protein Formulations Using a Modified Light Obscuration Sensor with Improved Detection Capabilities. Analytical Chemistry. 2015 Jun 16;87(12):6119-24 (2015).

5.   S. Kiese, Papppenberger, Astrid, Friess, Wolfgang, Mahler, Hanns-Christian. Shaken, not stirred: Mechanical stress testing of an IgG1 antibody. Journal of Pharmaceutical Sciences. 97:4347-4366 (2008).

6.   H.-C. Mahler, W. Friess, U. Grauschopf, and S. Kiese. Protein Aggregation: Pathways, Induction Factors and Analysis. Journal of Pharmaceutical Sciences. 98:2909-2934 (2009).

7.   J.G. Barnard, Singh, S., Randolph, T. W., Carpenter, J. F. Subvisible Particle Counting Provides a Sensitive Method of Detecting and Quantifying Aggregation of Monoclonal Antibody Caused by Freeze-Thawing: Insights Into the Roles of Particles in the Protein Aggregation Pathway. Journal of Pharmaceutical Sciences. 100:492-503 (2011).

8.   W. Jiskoot, Randolph, T. W., Volkin, D. B., Middaugh, C. R., Schoneich, C., Winter, G., Friess, W., Crommelin, D. J. A., Carpenter, J. F. Protein instability and immunogenicity: Roadblocks to clinical application of injectable protein delivery systems for sustained release. Journal of Pharmaceutical Sciences. 101:946-954 (2012).

9.   J.G. Barnard, Babcock, K., Carpenter, J. F. Characterization and quantitation of aggregates and particles in interferon- products: Potential links between product quality attributes and immunogenicity. Journal of Pharmaceutical Sciences. 102:915-928 (2013).

10.   J.S. Philo. Is any measurement method optimal for all aggregate sizes and types? AAPS Journal. 8:E564-E571 (2006).

11.   J.F. Carpenter, T.W. Randolph, W. Jiskoot, D.J.A. Crommelin, C.R. Middaugh, and G. Winter. Potential Inaccurate Quantitation and Sizing of Protein Aggregates by Size Exclusion Chromatography: Essential Need to Use Orthogonal Methods to Assure the Quality of Therapeutic Protein Products. Journal of Pharmaceutical Sciences. 99:2200-2208 (2010).

12.   B. Demeule, Palais, C., Machaidze, G., Gurny, R., Arvinte, T. New methods allowing the detection of protein aggregates A case study on trastuzumab. MAbs Journal. 1:142-150 (2009).

13.   L.O. Narhi, Jiang, Yijia, Cao, Shawn, Benedek, Kalman, Shnek, Deborah. A Critical Review of Analytical Methods for Subvisible and Visible Particles. Current Pharmaceutical Biotechnology. 10:373-381 (2009).

14.   S. Cao, Y. Jiang, and L. Narhi. A Light-obscuration Method Specific for Quantifying Subvisible Particles in Protein Therapeutics. Pharmacopeial Forum. 36:10 (2010).

15.   S. Zölls, Tantipolphan, R., Wiggenhorn, M., Winter, G., Jiskoot, W., Friess, W., Hawe, A. Particles in therapeutic protein formulations, Part 1: Overview of analytical methods. Journal of Pharmaceutical Sciences. 101:914-935 (2012).

16.   V. Filipe, A. Hawe, J.F. Carpenter, and W. Jiskoot. Analytical approaches to assess the degradation of therapeutic proteins. Trends in Analytical Chemistry. 49:118-125 (2013).

17.   Z. Hamrang, N.J.W. Rattray, and A. Pluen. Proteins behaving badly: emerging technologies in profiling biopharmaceutical aggregation. Trends in Biotechnology. 31:448-458 (2013).

18.   A. Hawe, Schaubhut, F., Geidobler, R., Wiggenhorn, M., Friess, W., Rast, M., de Muynck, C., Winter, G. Pharmaceutical feasibility of sub-visible particle analysis in parenterals with reduced volume light obscuration methods. European Journal of Pharmaceutics and Biopharmaceutics. 85:1084-1087 (2013).

19.   T. Werk, Volkin, D. B., Mahler, H. C. Effect of solution properties on the counting and sizing of subvisible particle standards as measured by light obscuration and digital imaging methods. European Journal of Pharmaceutical Sciences. 53:95-108 (2014).

20.   V. Filipe, Hawe, A., Carpenter, J. F., Jiskoot, W. Analytical approaches to assess the degradation of therapeutic proteins. Trends in Analytical Chemistry. 49:118-125 (2013).

21.   D.C. Ripple, Dimitrova, M. N. Protein particles: What we know and what we do not know. Journal of Pharmaceutical Sciences. 101:3568-3579 (2012).

22.   H. Zhao, M. Diez, A. Koulov, M. Bozova, M. Bluemel, and K. Forrer. Characterization of aggregates and particles using emerging techniques. In H.-C. Mahlerand W. Jiskoot (eds.), Analysis of aggregates and particles in protein pharmaceuticals, Wiley & Sons, Inc., 2012, pp. 133-167.

1.8 SUPPLEMENTARY MATERIAL
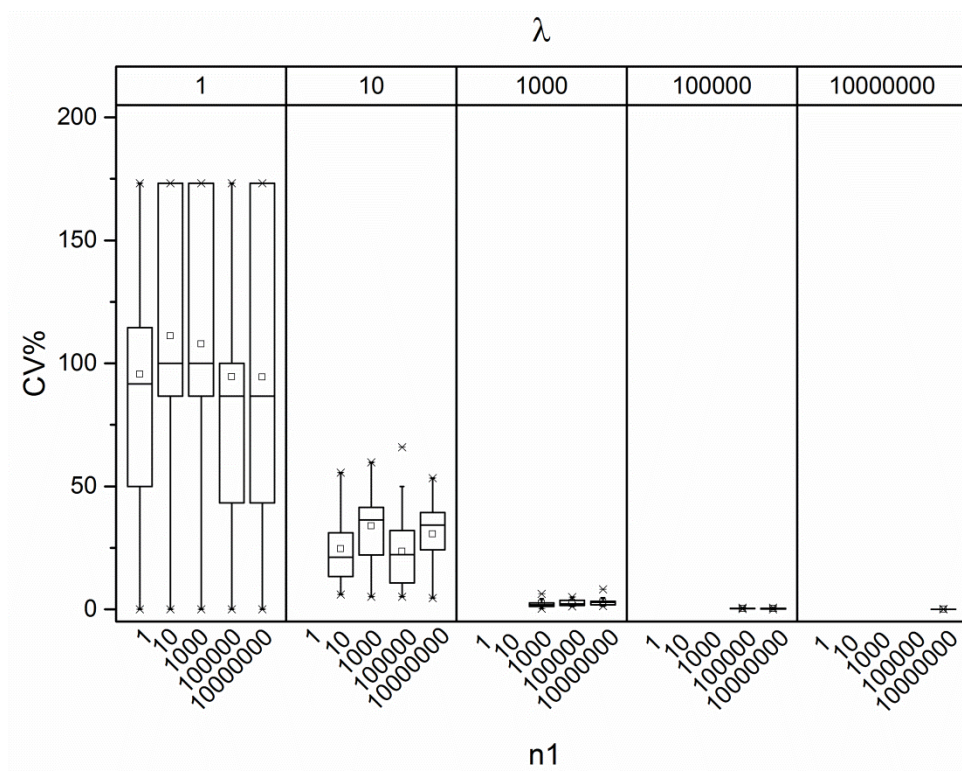
Figure S1.1 Boxplot of CV%, each estimated from 3 random values based on a Poisson distribution with expected number of particles λ and originating number of particles n1
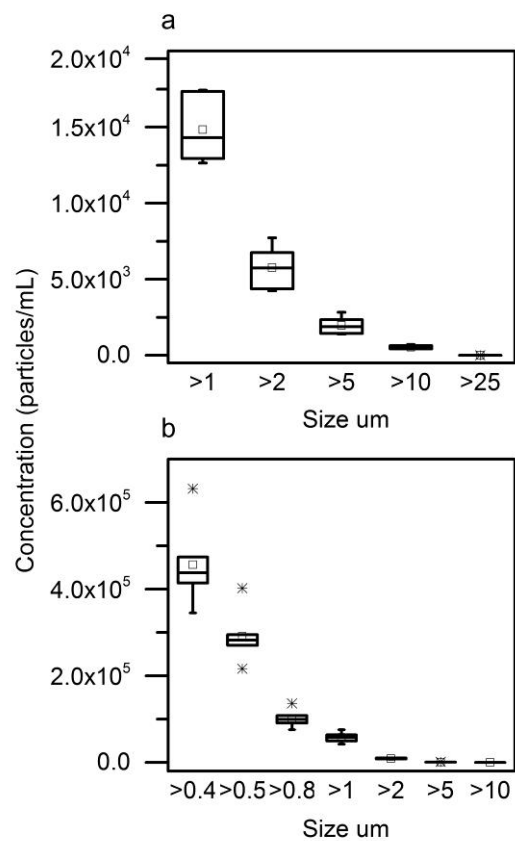
Figure S1.2 Pool variability in HIAC and CC. Variability of six independent and identically prepared pools of 10 units of PFS measured in HIAC (a) and CC (b). The large pool size originates low variability in the measurements
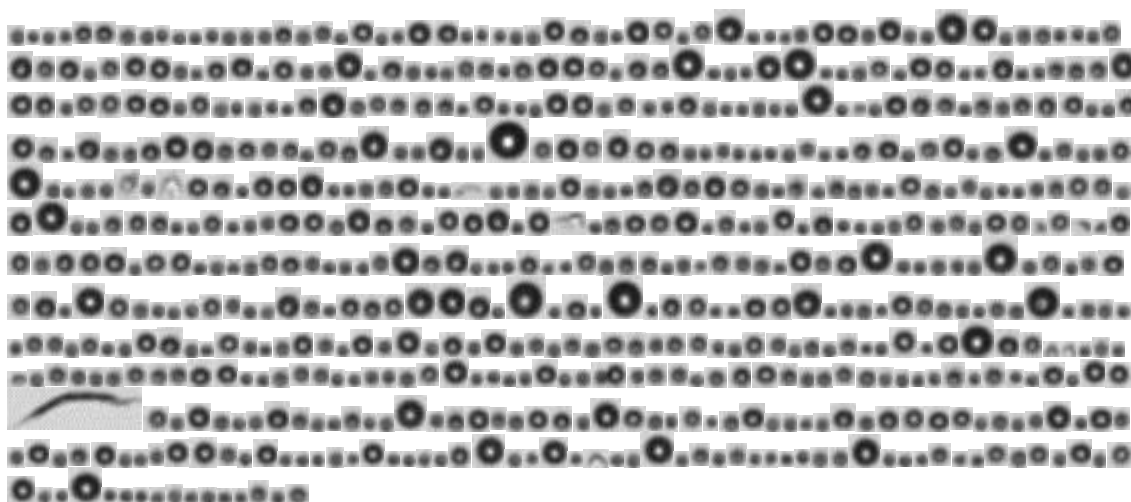
Figure S1.3 Collage of randomly selected MFI image and larger than 5 μm of the protein product used in this study. Mainly silicon oil-like particles can be observed

Table S1.1 Precision assessment of subvisible particle measurements using a low-concentration protein therapeutic product in pre-filled syringe Data is expressed in particles per mL

	Size um	Analyst 1[1]						Analyst 2						Overall[2]		
		run 1	run 2	run 3	average	std	CV%	run 1	run 2	run 3	average	std	CV%	average	std	CV%
HIAC	>2	6.49E+03	6.37E+03	6.72E+03	6.53E+03	173.9234	3	2.58E+03	2.58E+03	2.50E+03	2.55E+03	51.09795	2	4.54E+03	2178.937	48
	>5	2.40E+03	2.30E+03	2.26E+03	2.32E+03	70.46512	3	8.89E+02	8.52E+02	8.30E+02	8.57E+02	29.8161	3	1.59E+03	802.4135	51
	>10	4.82E+02	4.49E+02	4.22E+02	4.51E+02	30.04996	7	2.36E+02	1.99E+02	2.23E+02	2.19E+02	18.77054	9	3.35E+02	128.8525	38
	>25	1.20E+01	9.00E+00	9.00E+00	1.00E+01	1.732051	17	1.00E+01	6.00E+00	6.00E+00	7.33E+00	2.309401	31	8.67E+00	2.33809	27
MFI	>1	4.11E+04	4.23E+04	4.27E+04	4.21E+04	844.6238	2	1.52E+04	1.57E+04	1.57E+04	1.55E+04	312.3694	2	2.88E+04	14542.05	50
	>2	1.79E+04	1.92E+04	1.97E+04	1.89E+04	907.8044	5	5.88E+03	5.77E+03	5.85E+03	5.83E+03	60.56553	1	1.24E+04	7196.393	58
	>5	3.25E+03	3.78E+03	4.18E+03	3.74E+03	464.1802	12	1.14E+03	1.03E+03	1.16E+03	1.11E+03	68.94632	6	2.42E+03	1469.382	61
	>10	3.06E+02	5.37E+02	5.26E+02	4.56E+02	130.1428	29	1.61E+02	1.93E+02	1.79E+02	1.77E+02	16.40973	9	3.17E+02	173.8577	55
	>25	3.28E+00	1.64E+00	1.64E+00	2.19E+00	0.946854	43	1.64E+00	1.64E+00	4.92E+00	2.73E+00	1.893709	69	2.46E+00	1.372122	56
CC	>0.4	6.96E+05	6.24E+05	6.97E+05	6.72E+05	41895.39	6	6.05E+05	6.27E+05	6.22E+05	6.18E+05	11363.54	2	6.45E+05	40422.14	6
	>0.5	2.70E+05	2.73E+05	2.75E+05	2.73E+05	2657.693	1	4.11E+05	4.27E+05	4.24E+05	4.21E+05	8337.266	2	3.47E+05	81324.5	23
	>0.8	80150	82090	84830	8.24E+04	2351.368	3	1.69E+05	1.74E+05	1.73E+05	1.72E+05	2672.702	2	1.27E+05	49133.03	39
	>1	42220	44200	46660	4.44E+04	2224.32	5	1.00E+05	1.04E+05	1.06E+05	1.03E+05	2793.445	3	7.37E+04	32270.6	44
	>2	6273	6131	6276	6.23E+03	82.86334	1	16050	16540	16200	1.63E+04	251.0644	2	1.12E+04	5499.851	49
	>5	420	388.9	380	3.96E+02	21.00167	5	1199	1279	1219	1.23E+03	41.63332	3	8.14E+02	458.863	56
	>10	40	0	0	1.33E+01	23.09401	173	40	108.9	40	6.30E+01	39.77943	63	3.82E+01	39.81627	104

[1] Repeatability assessment
[2] Intermediate precision assessment
[3] E8 particles/mL

Table S1.1 *(continuation)*

	Size um	Analyst 1[1]						Analyst 2						Overall[2]		
		run 1	run 2	run 3	average	std	CV%	run 1	run 2	run 3	average	std	CV%	average	std	CV%
	>0.3	1.67E+05	9.65E+04	1.15E+05	1.26E+05	36552.47	*29*	1.10E+05	7.44E+04	2.08E+05	1.31E+05	69186.13	*53*	1.28E+05	49553.62	*39*
	>0.4	1.67E+05	9.65E+04	1.15E+05	1.26E+05	36552.47	*29*	1.10E+05	7.44E+04	2.08E+05	1.31E+05	69186.13	*53*	1.28E+05	49553.62	*39*
RMM (+)	>0.5	1.65E+05	9.56E+04	1.10E+05	1.24E+05	36625.86	*30*	1.09E+05	7.38E+04	2.07E+05	1.30E+05	69023.28	*53*	1.27E+05	49543.46	*39*
	>0.8	2.47E+04	1.18E+04	1.09E+04	1.58E+04	7720.751	*49*	1.26E+04	1.05E+04	3.01E+04	1.77E+04	10761.2	*61*	1.68E+04	8443.143	*50*
	>1	7.55E+03	4.41E+03	2.95E+03	4.97E+03	2350.574	*47*	4.24E+03	2.73E+03	8.71E+03	5.23E+03	3109.7	*59*	5.10E+03	2469.4	*48*
	>0.3	1.01E+05	1.75E+04	4.58E+03	4.10E+04	52338.63	128	1.04E+05	1.77E+04	2.80E+04	4.99E+04	47134.17	94	4.55E+04	44810.78	99
	>0.4	6.23E+04	1.06E+04	3.26E+03	2.54E+04	32177.86	127	5.82E+04	9.41E+03	1.51E+04	2.76E+04	26678.49	97	2.65E+04	26463.04	100
RMM (-)	>0.5	2.51E+04	3.55E+03	1.22E+03	9.96E+03	13166.15	132	2.01E+04	2.93E+03	4.72E+03	9.25E+03	9438.904	102	9.60E+03	10253.1	107
	>0.8	7.44E+02	2.15E+02	0.00E+00	3.20E+02	382.8842	120	3.20E+02	0.00E+00	1.05E+02	1.42E+02	163.1206	115	2.31E+02	280.6932	122
	>1	3.19E+02	0.00E+00	0.00E+00	1.06E+02	184.1747	173	2.07E+02	0.00E+00	1.05E+02	1.04E+02	103.5036	100	1.05E+02	133.6225	127
	>0.05	268.1198	246.736	280.991	2.65E+02	17.30289	7	343.3306	413.6359	314.6525	3.57E+02	50.92963	14	3.11E+02	60.76427	20
	>0.2	79.92221	50.10522	100.6841	7.69E+01	25.42418	33	19.57352	81.48103	47.48463	4.95E+01	31.00356	63	6.32E+01	29.46388	47
	>0.3	14.29503	9.372155	19.16112	1.43E+01	4.894508	34	2.340979	37.67165	7.930685	1.60E+01	18.99134	119	1.51E+01	12.43877	82
NTA[3]	>0.4	6.605697	1.742749	2.946583	3.77E+00	2.532673	67	0.735303	15.88422	2.490145	6.37E+00	8.28624	130	5.07E+00	5.662694	112
	>0.5	5.123745	0.455044	0.806469	2.13E+00	2.599972	122	0.482311	4.688885	1.295921	2.16E+00	2.231197	104	2.14E+00	2.166901	101
	>0.8	0.518275	0	0.33719	2.85E-01	0.263027	92	0.17525	0.22539	0.139476	1.80E-01	0.043157	24	2.33E-01	0.178138	77
	>1	0.036138	0	0.189032	7.51E-02	0.100346	*134*	0.049556	0.075002	0.004286	4.29E-02	0.035818	*83*	5.90E-02	0.069643	*118*

[1] Repeatability assessment
[2] Intermediate precision assessment
[3] E8 particles/mL

CHAPTER 2

Factors Governing The Accuracy Of Sub-Micrometer Particle Counting Methods

Anacelia Ríos Quiroz
Michael Adler
Joerg Huwyler
Hanns-Christian Mahler
Roland Schmidt
Atanas V. Koulov

2.1 ABSTRACT

A number of new techniques for particle characterization in biotechnological products have emerged in the last few decades. Although the pharmaceutical community is actively using them and many applications can be found in scientific literature, little is known about the analytical performance of these tools. With the aim of increasing our knowledge and understanding of said instruments, we have performed a systematic evaluation of the accuracy of the most commonly used particle counting instruments. Our results showed a marked, over-counting effect especially for low concentrated samples and particles fragile in nature. Furthermore, we established the relative sample size distribution as the most important contributor to an instrument's performance in accuracy counting. The smaller the representation of a particle size within a solution, the more difficulty the instruments had in providing an accurate count. A more thorough understanding of the capabilities of the different particle counting methods here provided will help correct the applicability and the results interpretation in particle assessment studies.

2.2 INTRODUCTION

Particulate matter is an important quality attribute of parenteral pharmaceutical formulations (1, 2). Lately, due to the new challenges that the emergence of biotechnological products have provoked, the assessment of particles in this type of products has received further attention (3-5). Specifically, concerns had been raised about the possible clinical relevance of protein particles in the submicron range (6-8). It is necessary to have analytical tools capable of the assessing and characterizing particles smaller than the current < 10 μm and < 25 μm limits established in the USP <788> and other harmonized compendial methods.

In the last decade, several instruments have been developed (or adapted) to monitor particles and to possibly support pharmaceutical development or even quality control (9-11). The most popular technologies available to date are NanoSight (Nano Tracking Analysis) (12, 13); Archimedes (Resonant Mass Measurement) (14-17); Coulter Counter (Electro Zone Sensing) (18, 19); Micro Flow Imaging and Flow Cam (Flow Imaging Microscopy) (20-25). However, each one of those emerging techniques tracks and explores different properties of the particulate matter in order to provide size and count information. Consequently, the different technical principle of each methodology implies different outcomes, both in terms of analytical performance (this and Chapter 1) and particle assessments (11). For example, whereas NanoSight combines light scattering with video recording of the Brownian motion of single particles; Archimedes uses frequency shifts and particle density values to estimate the weight of each particle. For a given sample, a hypothetical increase in viscosity will produce an apparent increase in size in NanoSight (particles would move slower) whereas the same change will produce an apparent decrease in Archimedes (particles would produce a smaller frequency shift). Although both methodologies can possibly account for such artefacts, it is important to notice that each technique will be affected in a different extend by the same given properties of the sample and by specific artefacts. Even when those two methodologies share a similar size range, the particle assessment performed by various methods will not necessarily compare. The latter highlights the importance of constructing a complete understanding of the analytical performance abilities of particle counting methodologies.

Some partial attempts had been made trying to evaluate the individual methods performance (12, 13, 17-19, 22-32), but to date no systematic analysis including a comparison between all the different methods using a number of different standard systems has been carried out. Recently, we reported "A Case Study With A Low-Concentration Therapeutic Protein Product In A Prefilled Syringe" ([Chapter 1](#)) describing the precision of the previously mentioned analytical tool box. The aim of the present paper, in contrast, is to study their accuracy. For the first time we took a realistic and integrative approach to evaluate the accuracy performance of sub-micron methods in a detailed and systematic fashion. Due to concerns

2.3 MATERIALS AND METHODS

Particle generation

Bovine serum albumin (BSA Sigma Aldrich; USA) MW ~67 kDa, formulated with phosphate buffer (DPBS 10x, GIBCO; UK) at 30 mg/mL as well as a monoclonal antibody (mAb) Roche Property calculated MW ~149 kDa, formulated with 51 mM sodium phosphate, 60 mg/ml trehalose dehydrate and 0.04% polysorbate 20 at ca 25 mg/mL were used as model proteins in our studies. Additionally, latex bead standards (Duke Standards; ThermoScientific, USA) were tested.

To generate sufficient amounts of protein particles, proteins were artificially stressed. For the ***BSA*** particles, BSA formulation was initially filtered through a 0.22 μm filter membrane (Millex GB PVDF membrane, Millipore; Ireland). A 50 mL tube (SARSTEDT; Germany) with 30 mL of protein solution was heated to 73 °C for 30 minutes using a Thermostat station (Eppendorf, Germany). The resulting solution was diluted 1:10 to a total volume of 10 mL with PBS 1x (DPBS 1x, GIBCO; UK) and homogenized by vortexing (VWR; Belgium). After centrifugation (Centrifuge 5810R, Eppendorf; Germany) at 1200G for one minute, the supernatant was collected and either the sample was used as initial micrometer-enriched stock or a nanometer-enriching procedure followed. For the ***mAb model A*** particles, mAb formulation was diluted 1:10 in PBS 10x (DPBS 10x, GIBCO; UK) followed by filtration through 0.22 um filter membrane (Millex GB PVDF membrane, Millipore; Ireland). Several 1.5 mL particle-free Eppendorf tubes (Biopure; Eppendorf; Germany) were filled with 1.3 mL of protein formulation using Eppendorf multippipete (Multippete stream, Eppendorf;

Germany) and 50 mL Combitips (Biopure, Eppendorf; Germany) at the slowest take-in and take-out speed. A Thermostat station (Eppendorf, Germany) was used to apply 73 °C heat stress for 7 minutes. A total of 24 tubes were pulled and either the sample was used as initial micrometer-enriched stock or a nanometer-enriching procedure followed. For the *mAb model B* particles, mAb formulation was initially filtered through 0.22 um filter membrane (0.22 µm PVDF Stericup, Millipore; USA). Several 1.5 mL Eppendorf tubes (Biopure; Eppendorf; Germany) were filled with 1.0 mL of protein formulation using Eppendorf multippipete (Multippete stream, Eppendorf; Germany) and 50 mL Combitips (Biopure, Eppendorf; Germany) at the slowest take-in and take-out speed. A Thermomixer station (Eppendorf, Germany) was used to apply 80 °C heat and 1400 rpm shake stress for 3 minutes. Using a silicon oil free 5 mL syringe (Norm-Ject luer lock; HSW, Germany) and a 27 G x 1½″ needle (100 Sterican; Braun, Germany), the volume of each tube were sucked in and out 20 times and collected in 2 mL Eppendorf tubes (Biopure, Eppendorf; Germany). After centrifugation at 540 G for one minute, the supernatant fractions of 24 tubes were collected and a final centrifugation step of 1200 G for 1 minute was applied. Either the sample was used as initial micrometer-enriched stock or a nanometer-enriching procedure followed. For the *latex bead* samples ThermoScientific size certified standards of different sizes were mixed in a proper ratio in water or isotone (Beckman Coulter Inc) to reach concentration and size distribution similar to that of the protein particles in the nano- and micrometer-enriched stocks. Depending on the size range specification for every instrument in the study, either a nano- or a micrometer-enriched stock was used.

Stock characterization

For the micrometer-enriched stock, samples were used in their original composition after the stress procedure. For the nanometer-enriched stock, filtration through 1.02 um filter (Acrodisc Versapor membrane; PALL Corp, USA) was combined with centrifugation steps until a suitable stock was produced not containing any large species. In all cases, the initial stocks were translucent solutions without visible particles. Vendor information of maximum concentration limits was considered to adjust initial instrument-specific stock counts. All the stocks were generated the day of analysis and were kept in lab conditions during each experiment. All the used material was extensively rinsed with particle free water (in house generated by several filtration (0.22 µm Millex GB PES membrane,

Millipore; Ireland) and degassing steps (Liquicel Membrane Contactors, Membrana; Germany) of bidestilated water)) and dried with filtered (0.22 um Millex GB PES membrane, Millipore; Ireland) air. For light obscuration (HIAC) and flow imaging instruments (MFI and FC), the micrometer enriched stock of the correspondent particle type was prepared. For electro zone sensing (Coulter Counter), resonant mass measurements (Archimedes) and nano tracking analysis (Nano Sight), a nanometer enriched stock was prepared.

Dilution procedure

Initial particle concentration of every stock was obtained measuring the stock in every single instrument per day of analysis. Several dilutions of the proper stock were prepared and measured in triplicate immediately after aliquoting that same day of stress. Dilutions were calculated in an instrument- and particle-specific way to achieve particle counts ranging from 10^1 to 10^8 particles per mL (with 4 target points per order of magnitude: 1.0, 2.5, 5.0 and 7.5) according to the specifications of each methodology. Final volumes of the dilutions were set considering: 1) minimum instrument requirements to assure at least triplicate measurements; 2) aliquot volume of at least 1 µL for easy handling with normal lab pipets; 3) dilution factor (DF) limits of 1.250 < DF > 50000.000 for the linearity experiments and 1.250 < DF < 500 for recovery experiments. Such dilution limits provided good profiles when non-stressed mAb formulation was diluted and protein in solution was then followed by UV-Vis absorption spectrometry as described later in the *Results* section. The assumption was applying the same handling procedure to the dilution of particles would lead to the isolation of particle- and instrument-related response, minimizing dilution artefacts. Dilutions were made and immediately measured in increasing concentration sequence. Aliquots were always taken from the initial stock. Stock stability was assessed by following the particle counts and size distribution at the beginning and at the end of each day's experiment allowing CV variations <15 %. Diluent solution was the correspondent fresh, particle-free and non-stressed protein solution (or water in the case of latex beads). For a given instrument and target concentration, the proportion stock:diluent was kept comparable along the different particle types.

Accuracy assessment

The average of the three experimental measurements was compared to the theoretical concentration and the ratio was expressed as a percentage. The recovery profile (one for each type of particle and analytical methodology) was built by plotting theoretical concentrations versus recovery percentage values. The initial approach considered all cumulative counts above the instrument's lower size limit of detection as follows: >0.03 μm for NTA; >0.2 μm for Archimedes; >0.60 μm for CC; >1.00 μm for MFI and FC; and >2.00 μm for HIAC. Additionally, a size-wise analysis considered cumulative particle counts in certain bins as follows: >0.03 μm, >0.05 μm, >0.2 μm, >0.3 μm, >0.4 μm and >0.5 μm for NTA; >0.2 μm, >0.3 μm, >0.4 μm and >0.5 μm >0.8 μm for RMM; >0.4 μm, >0.5 μm, >0.8 μm and >1 μm >2 μm and >5μm for CC; >1.00 μm, >2 μm, >5 μm, >10 μm and >25μm for MFI and FC; and >2.00 μm, >5 μm, >10 μm and >25 μm for HIAC.

Linearity assessment

The average of the three experimental measurements was plotted against the theoretical concentration. Data points were fit using linear regression analysis. For detailed evaluation, the linearity of the corresponding method was assessed considering the full concentration range studied and also by order of magnitude. Data was plotted using radar representations. Each linear fit parameter is represented in one axis of the radar plot. Scales were adapted to be common for all the instruments so that the better linear fit is represented by the smaller radar plot depicted area pointing to the r^2 axis.

Light obscuration, HIAC

A ROYCO System 9703, sensor HRLD400HC (Pacific scientific, New Jersey, USA) was used with a small volume method. Rinsing volume was set to 0.4 mL and 4 runs of 0.4 mL each were performed (sample volume was minimum 3 mL). Flow rate was set to 10 mL/min. The first run was discarded and the average ± standard deviation of the last three runs was reported. Blank measurements were performed at the beginning of the tests and in between family of samples (order of magnitude-based) using fresh particle-free water. The acceptance criterion for blanks was less than 5 particles > 1 μm. The suitability test per day of experiments consisted of the measurement of count standards of 2, 5 and 10 μm (COUNT-CAL Count Precision Standards, ThermoScientific; USA) with acceptance limits of ± 10% of the reported concentration for particles bigger than 1.3, 3.0 and 5 μm, respectively.

Micro flow imaging, MFI

A DPA 4052 instrument from Protein Simple was used. Cleanness of the 100 um flow cell was achieved every day of measurement by rinsing with 1% Tergazyme (Alconox Inc.; USA) solution for two minutes at maximum speed, soaking for one minute and finally flushing with particle free water for five minutes. Method parameters were set to 1 mL sample volume as termination type, 0.2 mL as purge volume, with "edge particle rejection" as well as "fill particle" options activated. The light optimization step was performed with the correspondent filtrated sample matrix. Either single or three independent runs of the same dilution were performed for blanks and particle samples, respectively. Blank measurements were performed at the beginning of the measurements and in-between family of samples (order of magnitude-based) using either fresh particle-free water (for latex standards) or fresh unstressed formulations (for protein particles). Acceptance criteria for blanks was less than 100 particles per mL > 1um. The suitability test per day of experiment involved 1) measurement of 5 µm count standards (COUNT-CAL Count Precision Standards, ThermoScientific; USA) with acceptance limits of ± 10% the reported concentration for particles >3 µm and 2) measurement of 5 µm size standard with acceptance limits of ECD mean of ± 25% the reported size and standard deviation <0.4.

FlowCam, FC

A benchtop model from Fluid Imaging Technologies was used. Camera parameters with a 10x magnification objective were set to 14 and 25 as threshold values for the dark and bright pixels, respectively. Camera rate was set at 20 frames per second. Sample volume was 1 mL using 0.2 mL for manual initial purge and background measurement. Any other parameter for the system suitability test and blank measurements were kept as those described for MFI measurements.

Coulter counter, CC

A CC4 model of Beckman Coulter with a 30 um aperture tube was used. For mAb particles, stock conductivity was enhanced by adding 4 µl/mL of a saturated NaCl solution to final conductivity values of ~16 mS. Stocks of BSA and latex particles were used without further modification since their correspondent PBS and isotonic matrix, respectively, allowed for acceptable conductivity values ~18 mS. The electrolyte jar was filled with the same buffer solution as that of sample's matrix. Method parameters were set to volume analysed 50 µl, consecutive runs 3, current 600 and gain 4. Aperture

tube cleanness was verified in between every sample with blank measurements <1000 particles/mL of isoton and unstressed formulations. The instrument was calibrated using 5 um size standards in the correspondent buffer with no more than 1% change to the accepted Kd values, (average of 5 independent determinations).

Resonant mass measurement, RMM, Archimedes

Resonant mass measurements were performed using Archimedes system (RMM0017 Generation 2) Affinity Biosensors, Santa Barbara, USA) equipped with a Hi-Q micro sensor. The sensor was calibrated using 1 μm Duke polystyrene size standards. The acceptance criterion was at least 90% of the particles within ± 10 % of the standard size. Prior to each sample, the system was rinsed as follows: matrix sample solution for two minutes, PCC54 detergent solution (ThermoScientific, Illinois, USA) for 2 minutes and particle-free water for ten minutes. A threshold of 0.04 Hz and 0.03 Hz for protein and polystyrene standards was applied, respectively. The data was collected and analysed using the software program ParticleLab version 1.8.570 (Affinity Biosensors, USA).

Nanoparticle Tracking Analysis, NTA

A NS200 instrument model LM20 from NanoSight with a 405 nm laser was used. The chamber was extensively flushed with filtered water (0.02 um (Anotop, Whatman) and cleanness was visually assessed using instrument's interface. Non-siliconized syringes (Norm-Ject, HSW, Tuttlingen, Germany) were used to load a 1 mL sample directly into the chamber. An initial volume of 0.6 mL was used to rinse out the flushing water, and with the remaining volume, three videos of 60 seconds were recorded using a replenished sample each time. Video recording settings were as follows: the best focus for a clear and sharp particle image was set. Starting from shutter equals to zero, this value was increased until no more new particles were visible on the screen. To avoid camera over exposition, the shutter was kept as low as possible. Starting for gain equals to zero, this value was increased until the contrast between the background and the particles was high and the actual particles were easily distinguished. To avoid the presence refractive rings, gain was kept as low as possible. A final slight adjustment of these three parameters together was made to obtain the best possible combination and the highest image quality. Among different runs of the same sample, strictly the same video-recording values were kept. Within series of samples, video-recording values were kept within narrow ranges but

higher importance was given to ensure all particles in a sample were tracked. The video analysis settings were as follows: the detection threshold value was set so that the software recognized every actual particle centre with a red cross. To avoid refractive rings interference, the blur value was set so that the area around every particle was clear and without the presence of noise particles (blue crosses). The applicability of these two settings was optimal throughout the video footage. The minimum track length was set to ten. The minimum expected particle size was set to automatic so that the software calculated it regarding the first 100 tracks. Considering all videos coming from the same sample were recorded under the same video quality settings, video analysis settings were also kept the same and batch analysis was performed. During measurement, temperature was recorded by a temperature sensor contained in the viewing unit. Sample viscosity was determined using a cone rheometer instrument (Anton Paar AG Switzerland, Zofingen, Switzerland) at 29 and 23 Celsius degrees. Viscosity values in steps of 0.1°C were interpolated and product-specific viscosity tables were loaded into the instrument's software. During video analysis, the proper viscosity values were automatically selected from previously loaded user viscosity tables

2.4 RESULTS AND DISCUSSION

Particle models
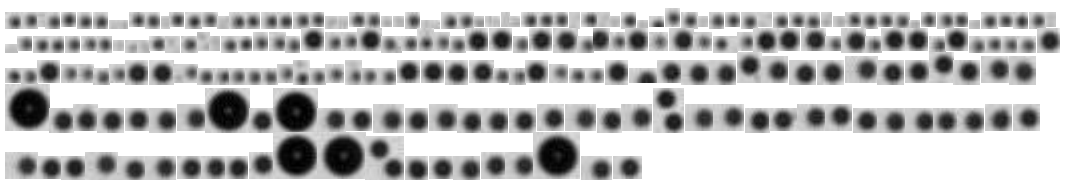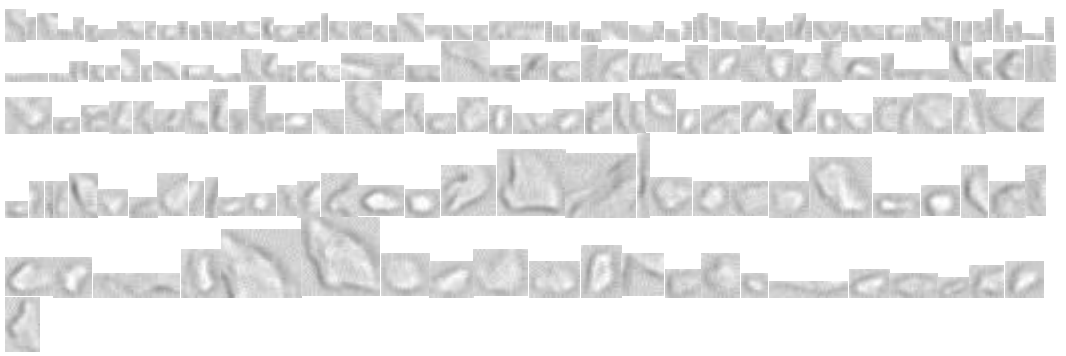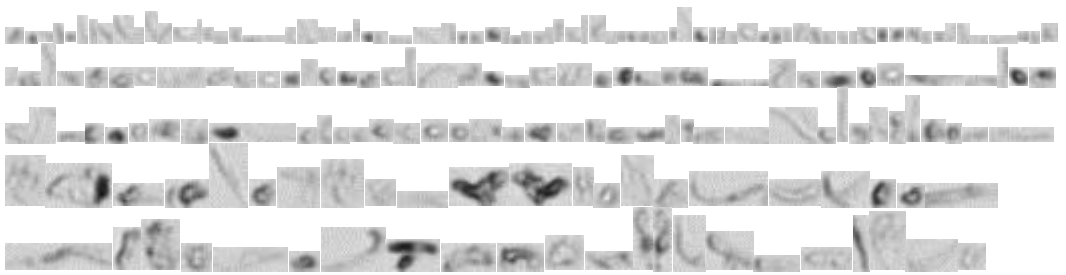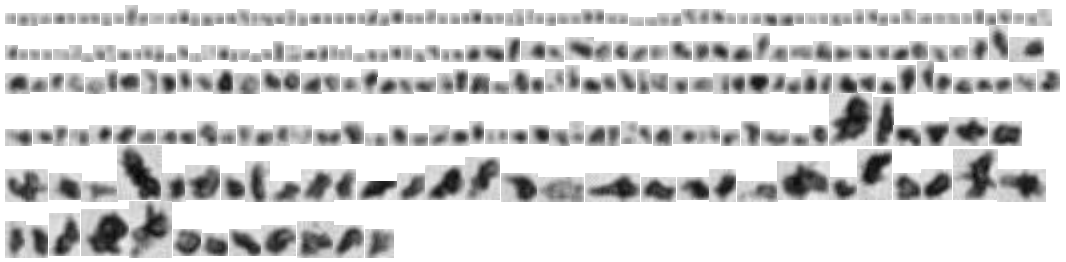
To identify morphology-related factors that may influence instrument performance, different particle models were generated. Typically used latex beads standards were used in a mixture of different sizes to mimic the heterogeneity of actual protein particle samples. In the best effort to generate particles under lab conditions, the applied stress to BSA and mAb formulations was unrealistically high. However, the generated samples showed characteristics of particle heterogeneity, matrix, morphology and pliability similar to actual protein particles in representative samples – although significantly higher in number. Table 2.1 shows randomly selected MFI images of the different particle models. In general, latex particles exhibited the characteristic round and dark shape whereas protein particles were highly amorphous. BSA and mAb-model A were both highly translucent with the former having better defined particle edges. In contrast, the higher stress applied to generate mAb-model B originated darker particles. Such characteristics, helped to challenge each of the instruments included in the

study. For example, the differences in translucency became a critical aspect for light obscuration and
flow imaging technologies.(33, 34) On the other hand, the different stress levels produced different
particle pliability that became interesting factor when performing dilutions.

Particle dilution

To overcome the lack of count standards in all the appropriate size and concentration ranges, dilutions
of well characterized samples had to be performed. To determine the best way to dilute particles, two
different schemes were tested. Scheme number 1 involved various intermediate stocks (a different one
per order of magnitude) and scheme number 2 used only one (so that all the aliquots were taken from

Table 2.1 Randomly selected and representative MFI images of the particle models used. To generate latex
samples, size standards were mixed. For the protein samples, different levels of heat stress were applied. In
contrast with the high sphericity of latex particles, protein particles are amorphous

Latex mixture	
BSA	
mAb model A	
mAb model B	

the same initial preparation). Using Fluorescein (as a model of a non proteinaceous and chromophore small molecule) and a non-stressed monoclonal antibody (mAb) formulation, dilutions were calculated following both dilution schemes to generate a broad set of samples covering five orders of magnitude Absorbance was then followed by SoloVPE technology and the concentration in mg/mL was directly obtained from the instrument. Performance of both dilution schemes were compared in terms of linear fit (intercept b, slope m, coefficient of correlation, r^2 and sum of squares total, SST) and confident intervals at 95%, with main focus in the lowest concentration ranges. Over the full concentration range both schemes correlated well with a linear fit (data not shown). However, a closer analysis per order of magnitude revealed for the lowest concentration range better m and r^2 values for scheme 2. This approach could require aliquot volumes as small as 1 µL and dilution factors as large as 5000 for the highest diluted samples, however it reduces the noise that can be introduced using several intermediate stocks. Hence, scheme 2 was chosen to dilute all the protein particles in the study. It allowed us to directly attribute observations to an instrument's performance, provided that dilution errors were shown to be minimized. Furthermore, several controls were also implemented (see also Materials and Methods): the size distribution of the stock solutions was noted at the beginning and at the end of the dilution series. Coefficients of variation values between initial and final concentration below 15% were considered as insignificant. This allowed for dilution set intra-comparability as all aliquots were taken from the same representative stock. This was the case for all the particles and instruments except for mAb-model A in MFI and FC; mAb-model B in MFI and FC; and latex beads in NTA (data not shown).

Accuracy of counting

In order to assess the factors governing the counting accuracy performance of different particle counting instruments, a highly integrative approach was taken. Important aspects like particle morphology, stability and size were considered. Dilutions of latex bead mixtures and artificially generated protein particles were prepared. That strategy helped to overcome the lack of count standards that i) covered the full concentration range of interest and ii) somewhat resembled the characteristics (morphology and size-wise) of relevant protein particle samples. Figure 2.1 shows the
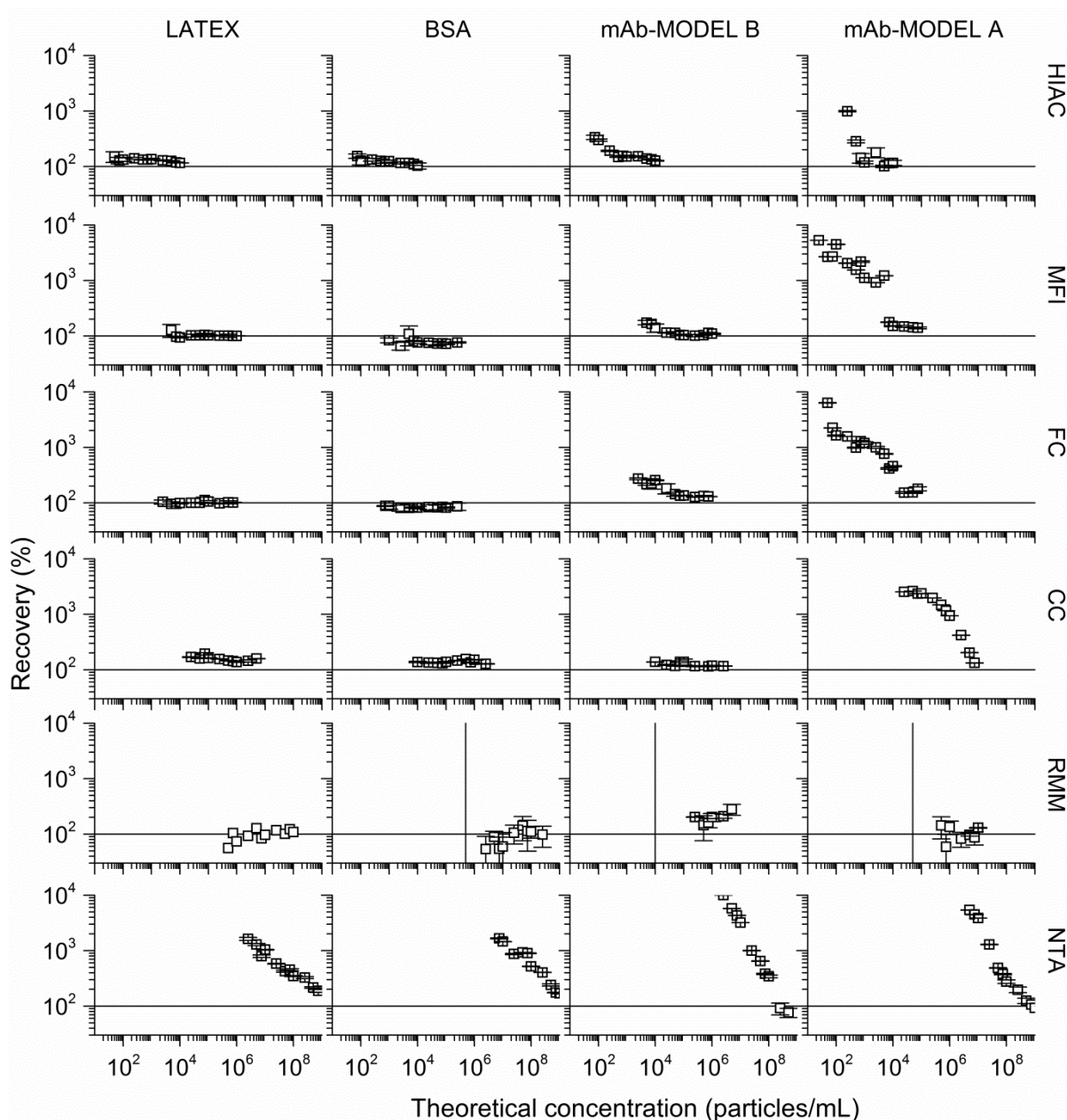
Figure 2.1 Accuracy of particle counting. The accuracy of eight different instruments was studied by following the recovery of four different particle models with a dilution scheme approach. Rows represent instruments ordered from top to bottom in micron to submicron and nano size ranges. Columns represent particle models ordered from left to right in comparatively decreasing levels of applied stress for its generation. Horizontal axes represent the theoretical particle concentration per mL of each independent sample of the dilution set. Vertical axes represent the calculated recovery, (theoretical concentration/experimental concentration*100), considering all counts above the instrument lower size limit of detection as follows: >0.03 μm for NTA; >0.2 μm for Archimedes; >0.60 μm for CC; >1.00 μm for MFI and FC; and >2.00 μm for HIAC. Ideal recovery of 100% is represented with the continuous horizontal line. For RMM, the vertical line indicates the lower limit of the concentration range studied and missing points

implies data not detected. For the rest of the instruments, missing points implies concentration not studied. Red symbols represent recoveries > 200%.

percentage ratio between the theoretical and experimental concentrations of each particle model (columns) and instrument (rows) included in the study. The experimental setup used in this research allowed for the detection of interesting factors governing accuracy performance of sub-micron methods. Results showed that the different particle nature of the models produced different recovery profiles. In general, the recovery % of total particle counts was good in the upper concentration ranges whereas a strong over-counting effect –mainly for the mAb particles– occurred in the lower concentration ranges. A more detailed evaluation on the recovery profiles demonstrated that, in most of the cases, instrument accuracy varied depending on the type of particle. Latex beads showed the best recovery profiles with a large majority of the values smoothly distributed around 100 % recovery (except for NTA). This confirmed the already established good performance of the instruments when measuring these typically used standard particles. Interestingly, the picture was different when using actual protein particles. Poorer profiles (recoveries >>> than 100%) were found i) as the particle nature changed from a high (and hence high optical density and particle stability) to lower level (and hence high translucency and pliability) of applied stress and ii) as the sample concentration decreased (except for RMM). It is important to note that the over-counting was more severe for the model mAb-A, which contained particles generated through the less severe stress level (as compare with model mAb-B and BSA). Since that model of particles is considered to be the most fragile the observed poor recovery can most likely be attributed to particle desintegration. In another interesting observation, for a given instrument, the starting concentration point of this striking over-counting effect varied depending on the particle model. That suggests that sample nature played an important role in the accuracy performance of the instrumentation. The over-counting here described, clearly reveals severe weaknesses in the accuracy performance of subvisible/submicron particle methods when realistic protein samples are measured (size-heterogeneous and proteinaceous samples). Most importantly, from a quality control point of view, this would lead to many false positive measurements.

Although dilution-related artefacts cannot be completely excluded as likely contributors to the poor accuracy at low concentrations, the exhaustive controls that were implemented (*see Materials and*

Methods section and further data not shown*)* severely limited their presence. Furthermore, the dilution methodology here implemented had already been successful reported in a previous publication (35). In another control, a series of fake dilutions (on which the same mixture proportions of stock : diluent was reproduced using only diluent) showed random recoveries (data not shown), whereas the results showed a clear tendency to higher recoveries. Finally, controls to exclude 1) likely dilution-induced artefacts and 2) sample polydispersity (in the case of latex particles) effects were also implemented. For 1) when counts standards were available (*i.e.* for 2, 5, 10 and 25 µm) the accuracy of counting was also analysed using the customary commercial and fixed concentration of 3000 particles/mL. This was also limited to those instruments in the micron size range. Results indicate good (> 95%) recoveries (not shown). For 2) the accuracy profile of latex dilutions of single sizes was also analysed. In this case, the overestimation of the counts that increased with every consecutive dilution was also observed (data not shown). Interestingly, as the initial concentration of this type of sample was not limited by the applied stress level as in the case of protein samples, much higher concentrations were possible to test. Results showed an undercounting effect that can be explained by sensor saturation (data not shown). However, the initial concentrations of the bead suspensions were calculated using the dry content of the suspensions as declared by the manufacturers. Such estimation may result in additional errors and present another important caveat when using this single-size approach means of the assessment. In conclusion, both previously described control experiments were not representative of the morphology, concentration and heterogeneity characteristics of the particles likely present in biotechnological products. These results showed that dilutions of (protein) particle-containing solutions are not recommended, unless a sound understanding of any instrument-specific effect is achieved and has been specifically qualified.

By visual assessment on plotted results, accuracy ranges can be defined per instrument and per particle type as shown in Table S2.1. However, these limits should not be considered as general. They just exemplify the application of a methodology that is useful in selecting, in a realistic product- and instrument-specific manner, the best accurate ranges for particle characterization. Below the indicated lower limits, all the instruments (except for RMM) demonstrated a propensity to over counting. This approach helps to overcome the difficulties that applying typical statistics would offer. For example,

there is little available data about the submicron particle burden of biotherapeutics. This is because of the limited application of subvisible particle analysis to the characterization and development stage not the routine quality control process. The former, in combination with the inherent product variability (1), can lead to unrealistically low control limits. The methodology here proposed is to define the lower limit of counting capabilities and also allow for the identification of important instrument-specific effects that were also encountered and will be discussed later in the corresponding section.

To further evaluate the root cause of the over-counting effect, in contrast with Figure 2.1 on which total particle counts were presented, a size-wise analysis was carried out to evaluate whether there was instrument accuracy (for a given particle model and instrument combination) bias towards specific size ranges (see Figure S2.1). Based on this representation, certain patters were identified and are presented in Figure 2.2 where both, stock concentration *(left axis)* and recovery percent *(right axis)* are plotted as a function of the particle size. Three different categories can be described: *Case I.* Good recovery along all the concentration ranges tested which do not vary with binned sizes. *Case II.* Recovery worsened as the sample concentration decreased and size bin increased. *Case III.* Poor recovery along all the concentration ranges tested, which did not vary with binned sizes. This important result highlights the impact that the relative size composition had on the method accuracy performance. Similarly, such an effect was already described in Chapter 1 on which the precision of particle counting instruments was also found to be sample-composition dependent. More importantly, as can be seen in Table 2.2, most of the recovery profiles described in Figure 2.1, fall into Case II (*see also* Figure S2.2) which implies that, not only instrument related artefacts, but also sample relative size composition has to be considered to interpret accuracy performance results.

Accuracy of sizing

The sizing accuracy of each method was evaluated using size standard polystyrene bead suspensions and is presented in Figure 2.3. The accuracy of sizing varied widely as a function of size, with all methods overestimating the size of the standards in their respective lower size range. For example, MFI overestimated the size of beads of 1 μm in diameter, CC overestimated the size of beads of 0.5 μm diameter, RMM overestimated the size of beads of 0.5 μm diameter and NTA
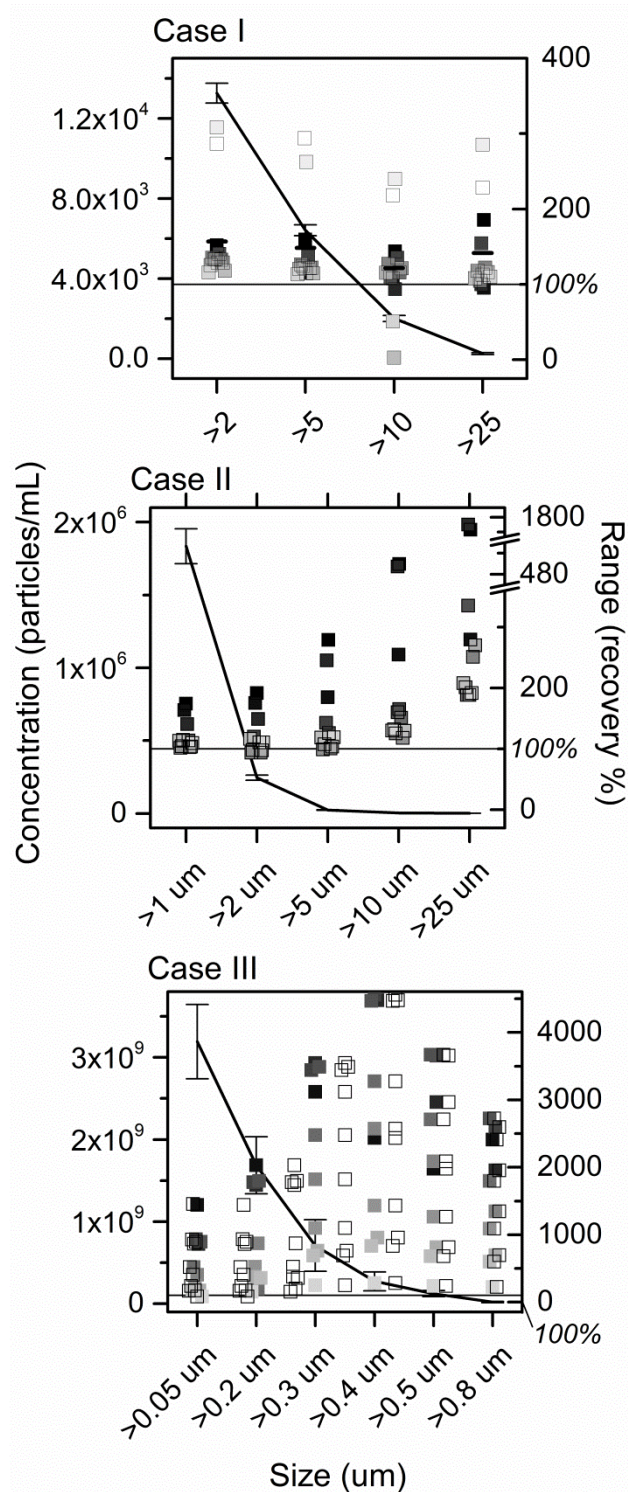
Figure 2.2 Identified categories that describe the relation between size distribution and method accuracy performance. The recovery profile presented in Figure 2.1 was analysed size wise and correlated with the size distribution of stocks from where dilutions were prepared. Horizontal axes represent cumulative size bins. Vertical left axes represent the particle concentration of the stock and error bars represent the related standard deviation of the measurements at the beginning and at the end of the experiment. Vertical right axes represent the recovery associated with each sample of the dilution set from high (black) to low concentration (red). Each panel exemplifies

typical encountered profiles that can describe the relation between accuracy and size distribution: Case I, accuracy is independent of particle concentration (ideal); Case II, better accuracy for those sizes with higher counts (inverse); Case III, poor accuracy

overestimated the size of beads of 0.05 μm diameter. Conversely, most methods underestimated the size of standards with diameters in the larger size range. In addition, the sizing accuracy in those sizes ends varied substantially as a function of concentration.

Linearity

The linearity assessment was carried out using the same four particle models and dilution approach previously described for the evaluation of the accuracy of counting. Analysis of all linear fit parameters (slope (m); intercept (b); regression coefficient (r^2) and sum of squares total (SST)) together in a radar plot representation offered a better insight on the instruments' linear performance. Similarly to the counting accuracy profiles, linearity assessment also showed differences depending on the type of particle analysed. However, general observations can be made based on instrument type. As indicated in Figure 2.4, by the smaller radar plot area pointing to the r^2 axis, the micron methods HIAC, MFI and FC showed better linearity performance than the submicron methods CC, RMM and NTA. With a more detailed evaluation of the linearity by order of magnitude, specific concentration ranges can be defined by each instrument and particle type. For example, while in the CC instrument the linear range for latex beads (considering $r^2 > 0.9$ and $m < 10$) was from 10^3 to 10^5 particles/mL, the mAb-model A particles range appeared to be narrower covering just concentrations as high as 10^5 particles/mL (see Figure S2.3a and Figure S2.3d). As already described for the accuracy assessment, poorer linear profiles were found i) as the particle nature changed from higher to lower levels of applied stress and ii) as the sample concentration decreased. As in the case of the accuracy lower limits proposed in Table S2.1, these linear ranges should not be interpreted as general but as the result of this specific experimental setup used to exemplify an integrative and realistic method evaluation approach.

Use of the instruments as complementary analytical techniques

All in all, not only the previously described accuracy and linear ranges of the instruments were different between particle types, but the particle measurements also displayed major discrepancies, as already observed in a previous stability study (see Chapter 1). These observed variations may have

different sources including instrument analytical deficiencies. The variety of methods investigated determined the reported particle size by assessing very different physical properties of the particle standards used for calibration. The accuracies of these methods are thus affected to varying degrees by the specific attributes of the polystyrene spheres. This difference is expected to affect the analysis of protein particles to an even greater degree, leading to substantial method-inherent differences in the total number of particles reported. Whilst the future availability of a protein or protein-like standard may allow different calibration procedures of these methods (possibly leading to an increase in accuracy), it is important to notice that sub visible particle instruments are frequently changing and both hardware and software- are constantly being updated. Aiming to improve analytical performance, there is currently a pump available for the NTA system (although in our experience it did not improve the performance of the method, see

Table 2.2 Based on the cases presented in Figure 2.2, the size-dependent accuracy response of each particle model and instrument combination was categorized.

Instrument	Particle model	Case I	Case II	Case III
HIAC	Latex	X		
	BSA		X	
	mAb-model B		X	
	mAb-model A			X
MFI	Latex	X		
	BSA		X	
	mAb-model B		X	
	mAb-model A		X	
FC	Latex	X		
	BSA		X	
	mAb-model B		X	
	mAb-model A		X	
CC	Latex		X	
	BSA		X	
	mAb-model B		X	
	mAb-model A		X	
RMM	Latex		X	
	BSA		X	
	mAb-model B		X	
	mAb-model A		X	
NTA	Latex		X	
	BSA			X
	mAb-model B		X	
	mAb-model A		X	
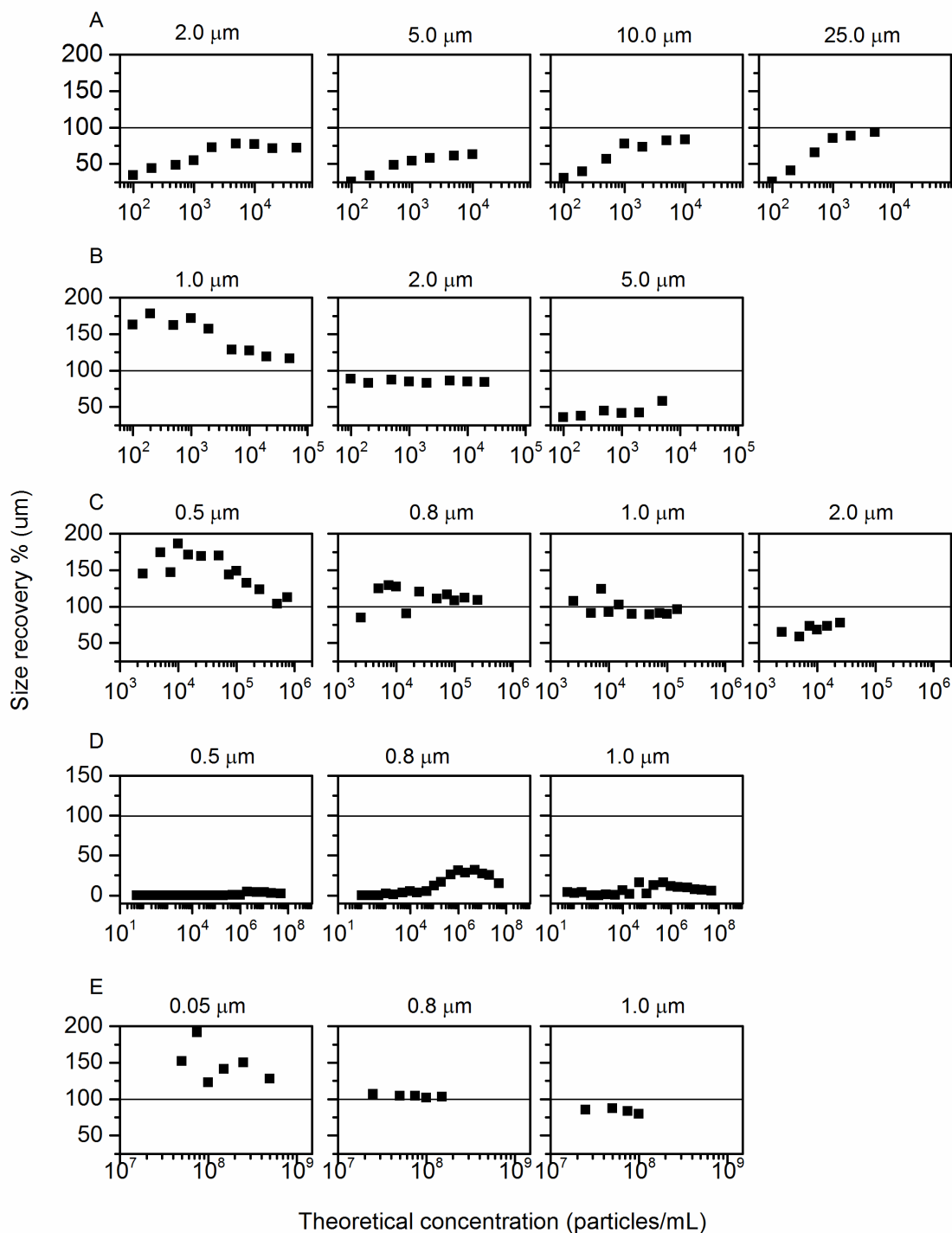
Figure 2.3 Size accuracy of A) HIAC, B) MFI, C) CC, D) RMM and E) NTA instruments with polystyrene of different sizes as indicated in the header of every panel

Chapter 4) and the incorporation of statistical tools for better particle classification using flow imaging technologies. Furthermore, although the "submicron gap" has been covered; a complete particle characterization (including micron and submicron size range) will synthesize the information coming from various instruments. Understanding their different principles, in addition to the assorted inherent

factors governing their performance, is essential if we are to fully understand to what extent they complement one another. To further this knowledge, Figure 2.5 shows the recovery percentage of four selected points of the dilution set of latex (Figure 2.5A) and mAb-model B (Figure 2.5B) particles plotted in a continuous size scale. Considering instrument's (vendor recommended concentration and size ranges) and the stock's limitations (dilution extend based on initial concentration as well as initial size distribution; *see Materials and Methods*) in regards to the specific setup of this experiment, a different combination of methodologies could provide information either in the nano (< 1 µm) or in the micron (> 1 µm) size range in a concentration dependent manner. Regardless of the considerations previously mentioned, these important observations should be considered: i) For a given particle size, particle counts varied depending on the methodology used as a reporter. However, comparable methodologies (*i.e.* MFI and FC) showed the closest recoveries. This highlights the impact of the different principles on the reported counts which will also lead to inherent differences in the precision (see Chapter 1) and accuracy of these measurements. ii) Variations described in i) followed a concentration dependent trend. For example, in the case of latex -at least in the upper size range- at 7.5×10^6 particles per mL the discrepancies between RMM and NTA were significantly reduced as compared to the 7.5×10^5 particles per mL dilution point. For mAb-B particles even higher concentrations may be needed to reflect this effect. In general, better accuracy performance was found in the upper concentration range of each instrument. iii) For latex particles along the dilution set, a certain concentration was reached in which recovery for all instruments at most of the sizes was not only ~100% but also comparable between them. This is the case of micron-range particles at 7.5×10^3 particles/mL and nano range particles at 7.5×10^6 particles/mL. However, for mAb-model A particles such consistency was not found at any concentration (neither for BSA and mAb-model B particles, data not shown). iv) There is lack of a suitable methodology than can accurately report low concentrations in the nano range and high concentrations in the micron range. For example, at 7.5×10^1 particles per mL, the only instrument that reported particle counts both for latex and mAb particles in the micrometer range was HIAC, whereas in the nanometer range no methodology reported values at such a low concentration. In contrast, at 7.5×10^5 particles per mL, in the micrometer range only MFI.
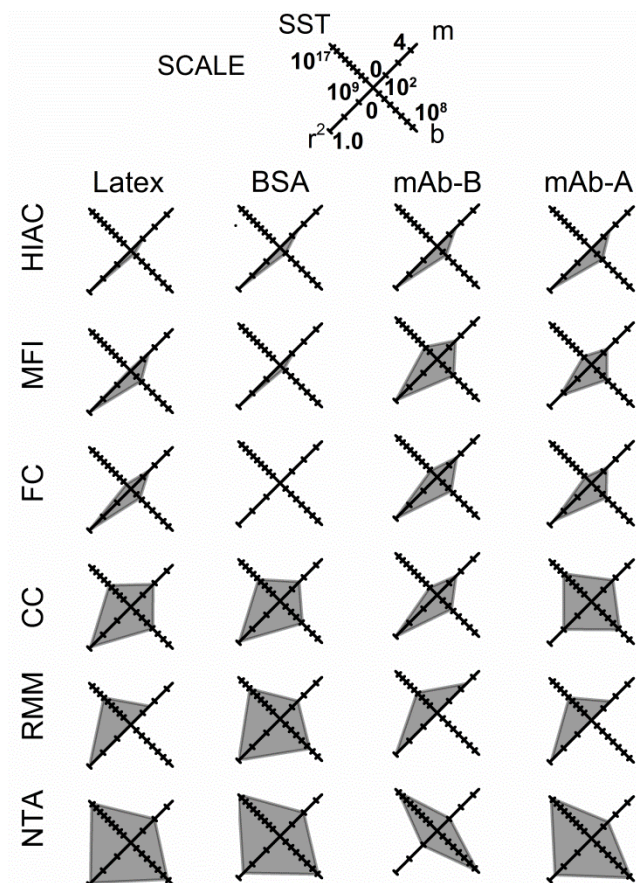
Figure 2.4 Independent dilution series of each particle type were measured in each instrument. The linearity performance was evaluated and each linear fit parameter is represented by one axis of the radar plot. Scales were adapted to be common for all the instruments so that the better linear fit is represented by the smaller radar plot depicted area pointing to the r2 axis

and FC reported information, whereas in the nanometer range RMM and NTA both did. This issue is something that will hopefully be assessed by further instrumentation developments. Interestingly, at this relatively high concentration, CC appeared in between the two size scales, however, a smooth transition was not observed.

Instrument-specific considerations

The use of identically prepared particle models for all the different techniques allowed for the identification of instrument-specific factors. This section will describe those observations. Interestingly, they revealed how the instrument fundament can bias count determinations as a result of different particle natures.
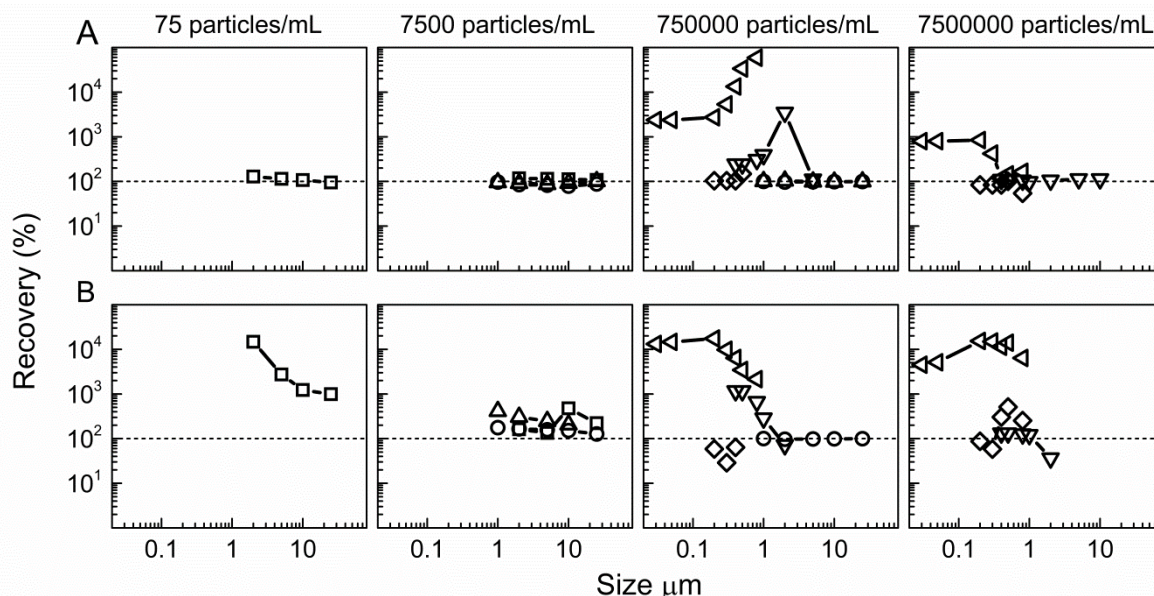
Figure 2.5 The recovery profile of 4 selected points (75; 7500; 750000 and 7500000 particles/mL) within the dilution set of A, latex and B, mAb-model B particles is presented including all the instruments as follows: □ HIAC; ○ MFI; △ FC; ▽ CC; ◇ RMM; ◁ NTA. This allows for data overlook in the complete size range (from >0.03 um (lower limit NTA) to >25 um (upper limit HIAC)). For a given concentration panel, only some of the instruments report data based on their specifications and sample composition. The horizontal axis represents the size of the particles and the vertical axis represents the recovery, (experimental/theoretical*100). At a given particle size and theoretical concentration, different instruments reported different experimental values hence different accuracy is associated. This effect is more severe for protein particles as compared with latex

For the flow imaging technologies, a clear difference was found in the recovery profile of mAb and that of latex or BSA models. . Provided that the same dilution and handling procedure was applied to all four particle preparations, this observation suggests a likely influence of the more complex particle matrix on which the mAb particles are immersed. It seems that a final protein formulation with all the typical excipients included might represent a major challenge for the camera-based techniques. It has been suggested that protein formulations can trap very small air bubbles (~1-2 μm) which cannot be discerned using morphological parameters or available statistical filters. The size-wise analysis presented in Figure S2.1b suggests this hypothesis is applicable. In the case of mAb-model A particles, even at high concentrations, -where other instruments showed good accuracy profiles- a strong over counting effect can be observed for the smallest >1 μm bin.

Another example in which the effect of particle morphology/nature could be identified is the CC instrument. This methodology bases its determinations on volume displacement. Assuming a spherical diameter for all particles (equivalent circular diameter determinations) morphology should not play a role in the measurements. This was confirmed by comparing the recovery profiles of latex, BSA and mAb-model B particles (Figure 2.1). Those examples showed similar good recoveries in both latex and protein. However, mAb-model A was the only model which exhibited a different profile. One possible cause of this observation is the high pliability of this model (a consequence of the relative low stress level applied to its generation) that could not endure the mechanical stress of the particle pumping through the glass tube orifice. Such mechanical stress due to particle transit inside the instrument has been suggested for other techniques (31) and is probably also present during particle dilution. These observations are of the highest importance given that CC is a technique that often requires particle dilution to increase sample conductivity. Our results clearly show how detrimental this practice can be in terms of particle integrity and accuracy of results.

The case of RMM exemplified a probabilistic effect already described in a previous publication of our group in which the precision assessment of particle counting instruments was carried out. In that study (Chapter 1) a poor precision for larger particle sizes was found to be rooted in a poor sampling effect due to low numbers of such particles whiting the entire sample size distribution. Similarly, in the present study, the tiny volumes that RMM uses challenged the limits of probabilistic detection (dashed lines Figure 2.1). Within our dilution study this effect is, of course, benchmarked by the initial concentration of the stock solutions. However, the same scenario would appear when measuring biotechnological products even without dilutions since their particle burden is generally low (2).

Finally, NTA appeared to be the least effective methodology included in this experimental design. In contrast with all other methodologies, not even latex beads showed a good recovery profile. Interestingly, in another set of experiments in which single sizes instead of a mixture of latex standards was used, the accuracy profile was acceptable (data not shown). Such contrasting results perfectly exemplify how important is to assess instrument accuracy using a realistic experiment design. In this specific case, the use of size-wise polydisperse samples allowed for the unmasking of strong over

counting effects. This behaviour was found to be consistent and even more pronounced in the case of the proteinaceous particle models.

Altogether, instrument-related artefacts were found to influence each one of the methodologies. Surely, particle characterization of biotechnological products constitutes a complex topic that offers many challenges. Some of them were illustrated by the different particle models used in this study. Despite the fact that only the Light Obscuration technology is currently considered in the regulatory frame; particle characterization at extended size ranges other than the >10 and >25 μm cut off values is recommended. In this regard, the careful use and interpretation of results when using any other techniques is strongly recommended.

2.5 CONCLUSIONS

The present study described the analytical assessment of the accuracy of subvisible and submicron particle counting instruments. We have shown that particle morphology and particle pliability are important factors that affect the performance of the instruments. The accuracy profiles appeared to be more different when measuring typically used latex beads standards than when measuring actual protein particles. Furthermore, a strong over-counting effect was found for the later especially at low concentration ranges and when particle stability was low. Among all the instruments tested, the nano tracking technology showed the strongest over-counting. For all techniques, the relative sample composition was found to be the most important factor, with improved accuracy for those particle sizes represented in the majority.

Our study showed how the specific analytical principles can impact the response of the instruments and which considerations should frame the interpretation of the results. All in all, the here illustrated experimental design should help define the ranges of particle and instrument specific counting capabilities. This represents an important tool in the applicability of the subvisible particle counting instruments in the research and development pharmaceutical arena

2.6 REFERENCES

1. J.F. Carpenter, Randolph, Theodore W., Jiskoot, Wim, Crommelin, Daan J. A., Middaugh, C. Russell, Winter, Gerhard, Fan, Ying-Xin, Kirshner, Susan, Verthelyi, Daniela, Kozlowski, Steven, Clouse, Kathleen A., Swann, Patrick G., Rosenberg, Amy, Cherney, Barry. Overlooking Subvisible Particles in Therapeutic Protein Products: Gaps That May Compromise Product Quality. Journal of Pharmaceutical Sciences. 98:1201-1205 (2009).

2. S.K. Singh, N. Afonina, M. Awwad, K. Bechtold-Peters, J.T. Blue, D. Chou, M. Cromwell, H.-J. Krause, H.-C. Mahler, B.K. Meyer, L. Narhi, D.P. Nesta, and T. Spitznagel. An industry perspective on the monitoring of subvisible particles as a quality attribute for protein therapeutics. Journal of Pharmaceutical Sciences. 99:3302-3321 (2010).

3. J. den Engelsman, Garidel, Patrick, Smulders, Ronald, Koll, Hans, Smith, Bryan, Bassarab, Stefan, Seidl, Andreas, Hainzl, Otmar, Jiskoot, Wim. Strategies for the Assessment of Protein Aggregates in Pharmaceutical Biotech Product Development. Pharmaceutical Research. 2011 Apr; 28(4): 920–933.

4. B. Demeule, Messick, S., Shire, S. J., Liu, J. Characterization of Particles in Protein Solutions: Reaching the Limits of Current Technologies. AAPS Journal. 12:708-715 (2010).

5. H. Mach, Arvinte, T. Addressing new analytical challenges in protein formulation development. European Journal of Pharmaceutics and Biopharmaceutics. 78:196-207 (2011).

6. A.S. Rosenberg, D. Verthelyi, and B.W. Cherney. Managing uncertainty: A perspective on risk pertaining to product quality attributes as they bear on immunogenicity of therapeutic proteins. Journal of Pharmaceutical Sciences. 101:3560-3567 (2012).

7. W. Wang, S.K. Singh, N. Li, M.R. Toler, K.R. King, and S. Nema. Immunogenicity of protein aggregates-Concerns and realities. International Journal of Pharmaceutics. 431:1-11 (2012).

8. J.G. Barnard, Babcock, K., Carpenter, J. F. Characterization and quantitation of aggregates and particles in interferon- products: Potential links between product quality attributes and immunogenicity. Journal of Pharmaceutical Sciences. 102:915-928 (2013).

9.   L.O. Narhi, Jiang, Yijia, Cao, Shawn, Benedek, Kalman, Shnek, Deborah. A Critical Review of Analytical Methods for Subvisible and Visible Particles. Current Pharmaceutical Biotechnology. 10:373-381 (2009).

10.   S. Zölls, Tantipolphan, R., Wiggenhorn, M., Winter, G., Jiskoot, W., Friess, W., Hawe, A. Particles in therapeutic protein formulations, Part 1: Overview of analytical methods. Journal of Pharmaceutical Sciences. 101:914-935 (2012).

11.   V. Filipe, Hawe, A., Carpenter, J. F., Jiskoot, W. Analytical approaches to assess the degradation of therapeutic proteins. Trends in Analytical Chemistry. 49:118-125 (2013).

12.   V. Filipe, Hawe, Andrea, Jiskoot, Wim. Critical Evaluation of Nanoparticle Tracking Analysis (NTA) by NanoSight for the Measurement of Nanoparticles and Protein Aggregates. Pharmaceutical Research. 27:796-810 (2010).

13.   M. Wright. Nanoparticle tracking analysis for the multiparameter characterization and counting of nanoparticle suspensions. Methods in Molecular Biology (Clifton, NJ). 906:511-524 (2012).

14.   T.P. Burg, Godin, M., Knudsen, S. M., Shen, W., Carlson, G., Foster, J. S., Babcock, K., Manalis, S. R. Weighing of biomolecules, single cells and single nanoparticles in fluid. Nature. 446:1066-1069 (2007).

15.   P. Dextras, Burg, T. P., Manalis, S. R. Integrated Measurement of the Mass and Surface Charge of Discrete Microparticles Using a Suspended Microchannel Resonator. Analytical Chemistry. 81:4517-4523 (2009).

16.   A.R. Patel, Lau, Doris, Liu, Jun. Quantification and Characterization of Micrometer and Submicrometer Subvisible Particles in Protein Therapeutics by Use of a Suspended Microchannel Resonator. Analytical Chemistry. 84:6833-6840 (2012).

17.   J. Panchal, J. Kotarek, E. Marszal, and E.M. Topp. Analyzing Subvisible Particles in Protein Drug Products: a Comparison of Dynamic Light Scattering (DLS) and Resonant Mass Measurement (RMM). AAPS Journal. 16:440-451 (2014).

18.   M.N. Rhyner. The Coulter Principle for Analysis of Subvisible Particles in Protein Formulations. AAPS Journal. 13:54-58 (2011).

19.   J.G. Barnard, Rhyner, M. N., Carpenter, J. F. Critical evaluation and guidance for using the Coulter method for counting subvisible particles in protein solutions. Journal of Pharmaceutical Sciences. 101:140-153 (2012).

20.   D.K. Sharma, P. Oma, M.J. Pollo, and M. Sukumar. Quantification and Characterization of Subvisible Proteinaceous Particles in Opalescent mAb Formulations Using Micro-Flow Imaging. Journal of Pharmaceutical Sciences. 99:2628-2642 (2010).

21.   R. Strehl, Rombach-Riegraf, V., Diez, M., Egodage, K., Bluemel, M., Jeschke, M., Koulov, A. V. Discrimination between silicone oil droplets and protein aggregates in biopharmaceuticals: a novel multiparametric image filter for sub-visible particles in microflow imaging analysis. Pharmaceutical Research. 29:594-602 (2012).

22.   G.A. Wilsonand M.C. Manning. Flow imaging: Moving toward best practices for subvisible particle quantitation in protein products. Journal of Pharmaceutical Sciences. 102:1133-1134 (2013).

23.   S. Zölls, Weinbuch, D., Wiggenhorn, M., Winter, G., Friess, W., Jiskoot, W., Hawe, A. Flow Imaging Microscopy for Protein Particle Analysis-A Comparative Evaluation of Four Different Analytical Instruments. AAPS Journal. 15:1200-1211 (2013).

24.   C. Kalonia, O.S. Kumru, I. Prajapati, R. Mathaes, J. Engert, S. Zhou, C.R. Middaugh, and D.B. Volkin. Calculating the Mass of Subvisible Protein Particles with Improved Accuracy Using Microflow Imaging Data. Journal of Pharmaceutical Sciences. (2014).

25.   T. Werk, Volkin, D. B., Mahler, H. C. Effect of solution properties on the counting and sizing of subvisible particle standards as measured by light obscuration and digital imaging methods. European Journal of Pharmaceutical Sciences. 53:95-108 (2014).

26.   J.S. Philo. Is any measurement method optimal for all aggregate sizes and types? AAPS Journal. 8:E564-E571 (2006).

27.   S. Cao, Y. Jiang, and L. Narhi. A Light-obscuration Method Specific for Quantifying Subvisible Particles in Protein Therapeutics. Pharmacopeial Forum. 36:10 (2010).

28.   A. Hawe, Schaubhut, F., Geidobler, R., Wiggenhorn, M., Friess, W., Rast, M., de Muynck, C., Winter, G. Pharmaceutical feasibility of sub-visible particle analysis in parenterals with reduced

volume light obscuration methods. European Journal of Pharmaceutics and Biopharmaceutics. 85:1084-1087 (2013).

29.   D. Weinbuch, Zolls, S., Wiggenhorn, M., Friess, W., Winter, G., Jiskoot, W., Hawe, A. Micro-flow imaging and resonant mass measurement (archimedes) - complementary methods to quantitatively differentiate protein particles and silicone oil droplets. Journal of Pharmaceutical Sciences. 102:2152-2165 (2013).

30.   S. Zölls, Gregoritza, M., Tantipolphan, R., Wiggenhorn, M., Winter, G., Friess, W., Hawe, A. How subvisible particles become invisible-relevance of the refractive index for protein particle analysis. Journal of Pharmaceutical Sciences. 102:1434-1446 (2013).

31.   D. Weinbuch, W. Jiskoot, and A. Hawe. Light obscuration measurements of highly viscous solutions: sample pressurization overcomes underestimation of subvisible particle counts. The AAPS Journal. 16:1128-1131 (2014).

32.   R. Vasudev, S. Mathew, and N. Afonina. Characterization of Submicron (0.1-1 mum) Particles in Therapeutic Proteins by Nanoparticle Tracking Analysis. Journal of Pharmaceutical Sciences. 104:1622-1631 (2015).

33.   S. Cao, N. Jiao, Y. Jiang, A. Mire-Sluis, and L.O. Narhi. Sub-visible particle quantitation in protein therapeutics. Pharmeuropa Bio & Scientific Notes. 2009:73-79 (2009).

34.   D.K. Sharma, D. King, P. Oma, and C. Merchant. Micro-Flow Imaging: Flow Microscopy Applied to Sub-visible Particulate Analysis in Protein Formulations. The AAPS Journal. 12:10 (2010).

2.7 SUPPLEMENTARY MATERIAL

Table S2.1 Lower limits of counting capabilities per instrument and particle type

	Latex	**BSA**	**mAb1-B**	**mAb1-A**
NTA	5.0×10^8	2.5×10^9	2.5×10^8	7.5×10^8
RMM	2.5×10^5	2.5×10^6	2.5×10^5	5.0×10^5
CC	2.5×10^3	2.5×10^3	7.5×10^4	7.5×10^6
FC	2.5×10^2	2.5×10^2	2.5×10^4	2.5×10^4
MFI	5.0×10^2	5.0×10^2	5.3×10^3	1.0×10^4
HIAC	5.0×10^1	5.0×10^1	2.5×10^2	5.0×10^2
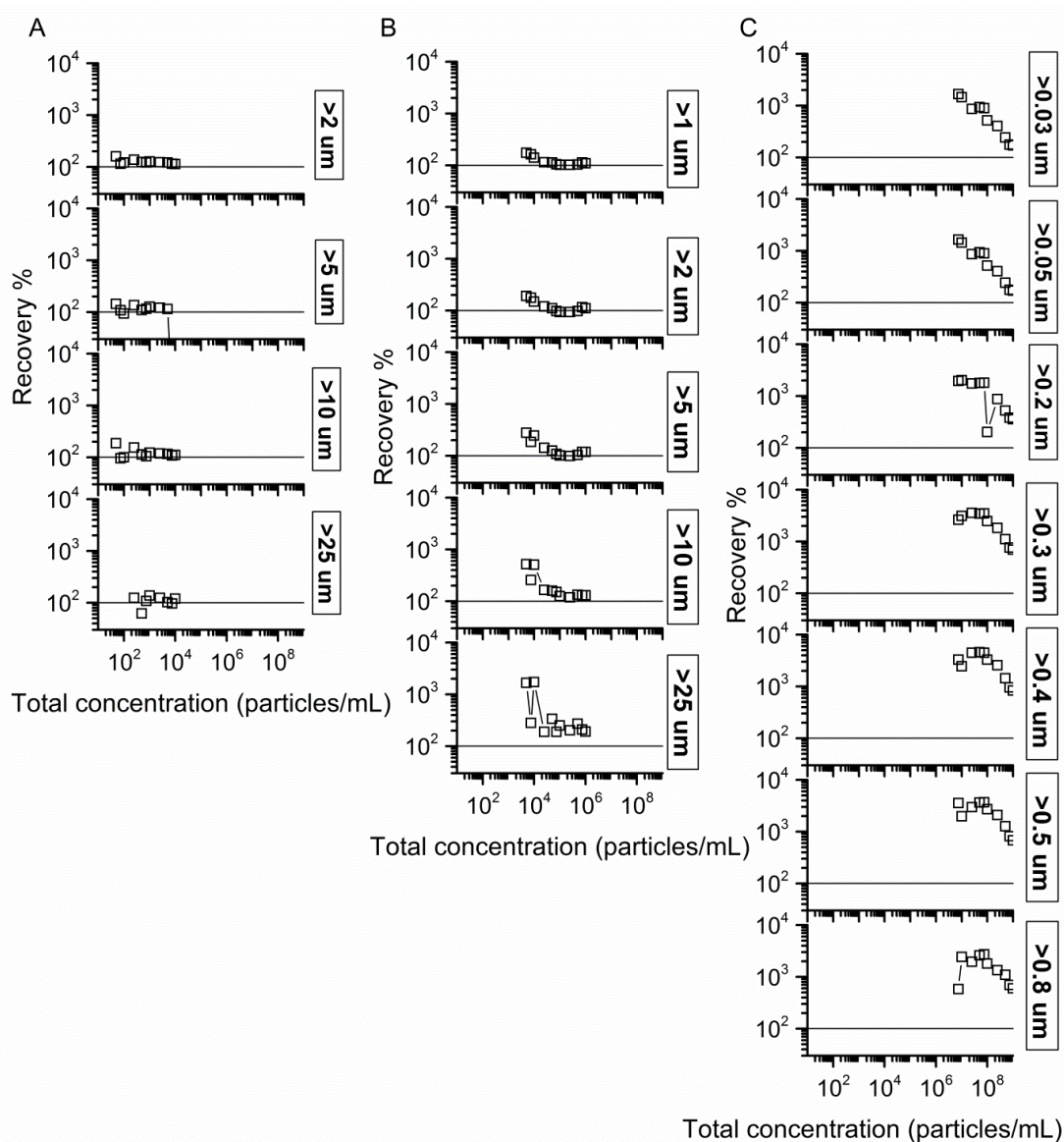
Figure S2.1a Examples of the recovery profile analyzed size-wise. Recovery profile of A) latex particles measured in HIAC; B) mAb-model B particles measured in MFI and C) BSA particles measured in NTA. Horizontal axes refer to the theoretical total particle concentration of each independent sample of the dilution set based on which the size-wise analysis was performed. Different panels represent the recovery profile of specific particle sizes in cumulative bins.
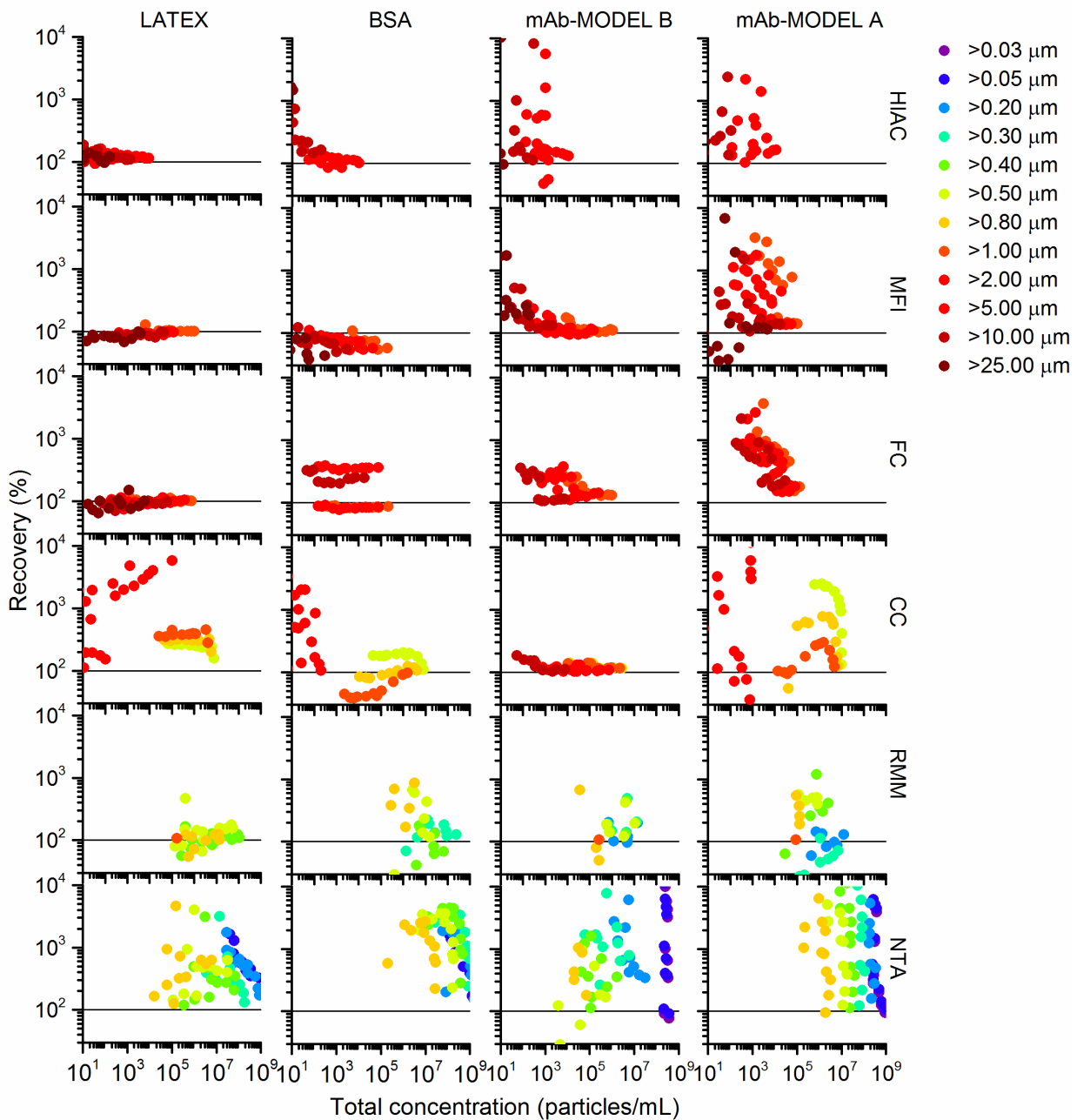
Figure S2.1b Recovery profile of all the counting instruments and particle models in scope analyzed per cumulative size bin. Horizontal axes refer to the theoretical total particle concentration of each independent sample of the dilution set based on which the size-wise analysis was performed. Vertical axes represents the calculated recovery, considering initial counts per bins as indicated by the different colors (theoretical concentration of a given bin/experimental concentration of the same bin*100).
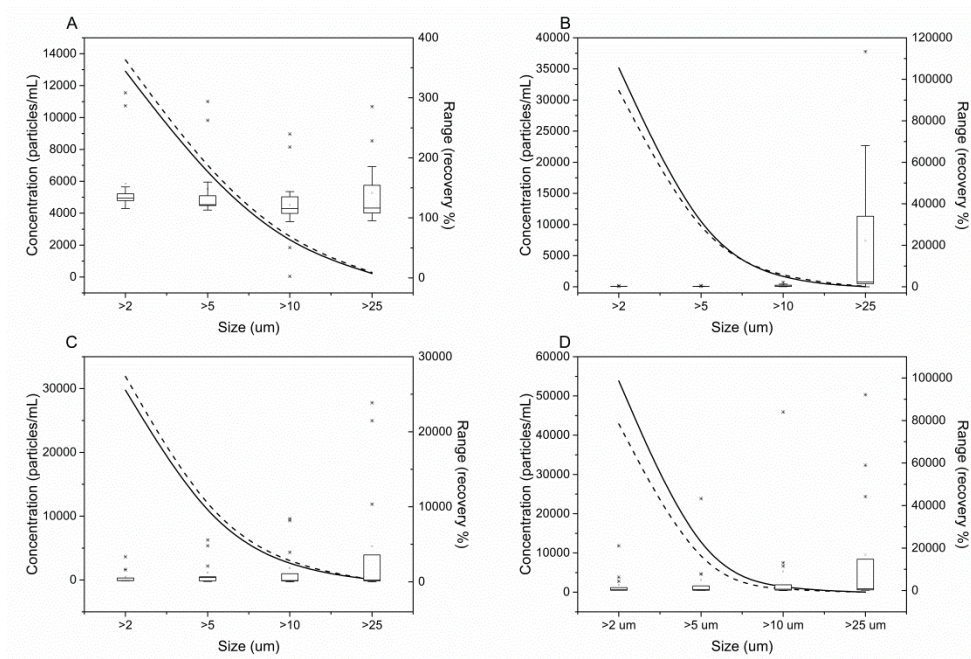
Figure S2.2a. Recovery profile per particle size for HIAC instrument The recovery profile per total particle counts of A, latex; B, BSA, C, mAb-model B and D, mAb-model A particles was analyzed size wise and correlated with the size distribution of stocks from which dilutions were prepared. Horizontal axes represent cumulative size bins. Vertical left axes represent the particle concentration of the stock at the beginning (continue line) and at the end (dashed line) of the experiment. Vertical right axes represent the recovery associated with each specific size along the full dilution set (box plot).
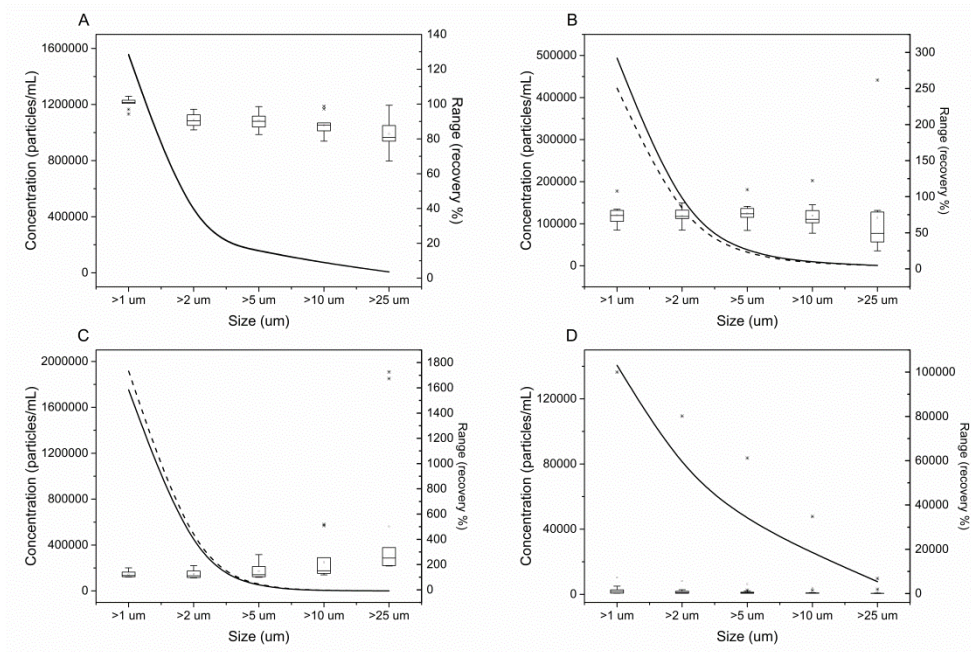
Figure S2.2b Recovery profile per particle size for MFI instrument. See legend Figure S2a
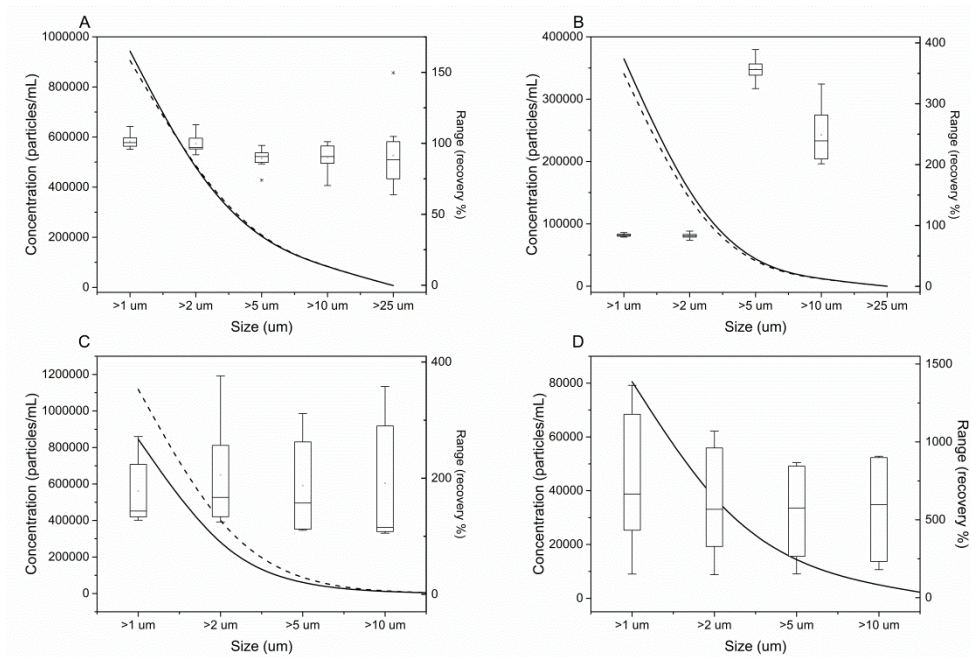
Figure S2.2c Recovery profile per particle size for FC instrument. See legend Figure S2a
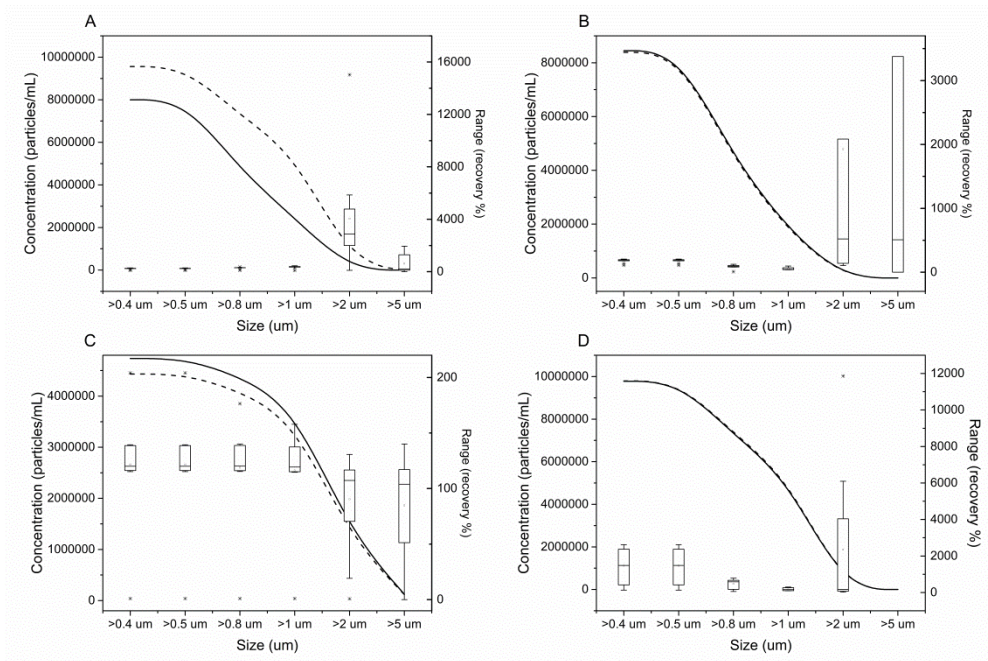
Figure S2.2d Recovery profile per particle size for CC instrument. See legend Figure S2a
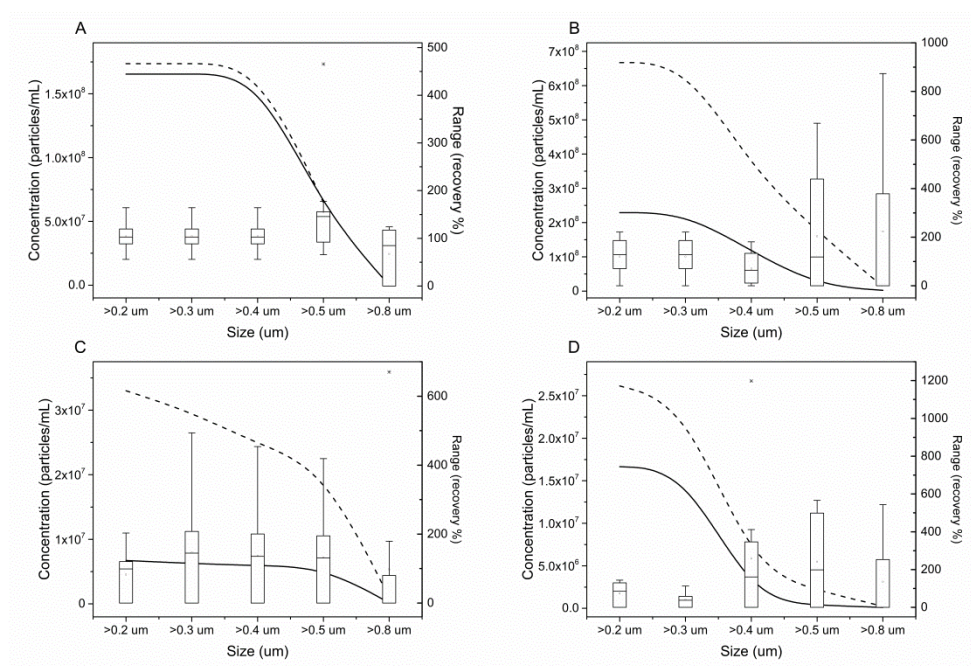
Figure S2.2e Recovery profile per particle size for RMM instrument. See legend Figure S2a
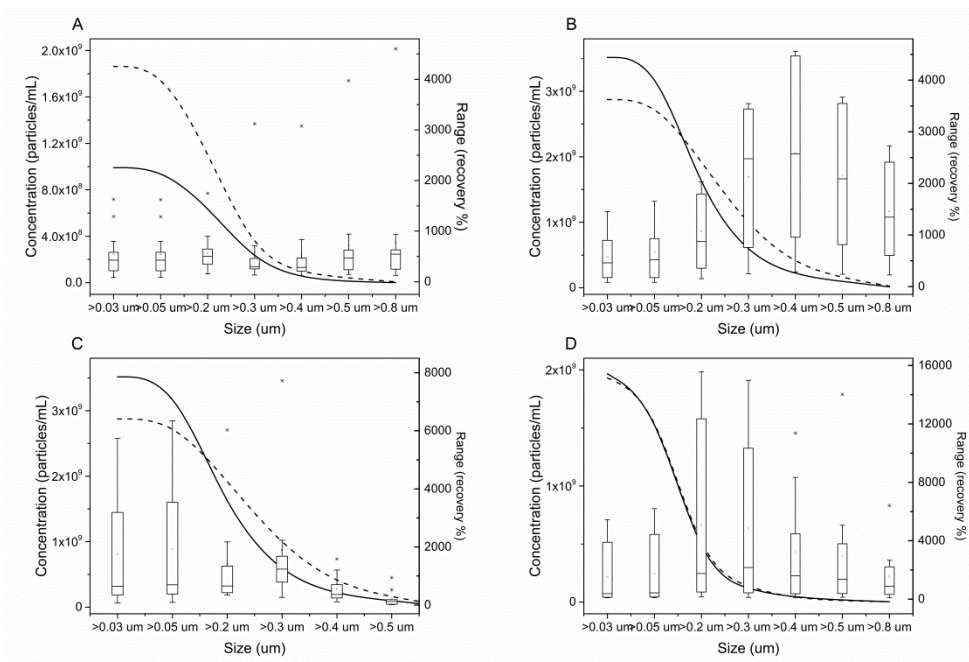
Figure S2.2f Recovery profile per particle size for NTA instrument See legend Figure S2a
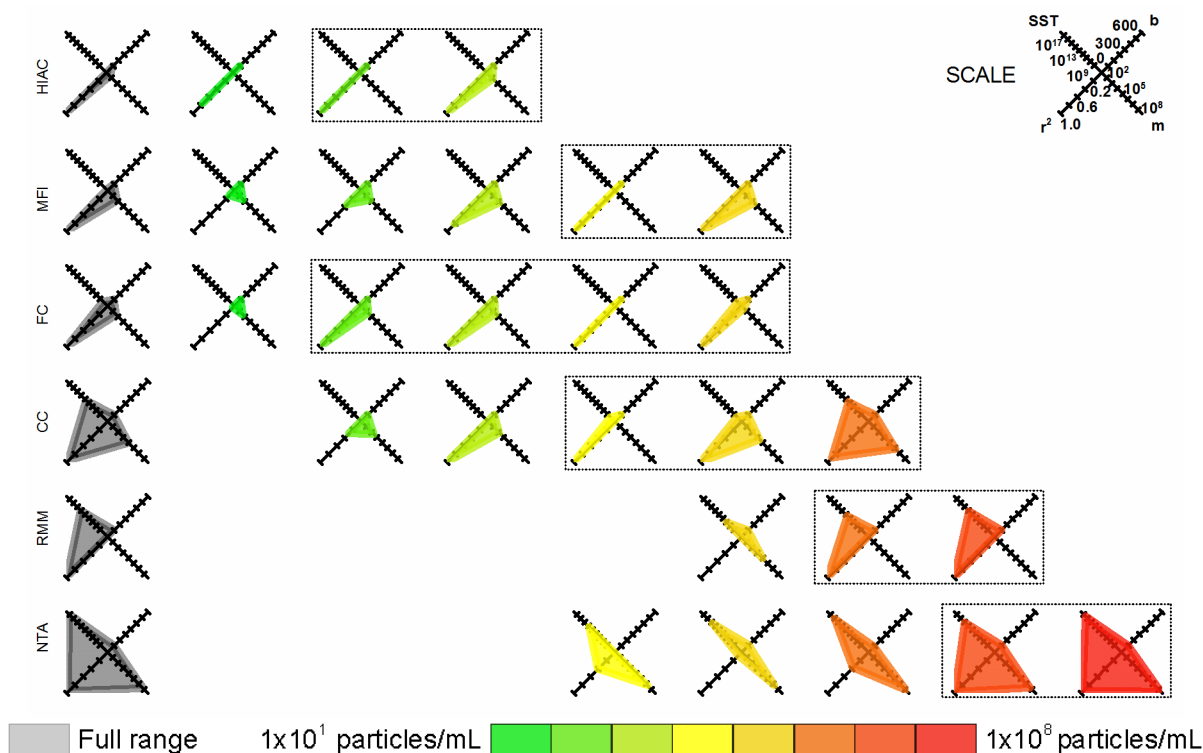
Figure S2.3a Linear assessment for latex particles A stock solution of the indicated type of particles was diluted to generate a broad set of samples benchmarked by instrument's concentration capabilities to measure in each instrument. The linearity assessment was performed by following all linear fit parameters (slope (*m*); intercept (*b*); coefficient of determination (*r²*) and sum of squares total (*SST*)) together in a radar plot representation. Scales were adapted to be common for all the instruments so that the better linear fit is represented by the smaller radar plot area pointing to the r^2 axis. Analysis was done considering the full size range (gray plots) and also per order of magnitude (color scale code from green=10 to red=100000000 particles/mL). Using internally defined criteria of m < 10 and r^2 > 0.9 optimal linear ranges are indicated by dotted boxes.
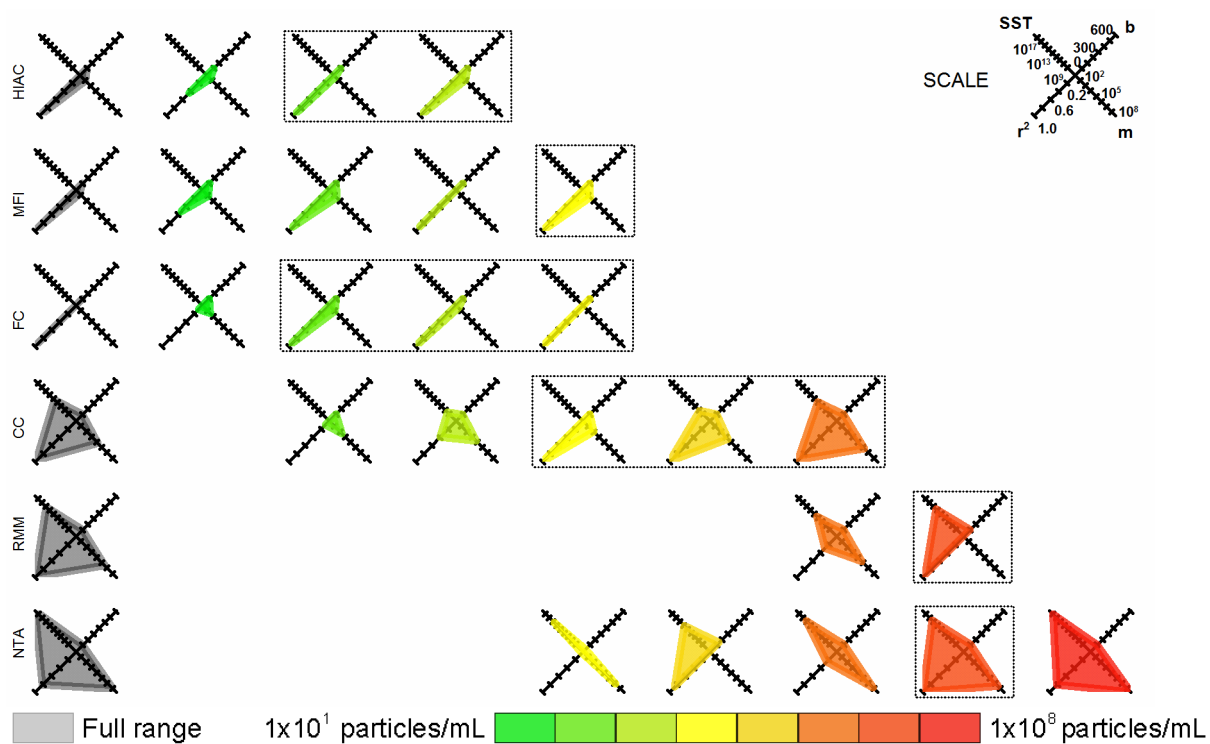
Figure S2.3b. Linear assessment for latex BSA particles See legend in Figure S2.3a
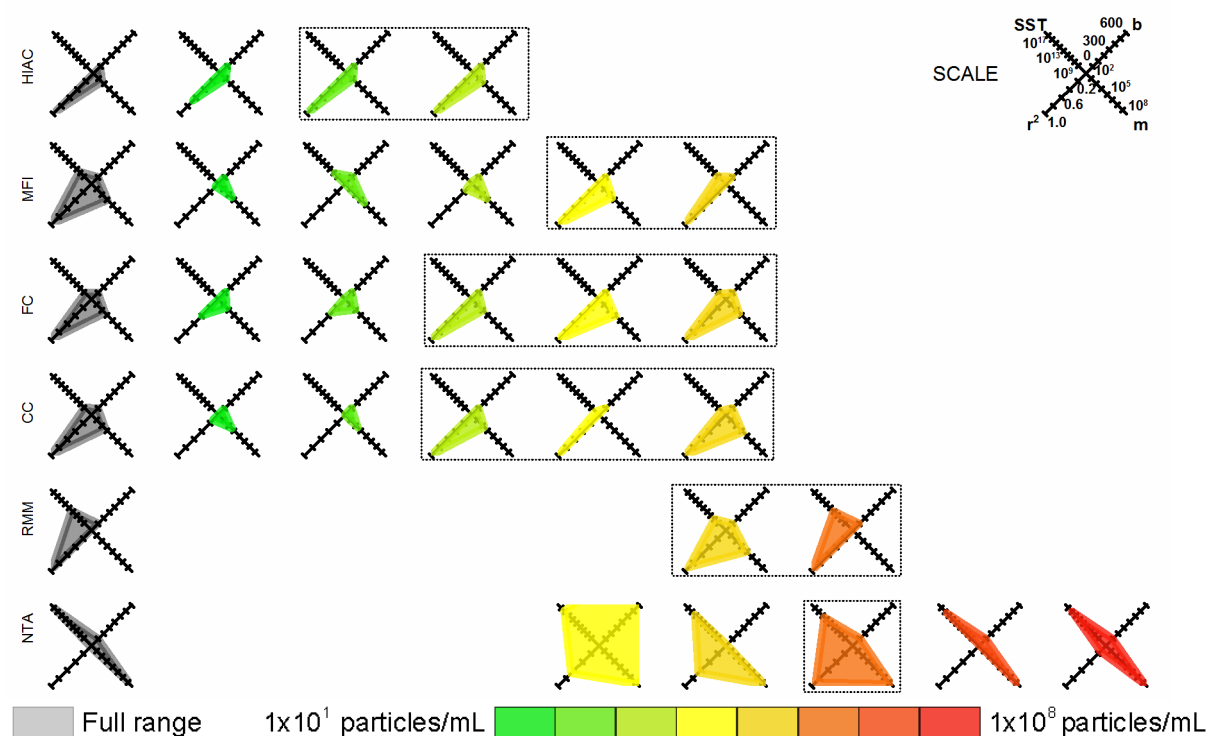
Figure S2.3c. Linear assessment for latex mAb-B particles See legend in Figure S2.3a
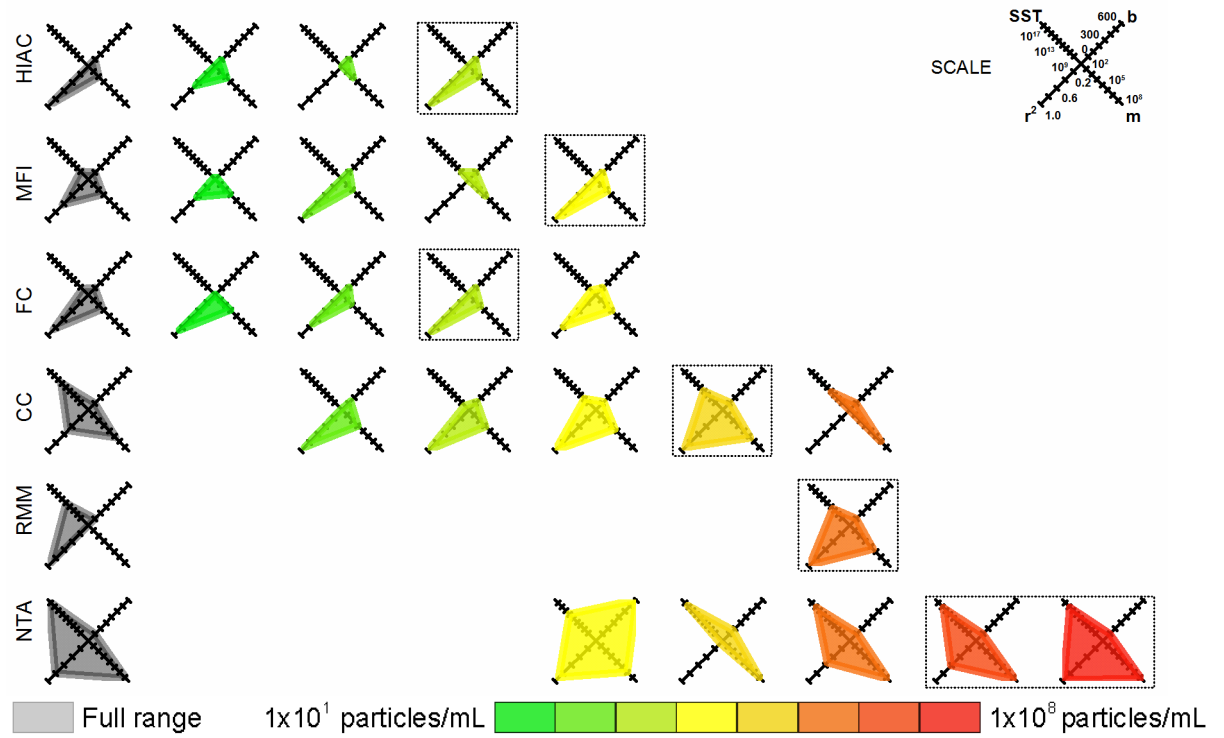
Figure S2.3d Linear assessment for latex mAb-A particles See legend in Figure S2.3a

CHAPTER 3

Measuring Subvisible Particles in Protein Formulations Using a Modified Light Obscuration Sensor with Improved Detection Capabilities

Anacelia Ríos Quiroz
Gabriela Québatte
Fabian Stump
Christof Finkler
Joerg Huwyler
Roland Schmidt
Hanns-Christian Mahler
Atanas V. Koulov
Michael Adler

CHAPTER 3. Measuring Sub-Visible Particles in Protein Formulations Using a Modified
Light Obscuration Sensor with Improved Detection Capabilities

91

3.1 ABSTRACT

Although light obscuration is the "gold standard" for subvisible particle measurements in biopharmaceutical products, the current technology has limitations with respect to the detection of translucent proteinaceous particles and particles of sizes smaller and around 2 µm. Here, we describe the evaluation of a modified light obscuration sensor utilizing a novel measuring mode. Whereas standard light obscuration methodology monitors the height (amplitude) of the signal, the new approach monitors its length (width). Experimental evaluation demonstrated that this new detection mode leads to improved detection of subvisible particles of sizes smaller than 2 µm, reduction of artefacts during measurements especially of low concentrations of translucent protein particles and higher counting accuracy as compared to flow imaging microscopy and standard light obscuration measurements.

3.2 INTRODUCTION

Despite the introduction of multiple new methodologies for characterization of sub-visible particles in parenteral formulations during the last decades, the light obscuration method (as described in USP chapter <788> (1) and Ph.Eur. 2.9.19.) is still the most reliable method for subvisible particle quantification applied in the pharmaceutical industry. The broad use of this technique, included as a compendial method since 1986, is the result of proven robustness and well understood performance. The method is based on the blockage of a constant source of light illuminating a photo-diode by particles passing through the flow-cell and measuring of the consequential drop in voltage. The size of individual particles is determined by relating the registered signal to a calibration curve built using reference polystyrene particles of defined sizes.

The light obscuration method was developed for measuring particles that are beyond the detection capabilities of visual inspection. The rationale for the introduction of measurement of sub-visible particles was the concern related to possible embolism or vein occlusion after intra venous (IV) administration. However, recently subvisible particle measurements have received further attention due to concerns that subvisible proteinaceous particles in protein therapeutics may have the potential to trigger immunological reactions (2-5). While the relevance of these concerns and the impact of subvisible particles on immunogenicity of biopharmaceuticals remain to be established, accurate and precise quantification of particles smaller than 10 μm is a major challenge to the current analytical methodology.

Analysis of particles in formulations of therapeutic proteins, including biotechnological products intended for routes of administration other than IV may be challenging. Important sample characteristics such as high viscosities (>6 cP up to 120 cP), limited sample volume (in many cases <2.5 mL), appearance characteristics (*e.g.* translucency, optical density), and particle stability (agglomeration, aggregation and particle rearrangement) need to be considered. The USP <787> (6) (officially applicable since August 2014) attempts to address some of these considerations that were originally pointed out in research papers (7, 8). For example, the new chapter provides some guidance for sample handling relevant to biotech products – e.g. recommendation against sonication.

Nevertheless, a number of challenges still remain to be tackled. For example, one of the main limitations of the light obscuration method is related to the ability for detection and sizing of relatively translucent particles which are typically present in biotechnological products (9, 10). The basis of this potential limitation is the discrepancy between the nature of the particles used for calibration (polystyrene beads) and the particles actually measured (proteinaceous and others). Whereas the former are optically dense and spherical, the latter vary in shape and more importantly – in optical density. As a rule, proteinaceous particles are less optically dense and therefore, a larger total surface area of a protein particle may be required to generate a comparable voltage drop to that generated by a polystyrene bead of equal size. The difference between the translucency of calibration standards and that of the measured particles likely results in a certain undersizing effect (11). One direct approach to solve this issue would be to change the material used for calibration. However, both the production of protein particles that fit the requirements of a standard material and the production of synthetic particles that resemble the morphology and optical properties of actual protein particles present major technical challenges. Although the second approach had been focus of ongoing efforts and partial success has been achieved (12, 13), still a lot remains to be desired with regard to practical implementation of such solution.

A methodology which claims to solve this quantification issue is the flow imaging microscopy technique. Despite the fact that in principle the detection of particles in this method should not be affected by particle morphology, it presents challenges of its own. For example, the detection of particles in flow imaging microscopy depends on the difference between the refractive indices of the medium and of the measured particles. Furthermore, in this technique the translucency of the measured particles affects the accuracy of particle sizing (9, 10, 14, 15). Because of these challenges, flow imaging microscopy does not necessarily present the best solution for particle quantification, although it remains a valuable tool for particle characterization.

Light obscuration method adaptions, such as lower measuring volumes and sample pressurization have already been studied (8, 16, 17). It has been demonstrated that analytical performance of modified light obscuration method may produce reliable results as the large volume modality. Benefits

CHAPTER 3. Measuring Sub-Visible Particles in Protein Formulations Using a Modified
Light Obscuration Sensor with Improved Detection Capabilities

95
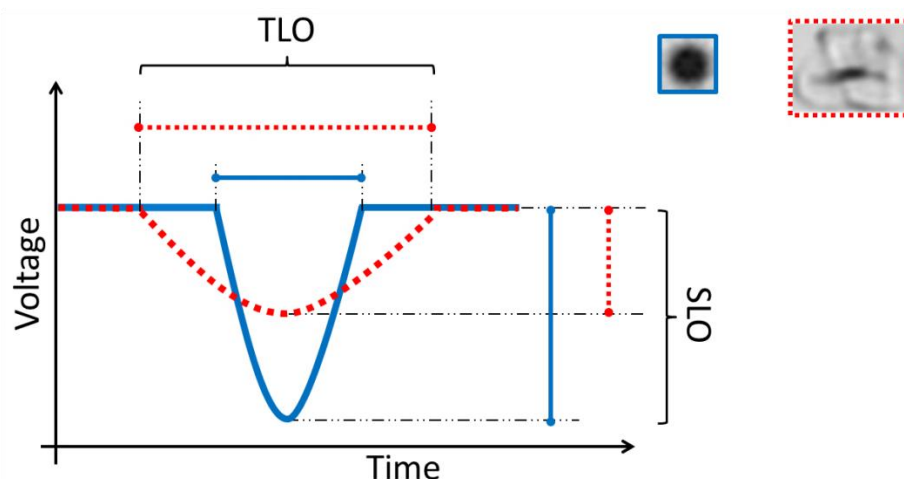
Figure 3.1 Schematic representation of the general principle of the Standard Light obscuration
technique (SLO) in comparison with the Time resolved Light Obscuration prototype (TLO).
Whereas SLO measures the height of the signal, TLO measures the width. For ····, despite the
light blockage is weaker as compare to ▬ given its higher translucency; when measured using
TLO a correct bigger size will be reported.

regarding improved counting accuracy, elimination of masking effects due to pooling procedures as
well as comparisons with other counting techniques have also been described (1-3). However, some
new opportunities still remain to be explored.

This present study aimed to evaluate a prototype of an optimized version of the existing standard light
obscuration method (hereafter referred to as SLO), which may allow the accurate monitoring of
particles in the 1-2 µm size range and reduce the alleged undersizing effects of translucent (*e.g.*
proteinaceous) particles (4-6). In addition to low volume and sample pressurization modifications, the
new approach offers an improved light obscuration sensor with a novel instrument configuration and
measurement mode represented in Figure 3.1. This new, time-resolved configuration (hereafter
referred to as TLO) enabled i) higher accuracy for low voltage drop signals coming from small
particles and ii) elimination of the influence of the morphology mismatch between standards used for
calibration (latex beads) and protein particles on the accuracy of the measurements. Both by means of
registering the width (time-resolved mode) instead of the height (standard mode) of the light
obscuration signal. This represents a new and innovative technique that measures the time course on
which the light is obscured rather than the intensity of this effect. Hence, particles resulting in very

low-intensity signals (*e.g.* translucent particles) can be sized more accurately by recording the time-span of the light blockage. We present the results of the evaluation and verification of this approach. Special attention was given to the counting accuracy of particles below 2 μm with an uneven optical density.

3.3 MATERIALS AND METHODS

Counting accuracy

Particle count standards (COUNT-CAL Count Precision Standards, ThermoScientific; USA) of 2, 5, 10, 15 and 20 μm were used. Manufacturer's reported concentration in particle/mL was 3000 ± 10 % for particles ≥1.3 μm; ≥3 μm; ≥7.5 μm; ≥10 μm and ≥15 μm; respectively.

Linearity and recovery

A broad set of dilutions was prepared using bovine serum albumin (BSA from Sigma Aldrich USA) particles generated as follows: a 30 mg/mL BSA formulation in PBS (DPBS, GIBCO UK) was initially filtered through a 0.22 μm filter membrane (Millex GB PVDF membrane, Millipore Ireland). A 50 mL tube (Sarstedt Germany) with 30 mL of protein solution was heated up to 73°C during 30 minutes using a Thermostat station (Eppendorf Germany). The resulting solution was diluted 1:10 to a total volume of 10 mL with PBS 1x (DPBS 1x, GIBCO UK) and homogenized by vortexing (VWR Belgium). After centrifugation (Centrifuge 5810R, Eppendorf Germany) at 1200 x g for 1 minute, the supernatant was collected to generate the "BSA stock" solution. The *dilution procedure* was standardized as follows: unstressed 40 mg/mL monoclonal antibody (mAb) formulation (consisting of a Roche proprietary reference IgG monoclonal antibody) was diluted with the correspondent buffer to generate a broad set of dilutions. The protein concentration in solution was followed by UV absorption using a SOLO VPE (C. Technologies; USA) spectrophotometer. When good linearity and recovery profiles were obtained, the same handling procedure and dilution extend was applied for the dilution of protein particles. The absence of dilution artefacts was confirmed by the excellent linearity profiles as described later in the Results section. Initial concentration of the daily-prepared BSA stock was defined accordingly to every independent instrument. Dilutions were calculated to achieve particle counts ranging from 10 to 10000 particles per mL and were measured immediately after aliquoting and

during the same day of stress. Minimum sample volume was set accordingly to instrument requirements to assure at least triplicate measurements. Maximum sample volume was set as needed to ensure stock aliquot of at least 1 µL. The diluent solution was the corresponding fresh filtered (0.22 µm PVDF Stericup, Millipore; USA) and non-stressed protein solution. All used material was extensively rinsed with particle free water (in house generated by several filtration and degassing steps (Liqui-cel Membrane Contactors, Membrana Germany) of bi-distilled water) and dried with 0.22 µm filtered (Millex GB PES membrane, Millipore Ireland) air prior use.

Particle size distribution

A stock solution of BSA particles prepared as described above was used. The same sample was measured in all the methods.

Morphology evaluation

The same preparations of mAb and ETFE (ethylene-tetrafluoroethylene) particles were measured in Flow imaging; Time resolved light obscuration and Standard light obscuration methods. mAb particles were generated as follows: a 25 mg/mL mAb formulation was diluted 1:10 in PBS (DPBS 10x, GIBCO UK) and filtrated through a 0.22 µm filter membrane (Millex GB PVDF membrane, Millipore Ireland). Formulation was subjected to heat stress (73°C for 7 minutes) using a Thermostat heat plate (Eppendorf, Hamburg Germany). ETFE particles were a gift from Dean Ripple (National Institute of Standards and Technology, Gaithersburg, Maryland USA).

Concentration and size dependency experiment

Two independently prepared stock solutions of mAb particles were used. Applying the dilution procedure already described independent dilution series were prepared and measured in Flow imaging and Time resolved light obscuration methods.

Standard light obscuration (SLO) measurements

A HIAC (ROYCO System 9703, sensor HRLD400HC, SKAN Basel, Switzerland) instrument with a small volume method was used as follows: rinsing volume was 0.2 mL and 4 runs of 0.4 mL each were performed at flow rate of 10 mL/min. The first run was discarded and the average ± standard deviation of the last 3 runs was reported. Cumulative particle counts per mL were obtained for sizes >2, >5, >10 and >25 µm. Data of particles >1 µm was considered just informative. Blank measurements were

performed at the beginning of the measurements and in between family of samples (order of magnitude-based). Acceptance criterion for blanks was less than 5 particles >1 µm. Suitability test per day of measurements involved the measurement of count standards of 2, 5 and 10 µm (ThermoScientific; USA) with acceptance limits of ± 10 % the reported concentration for particles bigger than 1.3, 3.0 and 5 µm, respectively. All stock samples were measured at the beginning and at the end of each measurement day to compare the particle concentration and size distribution. For dilution samples, counts >2 µm were compared to the theoretical values and the percentage correlation was reported as % recovery, (theoretical concentration/experimental concentration*100).

Time resolved light obscuration (TLO) measurements

A modified version of the standard light obscuration principle was used to monitor time-resolved changes in light blockage. The instrument was manufactured and modified by Markus Klotz GmbH (Burgholz, Germany), so that width measurements of the voltage drop due to particle's light obscuration effect could be measured. Additionally, as the sample was drawn at 40 mL per minute, the sample chamber was pressurized with nitrogen to avoid artefacts due to the presence of bubbles and/or air/liquid interface meniscus. Measurements were done accordingly with the small volume method described in the previous section.

Flow imaging (FI) measurements

An MFI instrument (DPA 4200 Brightwell Technologies Canada) equipped with a 100 µm flow cell was washed prior use with 1 % Tergazyme (Alconox Inc.; USA) solution during 2 minutes at maximum speed, soaking during 1 minute and finally flushing with particle free water during 5 minutes. Method parameters were 0.6 mL sample volume as termination type and 0.2 mL as purge volume. "Edge particle rejection" as well as "fill particle" option was activated. Light optimization step was performed with the correspondent filtrated sample. Cumulative particle counts per mL were obtained for sizes ≥1, ≥2, ≥5, ≥10 and ≥25 µm. Blank measurements were performed at the beginning of the measurements and in-between family of samples (order of magnitude-based) using fresh particle-free water. Acceptance criterion for blanks was less than 100 particles per mL > 1 µm. Suitability test per day of experiment involved 1) measurement of 5 µm count standards (ThermoScientific, Count-Cal; USA) with acceptance limits of ± 10 % the reported concentration for

particles >3 µm and 2) measurement of 5 µm size standard (ThermoScientific Duke Standard) with acceptance limits of Equivalent Circular Diameter (ECD) mean of ± 25 % the reported size and standard deviation <0.4. For stock samples, measurements at the beginning and at the end of the day of experiment were done and particle concentration was compared in the following bins: 1-2, 2-5, 5-10 and 10-25 µm. Size distribution in the 1 to 100 µm size range was also compared. For dilution samples, counts >1 µm were compared to the theoretical values and the percentage correlation was reported as % recovery, (theoretical concentration/experimental concentration*100).

3.4 RESULTS AND DISCUSSION

In order to evaluate the performance of the modifications made in the time-resolved light obscuration instrument (TLO), experiments to evaluate the count accuracy, linearity, recovery, size distribution, and morphology impact were carried out.

Counting accuracy

The counting accuracy of each instrument was evaluated by measuring the recovery of count standards of 2, 5, 10, 15 and 20 µm with a concentration of 3000 particles/mL (see Table S3.1). The SLO instrument configuration met supplier's criteria (recovery of ± 10 %) for 5, 10, 15 and 20 µm standards. However, for 2 µm count standard, the accuracy was not satisfactory with only 53 % recovery. This is not surprising as size specification of particles >1.4 µm is outside the lower size limit of the sensor. Interestingly, TLO showed accuracy within specifications for all the sizes including the smallest 2 µm standard. This suggests a major improvement of the new measuring mode and demonstrates that measuring the width instead of the height of the drop in voltage peak offers better accuracy for the minor signals produced by small (< 2 µm) particles. The FI measurements showed accuracy within specifications for all sizes.

Linearity and recovery

Although the SLO measurements are well suited for the low particle counts that are frequently found in biotechnological therapeutic products, concentrations below 100 particles/mL might represent a challenge for the analytical performance of counting instruments due to a poor signal to noise ratio. To
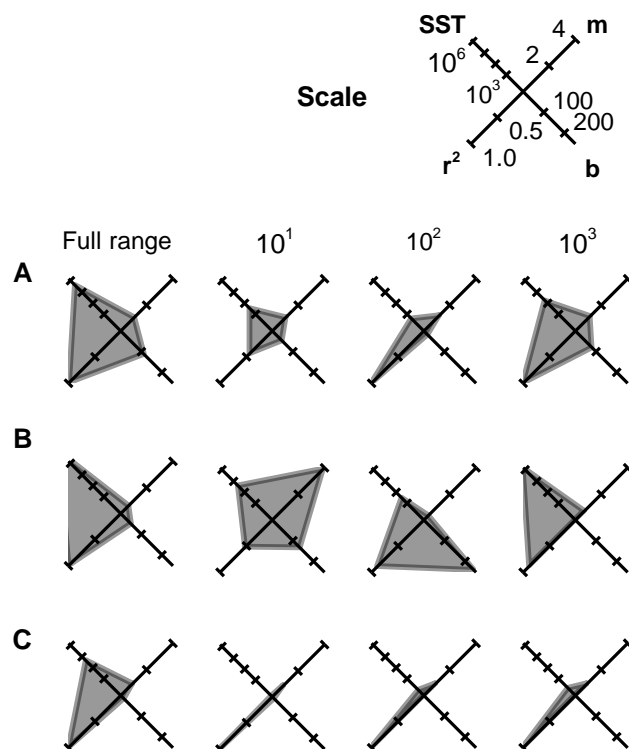
Figure 3.2 Linearity profile Independent dilution series of BSA heat stressed particles were measured in A, SLO; B, FI and C, TLO methods. The linearity performance was evaluated for the full concentration range studied (101 to 103 particles/mL) and also per order of magnitude. Each linear fit parameter is represented in one axis of the radar plot. Scales were adapted to be common for all the instruments. The best linear profile was found in the case of TLO, with the smallest radar plot depicted area pointed to the r2 axis.

evaluate the performance of the TLO method in this context, a stock solution of BSA protein particles was independently measured in SLO, TLO and FI instruments. Three different dilutions series were prepared using the initial stock concentration defined as per each respective technique and the theoretical concentrations were compared to the experimentally measured ones (see Table S3.2). To analyse the data, a linear model was assumed and the descriptors of the fit (slope, m; intercept, b; coefficient of correlation, r^2 and sum of squares total, SST) are presented in Figure 3.1 as radar plots (see also in Figure S3.1 and Table S3.3). Each axis have different scale (m 0-4; b 0-250; r2 0-1 and SST 301.5x106) adjusted so that the 12 representations displayed all the data. Thus, the smaller the plot area, the better the linear fit. Another advantage is that in contrast to other reports that consider only the coefficient of correlation value as reporter of the linear fit, this representation allows for a

CHAPTER 3. Measuring Sub-Visible Particles in Protein Formulations Using a Modified Light Obscuration Sensor with Improved Detection Capabilities

101
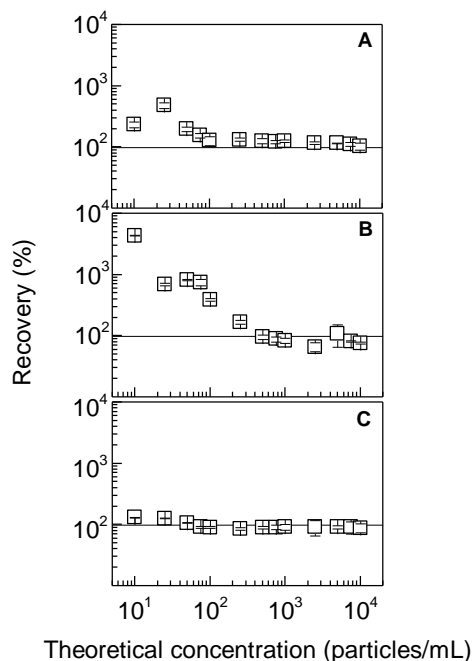
Figure 3.3. Recovery profile. Independent dilution series of BSA heat stressed particles ranging from 10 to 10000 particles/mL were measured in A, SLO; B, FI and C, TLO methods. The horizontal axis represents the theoretical concentration (for all sizes present in sample) and the vertical axis represents the recovery (theoretical concentration/experimental concentration*100). An overestimation effect in the lower concentration range was found. TLO instrument however showed good recoveries over the full concentration range.

stricter and more detailed evaluation of the linearity performance. For example, as can be seen in the case of FI measurements ([Figure 3.2B](#)), as the r^2 improves from 10^1 to 10^3 particles/mL, (0.52 to 0.88respectively), the SST worsens, (35000 to 1600000, respectively). It becomes also clear that at 101 particles/mL not only the r2 is poor but also an overestimation of almost 4 fold should be expected (m = 3.92). Interestingly, for the TLO measurements at the three orders of magnitude tested, a good linear fit was found (as indicated by the single line pointing to the r2 axis of the radar plots, see [Figure 3.2C](#)). Besides showing that sensor and instrument modifications in the new method improved the method linearity performance, this result also highlights that the dilution procedure and all the controls were successfully applied. Hence, this allowed us to exclude dilution artefacts and relate the observed response directly to instrumentation-related facts.

The results of the recovery assessment (assessed as experimental concentration/theoretical concentration × 100) reported in [Figure 3.2](#) also demonstrate exceptionally good performance of the TLO method. Whereas SLO and FI showed over counting effects (>150 %) around theoretical
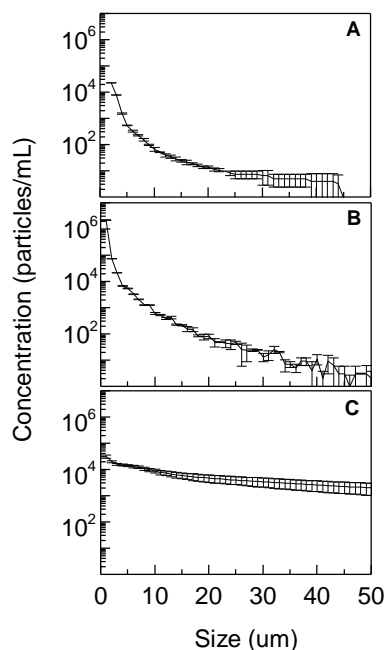
Figure 3.4 Size distribution of protein particles. Size distribution of the same BSA stock sample measured in A, SLO; B, FI and C, TLO. FI reported the higher total counts followed by TLO and SLO. A typical protein particle size distribution skewed to the right can be seen. TLO reported a tailing effect towards larger species

concentrations of 75 and 100 particles/mL, respectively, TLO showed good recoveries (85-130 %) along the entire dilution set.

Size distribution

A comparison between the particle size distribution measured by SLO, TLO and FI methods was carried out using BSA model particles. The results presented in Figure 3.4, showed some differences in the size distributions measured by the different instruments. Using SLO as a reference, counts for particles <5 µm were around 2 and 40 times higher for TLO and FI, respectively. On the other hand, for particles >5 µm, 120 and 9 fold times higher counts were found for TLO and FI, respectively.

To further inquire if the tailing effect observed in TLO was related to possible instability of the BSA particles, the size distribution of the count standards measurements described in the counting accuracy section was analysed. As can be seen in each column of Figure S3.2, the reported size distribution for the same standard varied between instruments. Whereas SLO results showed the usual decay size distribution, certain tailing effect was confirmed for TLO and in a lower extent, also for FI. This suggests that the tailing effect is not related with particle instability or nature, but rather to intrinsic
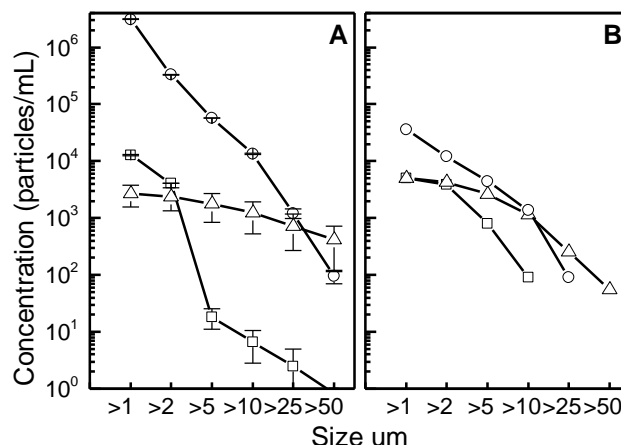
Figure 3.5 Morphology impact. Comparison of the cumulative counts of A) mAb protein and B) protein-like ETFE particles measured with the SLO □; FI ○ and TLO △ methods. For the ETFE model, similar results were found between TLO and FI for particles >5 μm

method characteristics. The analysis of the proportion of the total size distribution within ± 10 % of the reported size revealed that the tailing effect was more pronounced as the particle size increases. For example, in the TLO measurement of 2 μm count standard that proportion was close to 90 % (low tailing effect) whereas for the 20 μm count standard it dropped down to only 40 % (severe tailing effect). One possible explanation for the tailing effect could be the increased flow rate that was implemented in this instrument modification (from 10 to 40 mL/min). Although the latter likely contributes to the better accuracy of TLO, perhaps lower/intermediate rates can be examined in the future. Taken together these results demonstrate that despite the great improvements demonstrated by the excellent linearity and recovery profiles, the modified light obscuration method described here still presents challenges that remain to be addressed. Another interesting observation that can be made from the size distribution representation measured for the count standards is that although the same type of material was used in the three different measurements, only FI reported particles < ~2 μm for count standards of 5, 10, 15 and 20 μm, (see Figure S3.2). This can be explained by the detection of small, contaminating particles present in the standard solutions by FI.

Particle morphology and concentration

To further evaluate the instrument performance, morphology and concentration factors were considered. The goal was to understand if there were any attributes such as specific particle
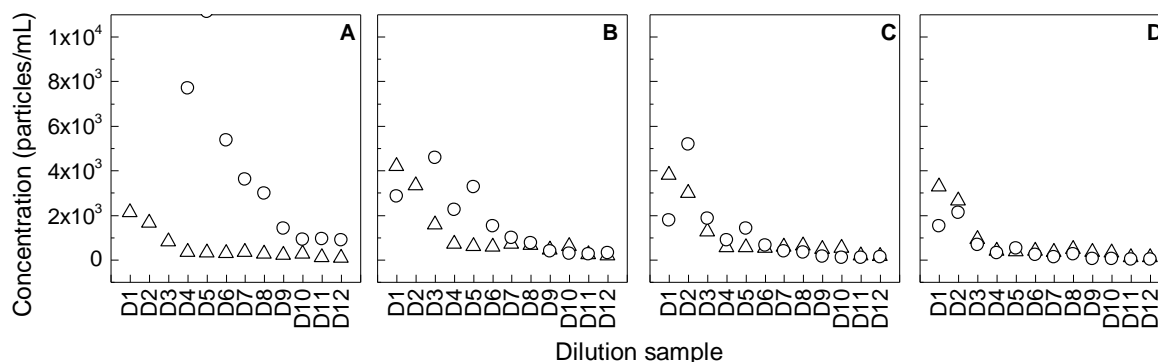
Figure 3.6 Comparison of the particle counts reported by FI $\bigcirc$ and TLO $\triangle$ of 2 dilutions series of mAb particles independently prepared. The horizontal axis represents the different dilution samples from D1=7500 particles/mL to D12=10 particles/mL in steps of 2.5 increase fold (theoretical values). The vertical axis represents the experimental particle concentration for different bins as follows: A) 1-2 μm, B) 2-5 μm, C) 5-10 μm and D) 10-25 μm. A better agreement between the 2 methodologies was found for the lowest concentrations and largest sizes

morphology, concentration and/or size range on which the TLO measurements showed a better agreement with the flow imaging technology. Such comparison would imply that implemented sensor and measurement's modifications positively overcome the alleged drawbacks of the light obscuration-based technique regarding the uneven optical density characteristic of protein particles. For the analysis of the morphology impact, mAb and ETFE (1) particle models were measured and the cumulative counts/mL was compared. The morphology characteristics of the particle models are described in Table S3.4. In general, mAb particles were less optically dense (more translucent) than the BSA particles used in this study. On the other hand, the ETFE particles presumably are highly stable (similar to latex beads) whilst retaining the typical morphology. The results of these measurements are presented in Figure 3.5. For both types of particles, FI reported the highest total counts of all three methods. This was also observed in the case of the BSA model particles (Figure 3.4), implying morphology aspects do not impact the sensitivity of FI. However, the discrepancy between FI and TLO was far less pronounced in the case of ETFE particles (Figure 3.5B) than in the case of mAb particles (Figure 3.5A) with a ratio FI/TLO of 7 and 1158, respectively. This observation

CHAPTER 3. Measuring Sub-Visible Particles in Protein Formulations Using a Modified Light Obscuration Sensor with Improved Detection Capabilities

105

can be attributed to the differences in the optical density between ETFE and proteinaceous particles smaller than 10 µm that still remain, although their shape is closely matched. (Figure S3.3).

Finally, the concentration impact was evaluated using mAb particles and the dilution scheme approach previously described. In contrast to the experiment shown in Figure 3.3 (on which the recoveries of particle dilutions were also followed) in this part of the work the focus was not on the total counts > 1 µm, but on defined size bins. Results are presented in Figure 3.6. The largest 10-25 µm particles, (Figure 3.6D), showed good agreement in all the concentration range tested. For the smallest particles 1-2 µm (Figure 3.6A), such comparability was observed only at low concentrations (around samples D1 to D3). The discrepancies in the smallest size-ranges were not surprising considering the largest particle counts in these size-ranges and also the strong over counting effect already demonstrated by FI (Figure 3.2). One hint of the potential contribution of small contaminating particles to this effect is seen in Figure S3.2. Although the exact ranges might vary for a different particle model, the results presented in Figure 3.5 and Figure 3.6 demonstrate that good agreement between light obscuration and flow imaging can be achieved even when measuring highly translucent particles using the TLO instrument configuration when concentration and size ranges are considered.

3.5 CONCLUSIONS

We have evaluated a novel light obscuration sensor and measuring mode which minimizes the interference of particle morphology by means of changing the measuring configuration from "intensity" to "pulse". The intended benefits of this approach were confirmed in terms of count accuracy, linearity and recovery as is indicated by the improved accuracy of counting polystyrene beads of 2 µm diameter and excellent linear and recovery response of protein particles in concentrations as low as 10 and up to 10000 particles/mL. Furthermore, it was demonstrated that despite the advantages that the flow-imaging technique offers, such as visualization of particles and characterization of particle morphology, an over counting effect is likely to be present. Thus, although flow imaging remains a valuable tool for particle characterization, its application to particle quantification remains to be evaluated.

 In contrast, the new modified light obscuration instrument demonstrated excellent accuracy, despite of the detected tailing which may need to be addressed in future instrument modifications (e.g. adjustments in the flow rate). It was also shown that the time-resolved approach successfully diminishes the morphology and optical density influence in the particle detection by the light obscuration principle.

Our work suggests that the pulse-width light obscuration-based approach offers major improvements for subvisible particle measurements in biotechnological therapeutic products by achieving a lower size limit of detection and elimination of particle morphology bias.

3.6 REFERENCES

1.   Carpenter JF, Randolph, Theodore W., Jiskoot, Wim, Crommelin, Daan J. A., Middaugh, C. Russell, Winter, Gerhard, Fan, Ying-Xin, Kirshner, Susan, Verthelyi, Daniela, Kozlowski, Steven, Clouse, Kathleen A., Swann, Patrick G., Rosenberg, Amy, Cherney, Barry 2009. Overlooking Subvisible Particles in Therapeutic Protein Products: Gaps That May Compromise Product Quality. Journal of Pharmaceutical Sciences. 98(4):1201-1205.

2.   Singh SK, Afonina N, Awwad M, Bechtold-Peters K, Blue JT, Chou D, Cromwell M, Krause H-J, Mahler H-C, Meyer BK, Narhi L, Nesta DP, Spitznagel T 2010. An industry perspective on the monitoring of subvisible particles as a quality attribute for protein therapeutics. Journal of Pharmaceutical Sciences. 99(8):3302-3321.

3.   Demeule B, Messick, S., Shire, S. J., Liu, J. 2010. Characterization of Particles in Protein Solutions: Reaching the Limits of Current Technologies. AAPS Journal. 12(4):708-715.

4.   Mach H, Arvinte, T. 2011. Addressing new analytical challenges in protein formulation development. European Journal of Pharmaceutics and Biopharmaceutics. 78(2):196-207.

5.   den Engelsman J, Garidel, Patrick, Smulders, Ronald, Koll, Hans, Smith, Bryan, Bassarab, Stefan, Seidl, Andreas, Hainzl, Otmar, Jiskoot, Wim Strategies for the Assessment of Protein Aggregates in Pharmaceutical Biotech Product Development. Pharmaceutical Research. April 2011, Volume 28, Issue 4, pp 920-933

6.   Barnard JG, Babcock, K., Carpenter, J. F. 2013. Characterization and quantitation of aggregates and particles in interferon- products: Potential links between product quality attributes and immunogenicity. Journal of Pharmaceutical Sciences. 102(3):915-928.

7.   Rosenberg AS, Verthelyi D, Cherney BW 2012. Managing uncertainty: A perspective on risk pertaining to product quality attributes as they bear on immunogenicity of therapeutic proteins. Journal of Pharmaceutical Sciences. 101(10):3560-3567.

8.   Wang W, Singh SK, Li N, Toler MR, King KR, Nema S 2012. Immunogenicity of protein aggregates-Concerns and realities. International Journal of Pharmaceutics 431(1-2):1-11.

9.   Filipe V, Hawe, A., Carpenter, J. F., Jiskoot, W. 2013. Analytical approaches to assess the degradation of therapeutic proteins. Trends in Analytical Chemistry. 49:118-125.

10.   Zölls S, Tantipolphan, R., Wiggenhorn, M., Winter, G., Jiskoot, W., Friess, W., Hawe, A. 2012. Particles in therapeutic protein formulations, Part 1: Overview of analytical methods. Journal of Pharmaceutical Sciences. 101(3):914-935.

11.   Narhi LO, Jiang, Yijia, Cao, Shawn, Benedek, Kalman, Shnek, Deborah 2009. A Critical Review of Analytical Methods for Subvisible and Visible Particles. Current Pharmaceutical Biotechnology. 10(4):373-381.

12.   Filipe V, Hawe, Andrea, Jiskoot, Wim 2010. Critical Evaluation of Nanoparticle Tracking Analysis (NTA) by NanoSight for the Measurement of Nanoparticles and Protein Aggregates. Pharmaceutical Research. 27(5):796-810.

13.   Wright M 2012. Nanoparticle tracking analysis for the multiparameter characterization and counting of nanoparticle suspensions. Methods in Molecular Biology (Clifton, NJ). 906:511-524.

14.   Burg TP, Godin, M., Knudsen, S. M., Shen, W., Carlson, G., Foster, J. S., Babcock, K., Manalis, S. R. 2007. Weighing of biomolecules, single cells and single nanoparticles in fluid. Nature 446(7139):1066-1069.

15.   Dextras P, Burg, T. P., Manalis, S. R. 2009. Integrated Measurement of the Mass and Surface Charge of Discrete Microparticles Using a Suspended Microchannel Resonator. Analytical Chemistry 81(11):4517-4523.

16.   Patel AR, Lau, Doris, Liu, Jun 2012. Quantification and Characterization of Micrometer and Submicrometer Subvisible Particles in Protein Therapeutics by Use of a Suspended Microchannel Resonator. Analytical Chemistry. 84(15):6833-6840.

17.   Panchal J, Kotarek J, Marszal E, Topp EM 2014. Analyzing Subvisible Particles in Protein Drug Products: a Comparison of Dynamic Light Scattering (DLS) and Resonant Mass Measurement (RMM). AAPS Journal. 16(3):440-451.

18.   Barnard JG, Rhyner, M. N., Carpenter, J. F. 2012. Critical evaluation and guidance for using the Coulter method for counting subvisible particles in protein solutions. Journal of Pharmaceutical Sciences. 101(1):140-153.

19.   Rhyner MN 2011. The Coulter Principle for Analysis of Subvisible Particles in Protein Formulations. AAPS Journal. 13(1):54-58.

20.   Sharma DK, Oma P, Pollo MJ, Sukumar M 2010. Quantification and Characterization of Subvisible Proteinaceous Particles in Opalescent mAb Formulations Using Micro-Flow Imaging. Journal of Pharmaceutical Sciences. 99(6):2628-2642.

21.   Strehl R, Rombach-Riegraf, V., Diez, M., Egodage, K., Bluemel, M., Jeschke, M., Koulov, A. V. 2012. Discrimination between silicone oil droplets and protein aggregates in biopharmaceuticals: a novel multiparametric image filter for sub-visible particles in microflow imaging analysis. Pharmaceutical Research. 29(2):594-602.

22.   Wilson GA, Manning MC 2013. Flow imaging: Moving toward best practices for subvisible particle quantitation in protein products. Journal of Pharmaceutical Sciences. 102(3):1133-1134.

23.   Zölls S, Weinbuch, D., Wiggenhorn, M., Winter, G., Friess, W., Jiskoot, W., Hawe, A. 2013. Flow Imaging Microscopy for Protein Particle Analysis-A Comparative Evaluation of Four Different Analytical Instruments. AAPS Journal. 15(4):1200-1211.

24.   Werk T, Volkin, D. B., Mahler, H. C. 2014. Effect of solution properties on the counting and sizing of subvisible particle standards as measured by light obscuration and digital imaging methods. European Journal of Pharmaceutical Sciences. 53:95-108.

25.   Kalonia C, Kumru OS, Prajapati I, Mathaes R, Engert J, Zhou S, Middaugh CR, Volkin DB 2014. Calculating the Mass of Subvisible Protein Particles with Improved Accuracy Using Microflow Imaging Data. Journal of Pharmaceutical Sciences.2015 Feb; 104(2):536-47.

26.   Cao S, Jiang Y, Narhi L 2010. A Light-obscuration Method Specific for Quantifying Subvisible Particles in Protein Therapeutics. Pharmacopeial Forum. 36(3):10.

27.   Weinbuch D, Jiskoot W, Hawe A 2014. Light obscuration measurements of highly viscous solutions: sample pressurization overcomes underestimation of subvisible particle counts. The AAPS Journal. 16(5):1128-1131.

28.   Hawe A, Schaubhut, F., Geidobler, R., Wiggenhorn, M., Friess, W., Rast, M., de Muynck, C., Winter, G. 2013. Pharmaceutical feasibility of sub-visible particle analysis in parenterals with reduced volume light obscuration methods. European Journal of Pharmaceutics and Biopharmaceutics 85(3):1084-1087.

29.   Philo JS 2006. Is any measurement method optimal for all aggregate sizes and types? AAPS Journal. 8(3):E564-E571.

30.   Vasudev R, Mathew S, Afonina N 2015. Characterization of Submicron (0.1-1 mum) Particles in Therapeutic Proteins by Nanoparticle Tracking Analysis. Journal of Pharmaceutical Sciences. 104(5):1622-1631.

31.   Weinbuch D, Zolls, S., Wiggenhorn, M., Friess, W., Winter, G., Jiskoot, W., Hawe, A. 2013. Micro-flow imaging and resonant mass measurement (archimedes) - complementary methods to quantitatively differentiate protein particles and silicone oil droplets. Journal of Pharmaceutical Sciences. 102(7):2152-2165.

32.   Zölls S, Gregoritza, M., Tantipolphan, R., Wiggenhorn, M., Winter, G., Friess, W., Hawe, A. 2013. How subvisible particles become invisible-relevance of the refractive index for protein particle analysis, Journal of Pharmaceutical Sciences. 102(5):1434-1446.

33.   Cao S, Jiao N, Jiang Y, Mire-Sluis A, Narhi LO 2009. Sub-visible particle quantitation in protein therapeutics. Pharmeuropa Bio & Scientific Notes. 2009(1):73-79.

34.   Sharma DK, King D, Oma P, Merchant C 2010. Micro-Flow Imaging: Flow Microscopy Applied to Sub-visible Particulate Analysis in Protein Formulations. The AAPS Journal. 12(3):10.

35.   Ríos Quiroz A, Québatte G, Stump F, Finkler C, Huwyler J, Schmidt R, Mahler H-C, Koulov AV, Adler M 2015. Measuring Subvisible Particles in Protein Formulations Using a Modified Light Obscuration Sensor with Improved Detection Capabilities. Analytical Chemistry. 2015 Jun 16;87(12):6119-24.

CHAPTER 3. Measuring Sub-Visible Particles in Protein Formulations Using a Modified
Light Obscuration Sensor with Improved Detection Capabilities

111

3.7 SUPPLEMENRATY MATERIAL
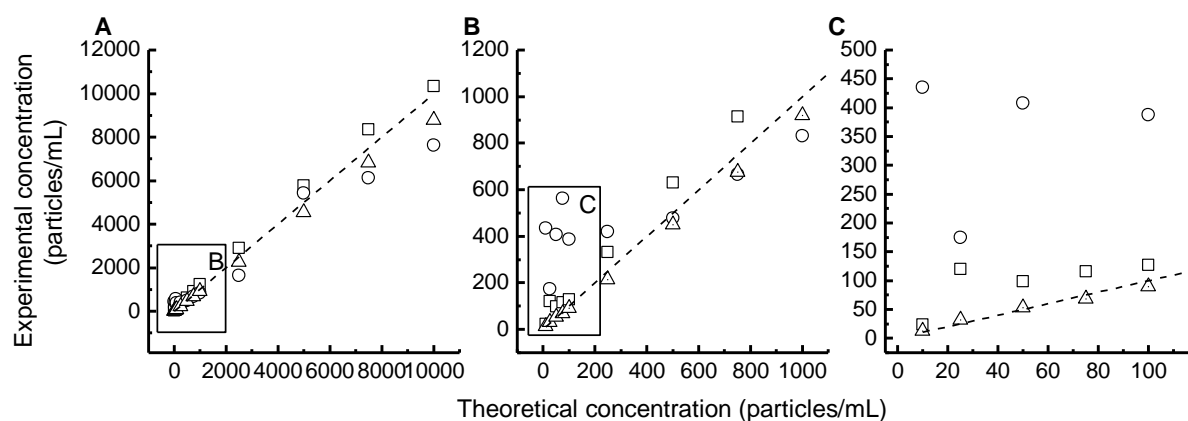
Figure S3.1 Several dilutions of BSA particles were prepared and measured in SLO □; FI ○ and TLO △. Graphs show the scatter plots of the theoretical versus the experimental concentration. The dotted line represents the ideal case. TLO showed a good performance even in the very low concentration range. Different panel represent different theoretical concentration ranges (particles/mL) as follows: A, 0-10000; B, 0-1000; C, 0-100.
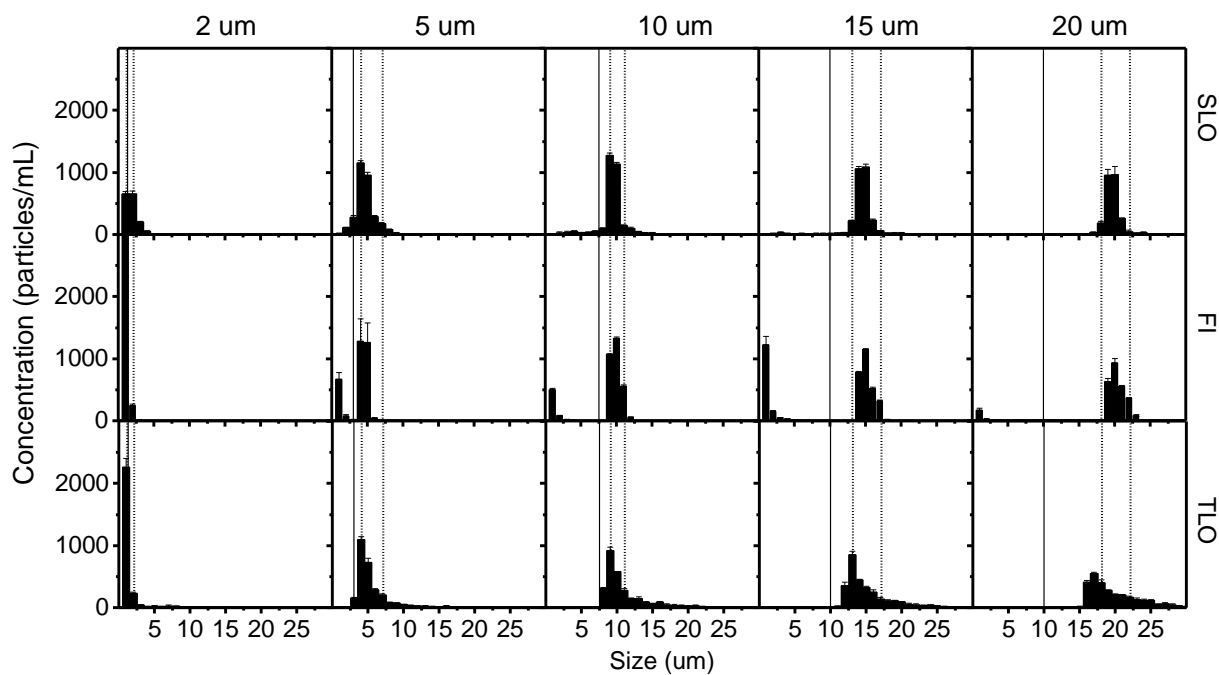
Figure S3.2 The size distribution of the corresponding measurements displayed in Figure 2 is presented. Quantification limits to fit count (supplier recommendations as follows: >1.3 μm for 2 μm; >3 μm for 5 μm; >7.5 μm for 10 μm and >10 μm for 15 μm and >15 μm for 20 μm) and size (authors' recommendations: ±10 % of the reported size) specifications are displayed with continuous and dotted lines, respectively
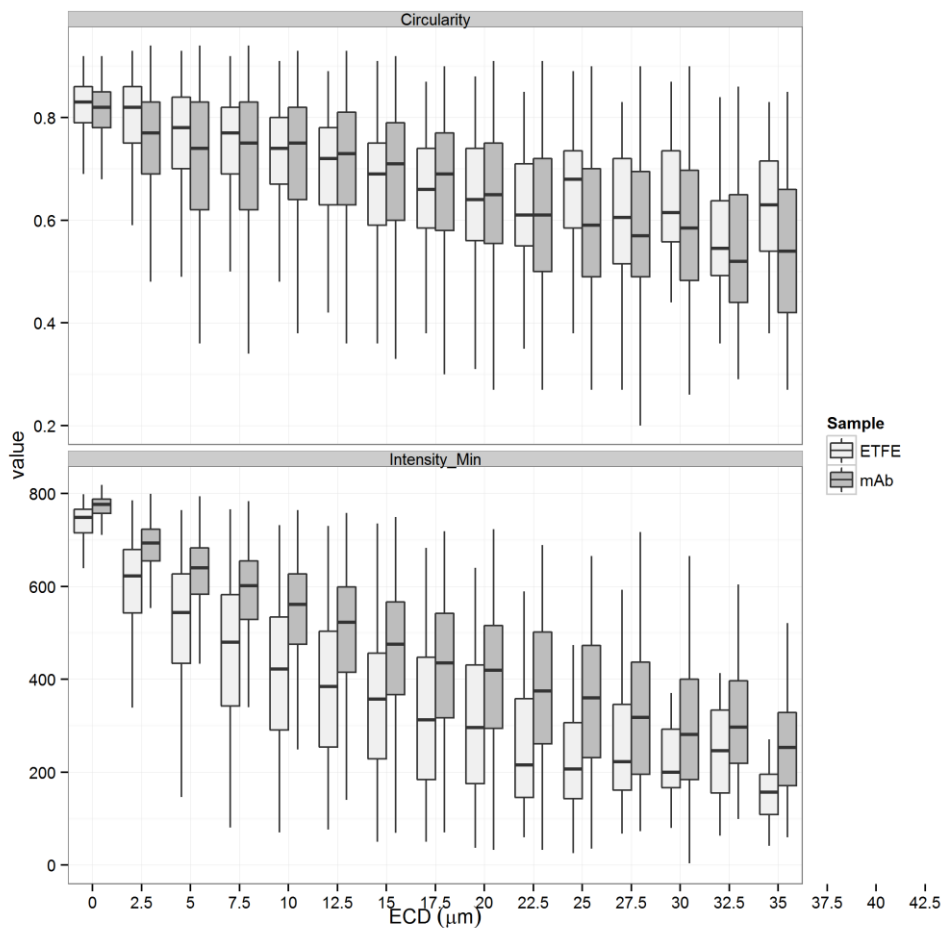
Figure S3.3 Morphological analysis of the mAb and ETFE particles measured by FI. Comparison of the particle shape (Circularity, upper panel) and darkness/translucency (Intensity Min, lower panel) parameters measured by MFI or ETFE (light grey) and mAb (dark grey). The data distributions were summarized in bins of 2.5 micrometers

Table S3.1 Polystyrene count standards of different sizes and 3000 particles/mL were measured in SLO, FI, and TLO. The recoveries in particles/mL ± standard deviation of 3 independent measurements are presented. Supplier specifications are ±10% recovery.

Standard	Counting accuracy (recovery %)		
	SLO	FI	TLO
2 µm	1596 ± 97	2833 ± 101	2807 ± 142
5 µm	2989 ± 75	3071 ± 58	2907 ± 36
10 µm	3016 ± 19	3028 ± 67	3128 ± 129
15 µm	2925 ± 24	2808 ± 27	3128 ± 129
25 µm	2828 ± 53	2753 ± 68	3065 ± 13

Table S3.2 Experimental concentrations of the dilution study. Theoretical and experimental concentration values of independent dilution sets of BSA particles measured in SLO, FI and TLO. For each dilution the mean and standard deviation of 3 measurements is presented
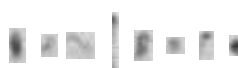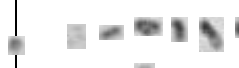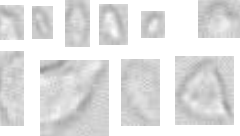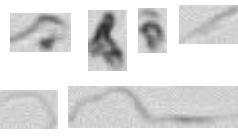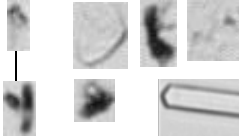
Theoretical concentration*	Experimental concentration* mean ± stdev of 3 measurements		
	SLO	FI	TLO
10	23 ± 6	435 ± 394	13 ± 173
25	120 ± 61	174 ± 64	32 ± 99
50	98 ± 16	408 ± 89	53 ± 103
75	116 ± 16	563 ± 528	68 ± 9
100	128 ± 26	387 ± 62	90 ± 47
250	332 ± 27	420 ± 53	213 ± 25
500	630 ± 72	478 ± 42	451 ± 28
750	915 ± 64	664 ± 57	674 ± 5
1000	1244 ± 75	832 ± 69	918 ± 15
2500	2911 ± 140	1653 ± 177	2267 ± 9
5000	5780 ± 124	5429 ± 2315	4546 ± 10
7500	8363 ± 643	6116 ± 88	6825 ± 7
10000	10339 ± 1350	7622 ± 248	8793 ± 4

* particles/mL

CHAPTER 3. Measuring Sub-Visible Particles in Protein Formulations Using a Modified
Light Obscuration Sensor with Improved Detection Capabilities

115

Table S3.3 The response of the experimental versus the theoretical particle concentration was modelled to a linear fit. For each order of magnitude, 4 points were included, (full range included 12 points). The following output parameters of the linear fit are presented: slope (ideal m=1), intercept (ideal b=0), coefficient of correlation (ideal r2=1) and sum of squares total (ideal SST=0)

Instrument	Linear fit parameter	Full range	10^1	10^2	10^3
SLO	m	1.06	1.04	1.21	1.12
	b	112.29	47.95	19.00	81.16
	r2	1.00	0.43	1.00	1.00
	SST	420000	3500	410	16000
FI	m	0.58	3.92	0.32	0.70
	b	50.23	132.01	243.39	-32.01
	r2	1.00	0.52	0.90	0.88
	SST	12000000	35000	2900	1600000
TLO	m	0.89	0.84	0.91	0.91
	b	15.38	7.92	-5.75	1.09
	r2	1.00	0.98	1.00	1.00
	SST	42000	35	90	130

Table S3.4 Morphological characterization of the particle models used. Representative randomly selected FI images of the particle models used are presented. The first 100 particles detected in the run were analysed and mean ± standard deviation values of the morphological parameters are reported

Size	Morphological parameter	BSA	mAb	ETFE
1-2 μm	ECD	1.24 ± 0.22	1.28 ± 0.25	1.27 ± 0.24
	Circularity	0.71 ± 0.08	0.78 ± 0.09	0.82 ± 0.06
	Aspect ratio	0.49 ± 0.15	0.65 ± 0.19	0.75 ± 0.14
	Intensity stdev.	9.53 ± 4.2	17.46 ± 11.36	18.73 ± 10.04
2-5 μm	ECD	2.93 ± 0.79	3.15 ± 0.86	3.08 ± 0.85
	Circularity	0.62 ± 0.08	0.73 ± 0.13	0.8 ± 0.09
	Aspect ratio	0.4 ± 0.13	0.62 ± 0.22	0.72 ± 0.16
	Intensity stdev.	17.68 ± 8.43	44.17 ± 31.83	58.72 ± 34.75
5-10 μm	ECD	6.82 ± 1.36	7.14 ± 1.42	7.08 ± 1.41
	Circularity	0.52 ± 0.1	0.69 ± 0.15	0.76 ± 0.11
	Aspect ratio	0.46 ± 0.2	0.61 ± 0.22	0.68 ± 0.16
	Intensity stdev.	26.28 ± 13.62	63.72 ± 44.04	89.56 ± 48.29
10-25 μm	ECD	14.12 ± 3.62	15.62 ± 4.22	14.26 ± 3.69
	Circularity	0.46 ± 0.14	0.59 ± 0.16	0.72 ± 0.11
	Aspect ratio	0.57 ± 0.22	0.49 ± 0.21	0.62 ± 0.16
	Intensity stdev.	43.53 ± 24.29	74.88 ± 46.39	127.57 ± 55.44

CHAPTER 4

Characterization of Sub-Visible Particles Using Nano Tracking Technology: Considerations for Method Development

Anacelia Ríos Quiroz
Joerg Huwyler
Hanns-Christian Mahler
Roland Schmidt
Atanas V. Koulov

CHAPTER 4. Characterization of Sub-Visible Particles Using Nano Tracking Technology: Considerations for Method Development

119

4.1 ABSTRACT

Within the framework of particle characterization methods for Biotechnological products, the current study aimed to provide a description of the variables that affect the performance of the Nano Tracking Analysis technique. The method of tracking particles under Brownian motion as they interact with a laser beam was evaluated using a LM20 NTA instrument from NanoSight. Sample- and instrument-related variables were studied using different model protein formulations, polystyrene nano-sized standards and one model of artificially generated protein particles. Experiments were designed to focus on dilution procedures, video recording settings and the precision of the size and concentration measurements. One of the study's main findings is that high protein concentration, or high particle polydispersity (typical characteristics of a biotechnological therapeutic product), can compromise the interpretation of NTA results. Furthermore, this methodology demonstrated a high sensitivity towards slight changes in the user-defined parameters, leading to high variability of the measurements. Greater reliability was found in the size determinations. Finally, the uncertainty in the calculation of the sample volume that is analyzed was found to be the main downside of this technique. Several variables were found to interfere with the Nano Particle Tracking assessments. The proper inclusion of the considerations here outlined to the development of sample-specific methods will surely increase the understanding of the results and contribute to the better performance of the technique in the frame of research and development activities.

CHAPTER 4. Characterization of Sub-Visible Particles Using Nano Tracking Technology: Considerations for Method Development

121

4.2 INTRODUCTION

Nano Tracking Technology (NTA) is a technique capable of measuring single particles in solution and reporting size and concentration data. The basis of the technique is tracking of *x, y* coordinates of the particles' Brownian motion for the calculation of the diffusivity (D_t) of individual particles:

$$D_t = \frac{(x,y)^2}{4}$$

NTA obtains the location of particles along the time (speed of the movements) using video recording. As signal enhancer, the instrument has a laser unit that applies light to the sample chamber that makes it interact with the surface of the suspended particles. When the light is scattered out of the particles, a charge-coupled device (*CCD)* (1) camera connected to a microscope objective generates a digital image. This image is then collected through many frames, creating a video of user-defined duration. Using an internal NTA algorithm, the tracking of each individual particle occurs, following user-defined parameters: *i)* Detection threshold set to the minimum brightness as compared to the background, above which a pixel will be considered as a particle. The higher the value, the lower the number of particles detected for a given frame; *ii)* Blur set to the area in pixels around any detected particle centre in which changes in pixel intensity (as compared to the background) will be assumed to proceed from that specific particle centre. The higher the value, the lower the noisy particles detected; *iii)* Minimum expected particle size set to the distance in pixels in which a particle will be searched from frame to frame in order to construct its trajectory. Particle centres detected outside this area will be considered as independent centres. The higher the value, the smaller the search area; *iv)* Minimum track length set to the minimum number of consecutive frames, after which the tracked particle will be included in the analysis. The higher the value, the better the statistical robustness of the analysis.

For size determinations, a hypothetical hard sphere that diffuses at the same speed of the tracked particles is assumed (2). Thus the hydrodynamic diameter (*d*) can be obtained according to a two-dimensional modified version of the Stokes-Einstein equation by multiplying temperature (*T*) of the measurement by the Boltzmann constant (K_B); and dividing by the product of *pi* (π), sample viscosity (η) and diffusivity (D_t):

$$d = \frac{TK_B}{3\pi\eta D_t}$$

For count determinations the average particle abundance (average number of particles per frame) is divided by the sample volume analysed.

In the field of Pharmaceutical Technology, NTA represents a potential methodology for the characterization of particulate matter in Biotechnological products. It has been used for several applications and summaries are available (3, 4). Interesting examples of its use include the classification of aggregates in order to help develop protein formulation strategies (5); seeding studies that follow likely particle growth from nano to micron range (6); size characterization of particles immersed in biological fluid or in primary containers (7, 8).

Although some partial evaluation studies have been published (9-13), the present paper aims for a guideline that can support the development of an adequate method for subvisible particle characterization using NTA. Two main aspects were considered: those inherent to the instrument itself and those imposed by the nature of the proteinaceous samples. Although our group has already conducted some research on this topic, (see Chapter 1 and Chapter 2), this present paper seeks to further explore specific effects and artefacts.

4.3 MATERIALS AND METHODS

Materials

Different Roche-property proteins were used in the study as indicated in the text. Protein-1 is a low-concentration 0.36 mg/mL pegylated protein of approximately 40 kDa. Protein-2 is a humanized monoclonal antibody of approximately 145 kDa, in a concentration of 180 mg/mL. Protein-3 is a humanized monoclonal antibody of approximately 149 kDa, in a concentration of 25 mg/mL. The final formulations were use freshly filtered through an 0.22 μm Millex GV PVDF Membrane (Merck Millipore Ltd, Ireland). Only for Protein-3 were two different stress models generated after filtration, as described later. National Institute of Standards and Technology (NIST) traceable polystyrene nanospheres size standards in an aqueous medium were purchased from Nanosphere Thermo

CHAPTER 4. Characterization of Sub-Visible Particles Using Nano Tracking Technology: Considerations for Method Development

123

Scientific, Fremont, California USA. Particle free water was generated in house by filtration of degassed (Liqui-cel Membrane Contactors, Membrana; Germany) and bidestilated water through i) 0.22 μm Millex GP PES Membrane (Merck Millipore Ltd, Ireland) and ii) 0.22 μm GP Stericup (Express Plus, Massachusetts, USA).

Methods

For the short-term *stability studies*, a recommended (5 °C), accelerated (25 °C/60% r.h.), and/or a stress condition (40 °C/75% r.h.) was used depending on the type of experiment and protein model. Total particle concentration and size distributions were analysed. For the *dilution study* using standards, nanoparticles of sizes 50 nm, 200 nm, 300 nm, 500 nm and 900 nm were used in a mixture of 10 %, 70 %, 12 %, 6 % and 2 % (v/v), respectively. This proportion was considered to be representative of what is typically found in polydisperse stressed protein samples (see Chapter 2). A final concentration of 1×10^9 particles/mL was adjusted assuming sphere volume for the particles and the solid content reported by the provider. From this stock, dilutions to achieve $(7.5, 5.0, 2.5 \text{ and } 1.0) \times 10^8$ particles/mL were prepared using particle free water (0.02 um Anotop 25, Whatman, Glattbrugg, Switzerland). Each dilution was video recorded in 60 second triplicates i) keeping the shutter and gain parameters constant and ii) making adjustments as needed according to the characteristics of each sample. The data was then analysed, comparing theoretical to experimental concentrations and that ratio was expressed as percentage. For the study of the *video recording time and MES* impact, artificially generated Protein-3 particles were used. Applied stress consisted of 2 h stirring a 5 mL sample in a 6 mL glass vial at 200 rpm in a magnetic multichannel stirring plate, using a Teflon bar of 6 x 15 mm. The stock solution along with 1:5; 1:10 and 1:80 dilutions (diluent was unstressed formulation 0.02 um Anotop 25, Whatman, Glattbrugg, Switzerland) were measured in triplicates at 4 different video durations (10; 30; 60 and 90 s) and 8 different MES values (30; 50; 80; 100; 150; 200; 250; 300 and 400). For the *intermediate precision,* 6x Protein-1 samples stored for 2 months at 5 °C were manually ejected into a Type I glass vial over a timespan of 20 to 25 seconds (s) each. Before measurements, pooled solutions were manually homogenized by repeated inversions of the vials. Intermediate precision was defined as the variance of the reported particle concentration values of triplicate consecutive measurements of identically prepared and independent samples performed by

different analysts on different days. For the *video recording settings*, 500 nm standard particles (Thermo Fisher Scientific) and the stressed model Protein-3 were used. Single measurements using all possible combinations of shutter (from 0 to 1000) and gain (from 0 to 400) in steps of approximately 50 units were applied. The standard was properly diluted with water to achieve a final concentration of 1×10^{8} particles/mL, according to the solid content of the standard solutions given by the manufacturer, and density of 1.05 g/cm3 (according to the manufacturer's certificate) for the polystyrene material. The stress condition on Protein-3 was applied by heating the formulation up to 73 °C for 7minutes using a Thermostat station (Eppendorf, Germany).

Nanoparticle Tracking Analysis (NTA)

The Nanosight NS200, LM20 equipped with a 405 nm laser and the NTA 2.2 version was used. Video images were collected at 37.8 frames per second. The detailed instrument handling has already been reported (see Chapter 2). Briefly, before each measurement, chamber cleanness was verified using 0.02 μm filtered water (Anotop 25, Whatman, Glattbrugg, Switzerland). Samples were injected using 1 mL sterile syringes (Norm-Ject, HSW, Tuttlingen, Germany). The first volume was used to rinse out the flushing water, and with the remaining volume, one to three videos (as indicated in the text) of 60 seconds were recorded using a replenished sample each time. Video recording parameters of shutter and gain were set to ensure that clear and sharp particle images were obtained. Initial gross focus was manually adjusted. Starting from shutter equals to zero, this value was increased until there were no new particles visible on the screen. Then, starting for gain equals to zero, this value was increased until the best possible contrast between the background and the particles was achieved. Final adjustments were done to find the best focus, shutter and gain combinations for the best screen visualization of particles. During the measurements, the temperature was recorded by a temperature sensor housed within the viewing unit of the instrument. Sample viscosity was determined using a cone rheometer instrument (Anton Paar AG Switzerland, Zofingen, Switzerland) at 29 and 23 Celsius degrees. Viscosity values in steps of 0.1°C were interpolated and product-specific viscosity tables were loaded in the instrument's software. Video analysis settings were set as follows: detection threshold value was set so that the software recognized every actual particle centre with a red cross. The blur value was set so that the area around every particle was clear and without the presence of noise

CHAPTER 4. Characterization of Sub-Visible Particles Using Nano Tracking Technology: Considerations for Method Development

125

particles (blue crosses). The applicability of these 2 settings was optimal for all video frames. The minimum track length was set to 10. The minimum expected particle size was set to automatic, so that the software calculated it based on the first 100 tracks. When video recording settings were similar, videos were analysed as batch, otherwise analysis parameters were optimized for each independent video. The summary data as *.csv* file as well as the 10 s video were generated for analysis.

4.4 RESULTS

Sample related considerations

Scatter of oligomeric species The applicability of NTA to the analysis of proteinaceous particles frequently offers the challenge of high scatter species of sizes smaller than the lower 30 nm limit of detection. To demonstrate this effect, a Protein-1 sample was stored for one week at 40 °C. As can be observed in Figure 4.1, the quality of the video was poorer when compared with the non-stress control sample. Horizontal stripes appeared, resembling an "old-TV" effect. This compromised the clear visibility of all the particles present (see also Video 4.1 and Video 4.2). To a lesser extent, this phenomenon was also observed in a short-term stability study when a different Protein-2 was stored for two months at 5 °C and 25 °C (see Video 4.3 and Video 4.4). The analysis of those samples reported a total concentration of (16.3 ± 4.9 and 4.5 ± 3.2) x 10^6 particles/mL, respectively (Figure 4.2A).

Trying to improve the quality of the videos and reduce the signal of oligomeric species (see Figure S4.1), a 1:10 dilution with unstressed formulation was performed. Such treatment positively impacted the video recording step (see Video 4.5 and Video 4.6) with better image quality. Furthermore, the inconsistent trend of lower counts at higher temperatures was reversed with a total concentration of (122.13 ± 82 and 247.6 ± 58.7) x 10^6 particles/mL for the 5 °C and 25 °C storage conditions, respectively (Figure 4.2B). Although this could suggest an unmasking effect of actual present particles, our group's recent publication had shown the likely over counting artefact that particle dilution can include in the analysis (see Chapter 2).

The effect of particle dilution was further studied using a mixture of latex beads and a previously reported dilution protocol (see Chapter 2). From a stock solution containing a mixture of different
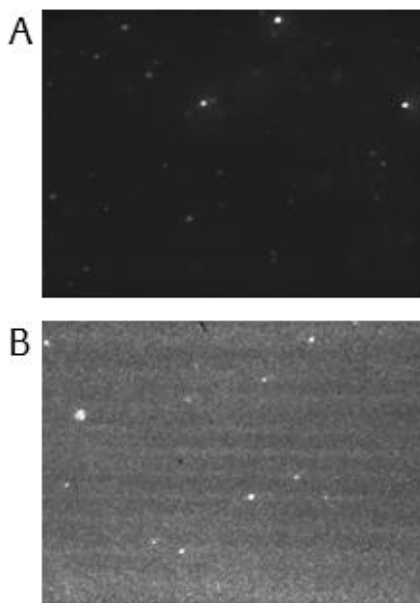
Figure 4.1 High scattering of oligomeric species. A low-concentration Protein-1 sample was stored for a week at A) 5 °C (control) and B) 40 °C (stress condition). The first frames of the NTA videos are presented. The old-TV effect in B) possibly compromises the good visibility of all the actual particles present.

nanoparticles, four independent dilutions were prepared. Each sample was then analysed i) using shutter and gain parameters accordingly to the best adjustments as per each independent sample and ii) using the same shutter and gain parameters as the ones used to define the initial concentration of the stock. Interestingly, it was possible to achieve acceptable recoveries around 100% only when the camera level was kept constant and equal to the one t used for the analysis of the undiluted sample (open symbols in Figure 4.3C). By contrast, when the camera level was adjusted to be optimal for each sample, the expected over counting effect was confirmed (closed symbols in Figure 4.3C). This would suggest that shutter and gain parameters should be kept constant among family of samples. However, the comparison of the first recorded frame, when the camera level was optimized (Figure 4.3A), with the frames in which the camera level was kept constant (Figure 4.3B), showed that some actual particles present were missed. On the other hand, following vendor recommendations of 20 to 100 centres per frame and more than 200 valid tracks to consider the analysis valid, both practices would be accepted (Figure 4.3E and Figure 4.3F). Notably, the size determinations remained stable independent of the recording adjustments (Figure 4.3D).
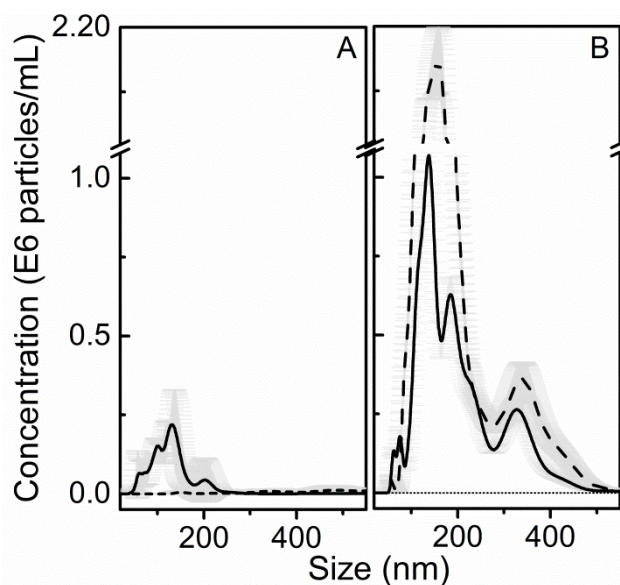
Figure.4.2 A Protein 2 formulation was stored for two months at 5 °C (—) and 25 °C (--). Samples were measured directly (A) and after 1:10 dilution (B). Fresh and 0.02 µm filtered formulation was used as diluent (·····). An apparent unmasking effect can be observed after dilution.

Video recording time and minimum expected particle size Video duration can be adjusted depending on sample concentration. For a low particle burden, the longest video length is recommended. By increasing the recording time, the number of possibly completed tracks also increases and enough statistical information is then collected to determine particle size and concentration. This aspect of the NTA system was challenged in terms of repeatability by using a highly concentrated sample and varying the video recording time from 10; 30; 60 and 90 seconds. Dilutions of 5; 10 and 80 fold were also measured.

Results indicated that the video duration had a smaller impact on the size determinations (overall CV of 15 %), ([Figure S4.2A](#)) but strong impact on the concentration determination factors (overall CV of 174 %). There was a tendency to apparent higher concentrations as the recording time increased, especially at higher dilution factors ([Figure 4.4](#)).

The effect of the minimum expected particle size as a function of the video duration was also studied. Each sample was recorded at MES values of 30; 50; 80; 100; 150; 200; 250; 300 and 400. This is represented in the box plots of [Figure 4.4](#). Concentration assessment was mostly independent of the MES value as indicated by the low variability of the assessments (except for the longest video duration
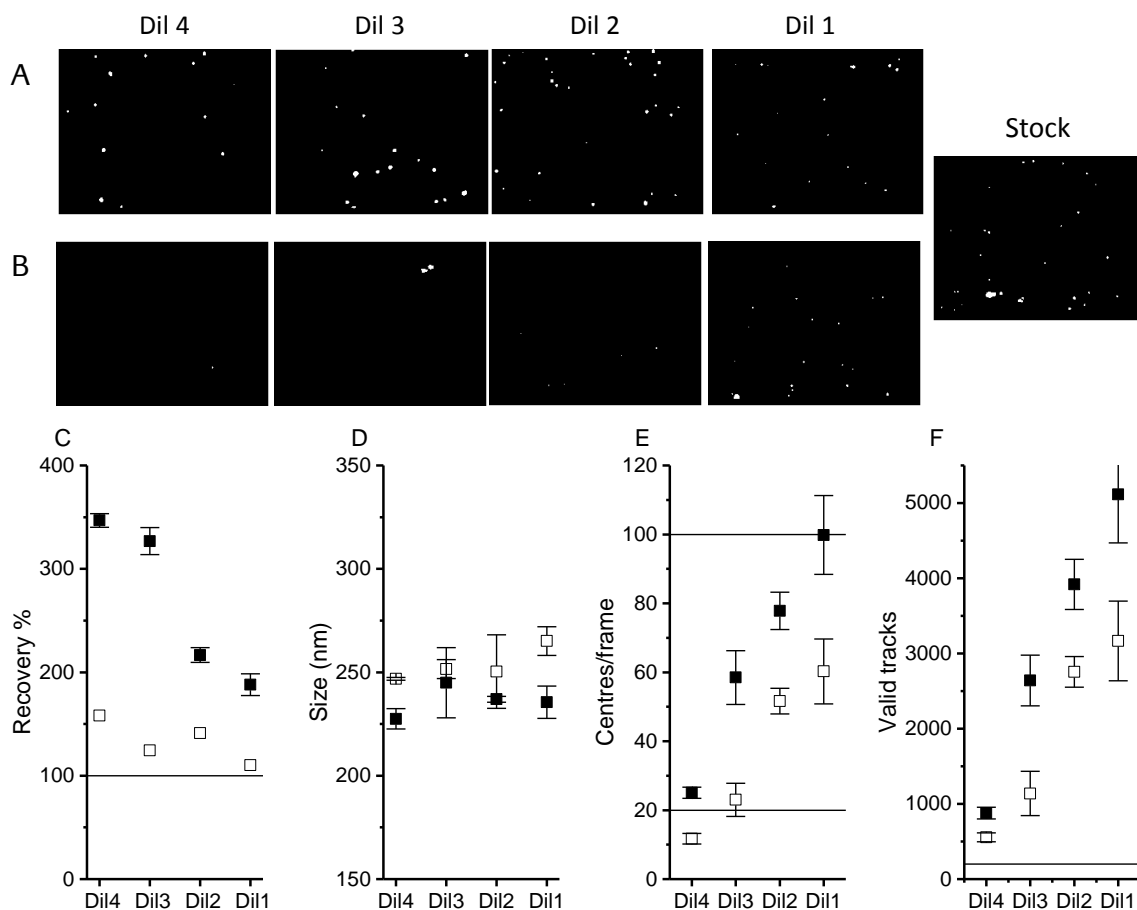
Figure 4.3 Video recording settings and accuracy of counting. Comparison of a mixture of latex particle beads measured in NTA when the video recording settings were adjusted for each independent sample (B, ■) and when they were kept constant for all sample sets (A, □). Images show the first frame of the video per each dilution, in a decreasing concentration from left to right. Although both video recording modalities report the dilution tendency, very noticeable discrepancies can be observed in terms of recovery (C). Size determination (D) as well as the control parameters centres/frame (E) and valid tracks (F) were less sensitive to the adjustments.

at the highest dilution factors). However, the size assessments, showed less robustness in front of MES changes.

Instrument related considerations

Precision In order to evaluate NTA robustness, two identically prepared Protein-1 samples stored for two months at 5 °C were measured independently on different days by different people. The quality of the videos recorded by each analyst was different (see Video 4.7 and Video 4.8) as well as the particle size distribution (see Figure S4.2). When a given video was analysed

CHAPTER 4. Characterization of Sub-Visible Particles Using Nano Tracking Technology: Considerations for Method Development

129
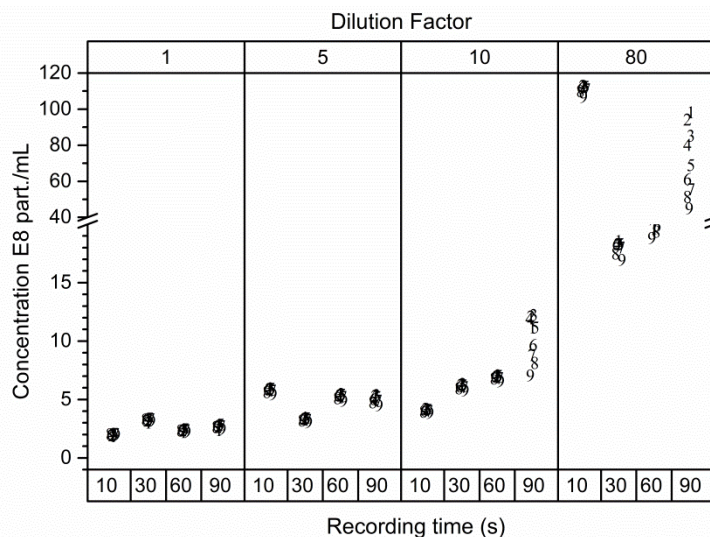
Figure 4.4 Effects of different video recording durations on the concentration determinations of a stressed protein model measured undiluted and at 5; 10 and 80 fold diluted with unstressed formulation. Numbers from 1 to 9 indicate single independent measurements of the same sample at the following different Minimum Expected particle Size (MES) values: 30; 50; 80; 100; 150; 200; 250; 300 and 400, respectively.

either by Analyst 1 (A1) or Analyst 2 (A2), the variability associated with the particle count determinations was lower as compared to the opposite scenario in which either A1 or A2 analysed a self-recorded video or a video recorded by another(Figure 4.5 and Table 4.1). Although both the video recording and video analysis are important steps, this experiment demonstrates that video recording is the more critical. These results also show that, even with highly experienced analysts, the intermediate precision of the technique is poor. It is important to notice that the analytical software appeared to be powerful and capable enough to account for the video differences in terms of size determinations (CV between A1 and A2, 1 %). Interestingly, the operator manipulation includes high variability to the measurements mainly to the concentration determination (CV between A1 and A2, 20 %).

Video recording settings From the previous experiments, it was found that choosing the right camera level is a sensitive parameter that can significantly vary the outcome of NTA measurements. Despite that, there is no clear guidance on how to select it and even highly experienced analyst have no standard optimal value settings. This becomes a critical point, especially when samples are not part of a stability study in which the unstressed material or the initial time point could serve as a reference. Consequently, a large scanning experiment was performed in which all possible combinations of
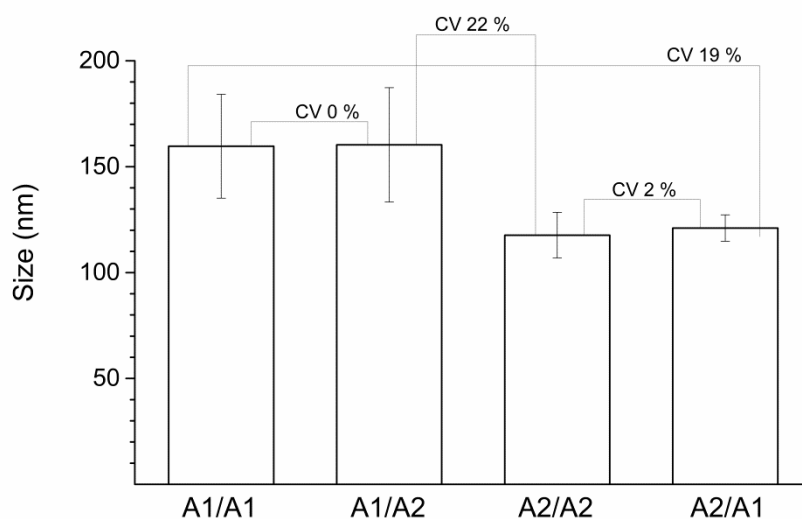
Figure 4.5 Intermediate precision – concentration assessment. The particle concentration of a protein sample independently assessed by two experienced analysts is presented. X axis follows the nomenclature: "Analyst who performed the video recording/Analyst who performed the video analysis". The variability of the measurements when a given video was analysed by different analysts (e.g. A1/A1 vs A1/A2) and the variability of the measurements when a designated person analysed either a self-recorded video or a video recorded by someone else (e.g. A1/A1 vs A2/A1) is presented as CV % values. More variability was found between videos recorded by different people.

shutter (from 0 to 1000) and gain (from 0 to 400) were applied to the analysis of a 500 nm polystyrene sample at a concentration of 1×10^8 particles/mL. In Figure 4.6 the results in particles/mL and mean size are presented. The mean values of all tested combinations were sample concentration of $(6.8 \pm 1.7) \times 10^8$ particles/mL and particle size of 432 ± 34 nm showing severe overestimation of the concentration and an undersizing by 13 % (Table 4.2).There was a broad range of possible shutter and gain combinations that fit the criteria of more than 200 completed tracks and 20-100 centres/frame for the analysis to be considered valid (black symbols in Figure 4.6). Interestingly, for a given gain value, small changes of 50 units in shutter consistently produced changes in the particle concentration (CV range 15-40 %) to a lesser degree, in the size determination as well (CV range 3-9 %) (Table 4.2). This effect was more pronounced in the largest gain values in which the number of invalid analysis also increased (grey symbols in Figure 4.6). Only around gain = 100 a certain stability was found in the concentration results. However, at this gain level the size results showed high variability. The opposite situation of stable results in terms of size, but high variability for the particle concentration assessment

CHAPTER 4. Characterization of Sub-Visible Particles Using Nano Tracking Technology: Considerations for Method Development

131

was found at gain = 50. The same experiment was carried out using a model of artificially generated protein particles. In that case, the acceptance criteria for valid tracks and centres per frame constrained the possible adjustments to a much narrower window than that of the polystyrene measurements (Figure S4.6). Although in that range the concentration assessment was stable, the size determinations presented a much higher variability when compared to latex beads.

Camera field of view To further investigate in the possible reasons for the results variability due to the video recording settings, the sample volume was analysed in greater detail. The sample chamber dimensions were 80 x 100 x 10 µm which gives a field of view of 8×10^{-8} mL. The consequences of measuring of such a small volume have been already discussed (see Chapter 1). One attempt to correct for this shortcoming was the injection of the sample using a pump to increase the amount of volume sampled. However, in our experience this was not enough to correct the low accuracy (Figure S4.3). Given the average counts of particles/frame and the equivalent particle concentration in the analysis report, it is possible to reverse calculate the volume that was assumed for each measurement. For example, in the case of the 500 nm particles measured at gain = 0 and shutter = 24, the average number of particles/frame was 7 and the reported concentration was 0.94×10^{8}. Thus a sample volume of 7.4×10^{-8} mL was estimated. In contrast, when gain = 0 and shutter = 1004, average number of particles/frame was 35 and the reported concentration was 5.49×10^{8}. Thus a sample volume of 6.5×10^{-8} mL was estimated. This trend of lower apparent volumes as the shutter value increase was also found for the larger gain values (Figure 4.7 and Table S4.1).

Table 4.1 Intermediate precision assessment. Video recording and video analysis parameters of the measurement of a protein sample identically prepared and independently measured by two different analysts on different days.

Video recording	Analyst 1 (A1)						Analyst 2 (A2)					
	Video 1		Video 2		Video 3		Video 1		Video 2		Video 3	
Shutter	1265		1265		1265		299		299		299	
Gain	253		283		268		299		377		377	
Video analysis	A1	A2	A1	A2	A1	A2	A1	A2	A1	A2	A1	A2
Blur	7	7	7	7	7	7	7	9	7	9	7	9
Detection Threshold	7	9	8	11	8	10	14	12	14	13	14	11
Min Track Length	10	10	10	10	10	10	10	10	10	10	10	10
Min Expected Size	50	100	50	100	50	100	100	50	100	50	100	100
Results	Mean			Stdesv			Mean			Stdesv		
Concentration	2.66E+08			1.72E+07			3.58E+08			5.09E+07		
Size	139			30			141			28		
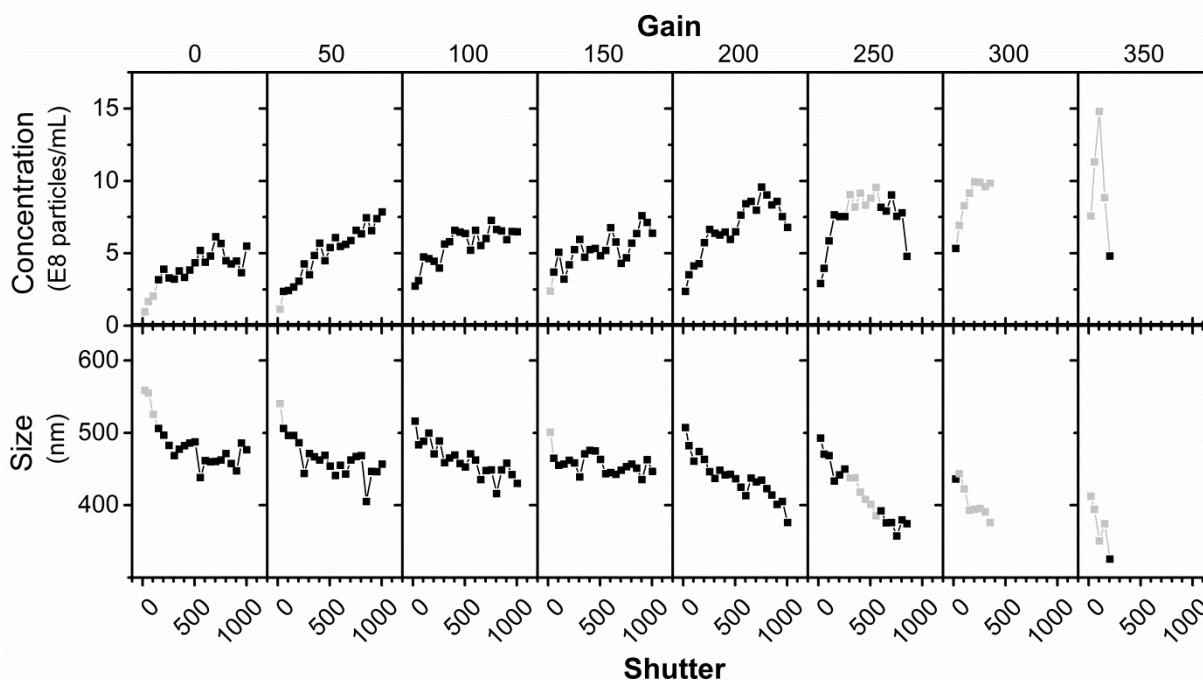
Figure 4.6 Scanning of the video recording settings using latex beads. A 500 nm latex solution with a concentration of 1 x 10^8 particles/mL was measured in NTA. Different video recording settings were applied to cover a broad combination of shutter and gain values. Each panel represents a fixed gain from 0 to 350 in steps of 50 units. The X axis represents a fixed shutter value from 0 to 1004 in steps of 50 units. The Y axis represents the concentration (upper row) and the size results (lower row). Considering limits of 20-100 centres/frame and more than 200 completed tracks, valid ■ and invalid ■ tracks are presented.

4.5 DISCUSSION

Particle characterization in biotherapeutics covers a broad range of sizes from visible particulate matter (> 150 μm) down to oligomers or soluble aggregates (< 100 nm) (1). The Nanoparticle Tracking Technology (NTA) by NanoSight is capable of covering parts of the lower size range of interest (30 nm up to 1 μm) that before was only partially covered by other techniques like SEC or DLS. The theoretical basis of Brownian particle motion applied to size determinations has been broadly studied (2). Unpublished data from our lab suggests, however, that given the irregular shape of protein particles, the same estimations may be different when working with non-sphere and uneven optically dense particles. Furthermore, despite the great potentiality of NTA and the importance of collecting particle information in the nanometre range, in this study we explored specific effects that can influence the accuracy of the results. Such effects were divided in sample- and instrument-related.

CHAPTER 4. Characterization of Sub-Visible Particles Using Nano Tracking Technology: Considerations for Method Development

133

The first part focused on the likely incompatibility of biotechnological samples analysed by NTA. The later in turn, describes a more in-depth analysis of the technique's drawbacks that were outlined in recent publications (Chapter 1 and Chapter 2). The main sample-related issue appeared to be the typically high concentration of biotherapeutic samples. Although the monomer signal cannot be individually resolved, this weak scatter light can interfere with the resolution of other particles present. This phenomenon is normally accompanied with an increase in the percentage of oligomers detected by SEC (Figure S4.1) and produces the "*old-TV*" effect illustrated in Figure 4.1. This can be attributed to the noisy signal of these species resulting in poor video quality (Video 3 and Video 4). Furthermore, an apparent decrease in counts of around 70 % after two months storage at 25 °C could be detected (Figure 4.2A). This finding is in line with a previously reported stability study in which a different protein model showed a decrease in the particle concentration of 40 % and 80 % after two months storage at 25 °C and 40 °C, respectively (see Chapter 1). One common practice to improve the analysis of this type of samples is dilution with unstressed material (3, 4). By these means, soluble aggregates (oligomeric species) return to solution and the video recording improves. This step did, however, i) make particles appear sharper (Video 5 and Video 6) and ii) reverted the particle concentration assessment to the expected trend of higher counts at higher temperatures (Figure 4.2B). This unmasking effect is likely to add other artefacts. It is important to note that, besides particle dilution, this effect is also present within the stability studies in which any changes in the particle

Table 4.2 Size and concentration results of the scanning experiment. Dispersion descriptors at fixed gain values of the size and concentration assessments of a latex bead sample measured at different shutter values ranging from 0 to 1006 in steps of 50 units.

Gain	Size (nm)				Concentration (E8 particles/ml)			
	Mean	**Stdesv**	**CV%**	**Range[1]**	**Mean**	**Stdesv**	**CV%**	**Range[1]**
0	470.6	15.7	3	58.6	4.4	0.9	20	2.9
50	453.5	16.6	4	66.4	5.8	1.2	21	4.3
100	458.3	20.7	5	83.6	5.9	0.9	15	3.3
150	455.2	11.5	3	40.2	5.4	1.1	21	4.4
200	434.6	25.5	6	106.4	6.9	1.7	24	6.1
250	412.1	35.4	9	112.8	7.7	1.5	20	5.6
300	406.3	24.3	6	67.4	8.6	1.7	20	4.6
350	371.3	34.4	9	86.8	9.5	3.8	40	10.0

[1] Max-Min
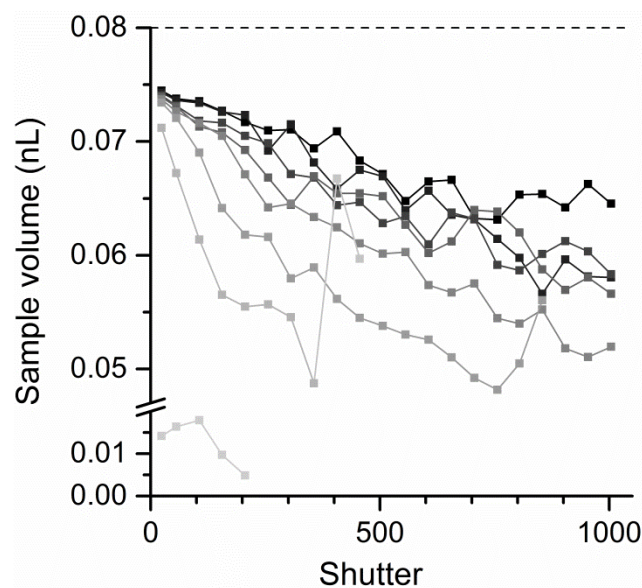
Figure 4.7 Sample volume as a function of gain and shutter. From the experiment reported in Figure 6 the ratio: (average number of centres per frame)/(concentration) was calculated to obtain the related sample volume (Y axis) as a function of all possible combinations of shutter (X axis) and gain (increasing from 0 ■ to 350 ■ in steps of 50 units) values. All values were inferior to the actual chamber volume of 0.08 nL (chamber dimensions: 80 μm x 100 μm x 10 μm).

population will force the camera level to be adjusted. Furthermore, given the narrow concentration range in which NTA optimally works, some samples require dilution even without the oligomer scatter issue. One such artefact is the over counting that appears as the dilution factor increases. This detrimental effect in the counting accuracy of the technique was already described in Chapter 2. Another related artefact is the video recording parameters that diluted samples require as compared with the original, undiluted ones. As dilution makes the background clearer, higher shutter and gain values are generally needed to visualize all the particles present. This change in the camera level potentially compromise sample comparability. When a given sample was video-recorded by applying the shutter and gain settings that were optimal for the undiluted sample or by applying the new camera level necessary for the optimal visibility after dilution, the variability in the particle concentration assessment was higher than 30 %, with better accuracy for the former settings (Figure 4.3C). Interestingly, in terms of size the variability was lower than 8 % (Figure 4.3D). This suggests higher robustness in particle sizing rather than in particle counting for the NTA methodology. This statement is also supported by the lower variability obtained in the scanning experiment for the mean size values

CHAPTER 4. Characterization of Sub-Visible Particles Using Nano Tracking Technology: Considerations for Method Development

135

(CV < 9 %) as compared to the particle concentration ones (CV > 15 %) ([Figure 4.6](#) and [Table 4.2](#)). From this experiment, it becomes clear that the better practice is to keep the camera level unmodified and equal to that of the undiluted original sample. Despite the risk of missing actual present particles ([Figure 4.3A-B](#)), this will ensure a camera level comparability and thus comparability of the results as well.

Both previously described effects, the over counting and the incomparable camera levels, are related to the field of view resulting from specific shutter and gain combinations. This was studied in the second part of this research paper where the focus was the instrument-related artefacts. To calculate sample volume, the X and Y axis are fixed by the dimensions of the sample chamber. However, the Z axis is defined by the depth of the laser beam and, thus, influenced by the magnitude of the video recording settings. As shown in [Figure 4.6](#), NTA assumes a different volume per sample according to the shutter and gain values. That generates a specific apparent volume that can be as low as 0.005 nL ([Table S4.1](#)). However, the chamber dimensions (80 μm x 10 μm x 100 μm) are unchangeable and so is the 0.08nL volume of the sample to be analysed. As the instrument does not correct for this, the detected number of particles is related to an erroneous lower volume which partially contributes to the over counting effect. Furthermore, it has to be considered that for a heterogeneous sample, the apparent volume in which a small particle is immersed is larger than that for a larger particle. This estimation is difficult to assess, though.

One of the most generalized perceptions when working with NTA is the highly experienced analysts that the technique requires. However, the intermediate precision evaluation showed that, even for experienced analysts, the technique produces highly variable results. The fact that the methodology lacks of controls capable of guiding users to a standardized video recording procedure resulted in particle concentration differences of 21 % between the two Analysts ([Table 4.1](#)). (Interestingly, the impact on size determinations was minimal with a CV between Analyst 1 and Analyst 2 of only 1%. This result is in accordance with previously discussed results on which size showed also better robustness). The main difference was the shutter level that each analyst assigned (Analyst 1 = 1265 and Analyst 2 = 299). After discussion with both analysts about the criteria they used to perform the video recording, we learned that Analyst 1 prioritized the contrast of the major particle population.

Analyst 2, on the other hand, paid greater attention to clear visibility and good recordings of all actual particles. Although the image quality of both sets of videos was highly similar (see Video 7 and Video 8 as examples), the slightly brighter background obtained using a lower shutter value may have allowed the dimmest particles to be better recorded. This is reflected in the higher concentration and narrower size distribution obtained by Analyst 2 (Figure S4.2C) as compared to Analyst 1 (Figure S4.2A). Finally, this intermediate precision experiment showed that the NTA software has a good performance. Given a video, regardless of who performed the analysis, the results had low variability in terms of particle concentration with CV < 6 % (Figure 4.4). However, when a given person analysed a self-recorded video or a video recorded by another, the variability was much larger (CV > 20 %). This suggests that video recording is the most critical and user-dependent step. The same observations were also done for the size assessment (Figure S4.5).

The experiments about the video recording settings (Figure 4.3) and the intermediate precision (Figure 4.4) showed the importance of the right shutter and gain parameters selection. This will allow for good accuracy of counting, sample to sample comparability and high intermediate precision as demonstrated in the previously described experiments. To define the video recording parameters, a methodology comprising many variations was utilized in a scanning experiment (Figure 4.5 and Figure S4.3). This allowed all possible shutter and gain combinations to be tested. Although some combinations were clearly inappropriate and produced over exposed images (Figure S4.6), this approach defined a range in which shutter and gain changes produced no change in the concentration and size determinations. Such a range could be then defined as a range to limit all the possibilities for the comparable analysis of a family of samples (different time points, different dilutions, different analyst etc.). Surprisingly, the range that was identified to obtain relatively constant concentrations was different than the range needed to obtain constant size values. This means that although NTA is capable of giving both types of information, a different optimal setting is required for each one. In contrast to the experiment using polystyrene nanoparticles, the experiment with artificially generated protein showed a much narrower range for achieving a valid analysis. This can be attributed to differences in the refractive index of the protein particles and heterogeneity of the sample. This is also

CHAPTER 4. Characterization of Sub-Visible Particles Using Nano Tracking Technology: Considerations for Method Development

137

consistent with other studies that reported different instrument performance depending on the particle nature (see Chapter 2).

One of the most notable facts about the NanoSight Company is the number of NTA generations available on the market. Although the present evaluation was done using one of the first models, it is possible that some labs still work with the LM20 version. Maintaining an up-to-date particle laboratory requires a costly investment that, in some cases, is not easy to justify provided the immaturity of most of the incoming techniques. We are aware, however, that important improvements have been made to the NTA newest generation, *e.g.* automatic focus is now available.

4.6 CONCLUSIONS

The evaluation presented here demonstrates that NTA measurements are highly dependent on user-selected settings. Therefore, the real meaning of any measurement has to be analysed in a number of sample, instrument and analyst-related contexts. This may eclipse the relevance of the outcomes and, more importantly, the applicability of the technique in quality control environments. However, this technique offers flexibility in line with current research tasks. In this regard, the experimental evaluation of this technique might be useful in developing product-specific methods to support further nanoparticle characterization studies

4.7 REFERENCES

1.   USP. General Chapters: <788> Particulate Matter in Injections, Pharmacopeial Forum: Volume No. 28, pp. USP32-NF27.

2.   J.F. Carpenter, Randolph, Theodore W., Jiskoot, Wim, Crommelin, Daan J. A., Middaugh, C. Russell, Winter, Gerhard, Fan, Ying-Xin, Kirshner, Susan, Verthelyi, Daniela, Kozlowski, Steven, Clouse, Kathleen A., Swann, Patrick G., Rosenberg, Amy, Cherney, Barry. Overlooking Subvisible Particles in Therapeutic Protein Products: Gaps That May Compromise Product Quality. Journal of Pharmaceutical Sciences. 98:1201-1205 (2009).

3.   V. Filipe, Hawe, Andrea, Jiskoot, Wim. Critical Evaluation of Nanoparticle Tracking Analysis (NTA) by NanoSight for the Measurement of Nanoparticles and Protein Aggregates. Pharmaceutical Research. 27:796-810 (2010).

4.   S.K. Singh, N. Afonina, M. Awwad, K. Bechtold-Peters, J.T. Blue, D. Chou, M. Cromwell, H.-J. Krause, H.-C. Mahler, B.K. Meyer, L. Narhi, D.P. Nesta, and T. Spitznagel. An industry perspective on the monitoring of subvisible particles as a quality attribute for protein therapeutics. Journal of Pharmaceutical Sciences. 99:3302-3321 (2010).

5.   W. Jiskoot, Randolph, T. W., Volkin, D. B., Middaugh, C. R., Schoneich, C., Winter, G., Friess, W., Crommelin, D. J. A., Carpenter, J. F. Protein instability and immunogenicity: Roadblocks to clinical application of injectable protein delivery systems for sustained release. Journal of Pharmaceutical Sciences. 101:946-954 (2012).

6.   USP. General Chapters: <787> Subvisible particulate matter in therapeutic protein injections, Pharmacopeial Forum: Volume No. 28, pp. USP32-NF27.

7.   S. Cao, N. Jiao, Y. Jiang, A. Mire-Sluis, and L.O. Narhi. Sub-visible particle quantitation in protein therapeutics. Pharmeuropa Bio & Scientific Notes. 2009:73-79 (2009).

8.   S. Cao, Y. Jiang, and L. Narhi. A Light-obscuration Method Specific for Quantifying Subvisible Particles in Protein Therapeutics. Pharmacopeial Forum. 36:10 (2010).

9.   S. Zölls, Gregoritza, M., Tantipolphan, R., Wiggenhorn, M., Winter, G., Friess, W., Hawe, A. How subvisible particles become invisible-relevance of the refractive index for protein particle analysis. Journal of Pharmaceutical Sciences. 102:1434-1446 (2013).

10.   T. Werk, Volkin, D. B., Mahler, H. C. Effect of solution properties on the counting and sizing of subvisible particle standards as measured by light obscuration and digital imaging methods. European Journal of Pharmaceutical Sciences. 53:95-108 (2014).

11.   H. Zhao, M. Diez, A. Koulov, M. Bozova, M. Bluemel, and K. Forrer. Characterization of aggregates and particles using emerging techniques. In H.-C. Mahlerand W. Jiskoot (eds.), Analysis of aggregates and particles in protein pharmaceuticals, Wiley & Sons, Inc., 2012, pp. 133-167.

12.   D.C. Ripple, Dimitrova, M. N. Protein particles: What we know and what we do not know. Journal of Pharmaceutical Sciences. 101:3568-3579 (2012).

CHAPTER 4. Characterization of Sub-Visible Particles Using Nano Tracking Technology: Considerations for Method Development

139

13.   D.C. Ripple, C.B. Montgomery, and Z. Hu. An Interlaboratory Comparison of Sizing and Counting of Subvisible Particles Mimicking Protein Aggregates. Journal of Pharmaceutical Sciences. (2014).

14.   J.S. Pedersen, Persson, Malin. Unmasking Translucent Protein Particles by Improved Micro-Flow Imaging (TM) Algorithms.

15.   G.A. Wilsonand M.C. Manning. Flow imaging: Moving toward best practices for subvisible particle quantitation in protein products. Journal of Pharmaceutical Sciences. 102:1133-1134 (2013).

16.   A. Hawe, Schaubhut, F., Geidobler, R., Wiggenhorn, M., Friess, W., Rast, M., de Muynck, C., Winter, G. Pharmaceutical feasibility of sub-visible particle analysis in parenterals with reduced volume light obscuration methods. European Journal of Pharmaceutics and Biopharmaceutics. 85:1084-1087 (2013).

17.   D. Weinbuch, W. Jiskoot, and A. Hawe. Light obscuration measurements of highly viscous solutions: sample pressurization overcomes underestimation of subvisible particle counts. The AAPS Journal. 16:1128-1131 (2014).

18.   B. Demeule, Messick, S., Shire, S. J., Liu, J. Characterization of Particles in Protein Solutions: Reaching the Limits of Current Technologies. AAPS Journal. 12:708-715 (2010).

19.   J.G. Barnard, Rhyner, M. N., Carpenter, J. F. Critical evaluation and guidance for using the Coulter method for counting subvisible particles in protein solutions. Journal of Pharmaceutical Sciences. 101:140-153 (2012).

20.   S. Southall, A. Ketkar, C. Brisbane, and D. Nesta. Particle analysis as a formulation development tool American Pharmaceutical Review:5 (2011).

4.8 SUPPLEMENTARY MATERIAL
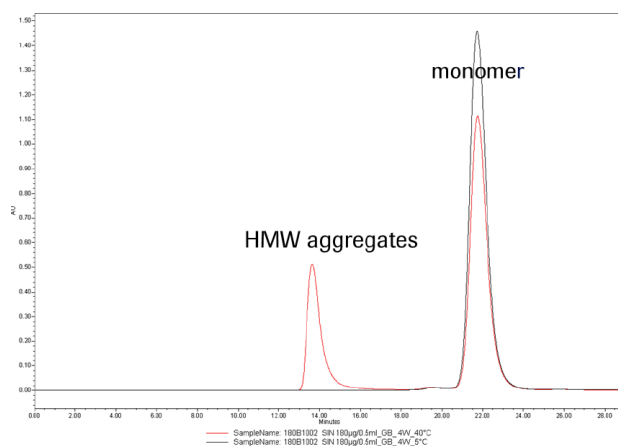
Figure S4.1 Chromatograms of Protein-1 °C at 5 and 40 °C showing increase in high molecular weight species after stress**.** SE-HPLC is run on silica-based size exclusion column (TOSOHaas TSKgel G4000SWXL 7.8mm ID, 30 cm length) using isocratic elution with sodium phosphate buffer containing sodium chloride, diethylene glycol and ethanol. (0.02M sodium phosphate, 0.15M sodium chloride, 1% V/V diethylene glycol, 10% ethanol v/v, pH 6.8). Chromatography was performed using a Waters 2695 HPLC Alliance System equipped with a Waters PDA 2996 detector or with a Waters Dual Absorbance Detector 2487. The detection wavelength was set at 210 nm with a flow rate of 0.4 mL/min

CHAPTER 4. Characterization of Sub-Visible Particles Using Nano Tracking Technology: Considerations for Method Development

141
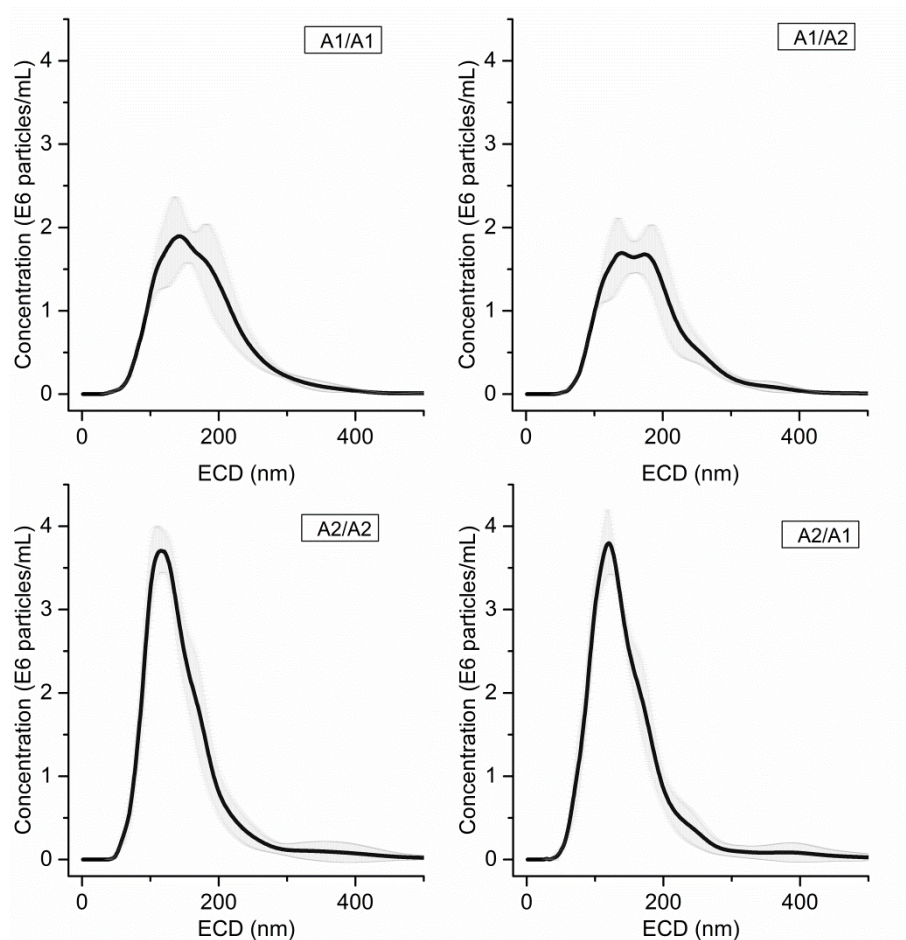
Figure S4.2 Size distribution of the intermediate precision assessment. The size distribution of a Protein-2 sample independently assessed by two experienced analysts is presented. Panel labels follow the nomenclature: "Analyst who performed the video recording/Analyst who performed the video analysis". When two different people analyzed the same video, the size distribution showed small variations. By comparison, when the same person analyzed two different videos, major differences were observed. This experiment suggests that video recording is the most critical step to ensure measurement comparability.
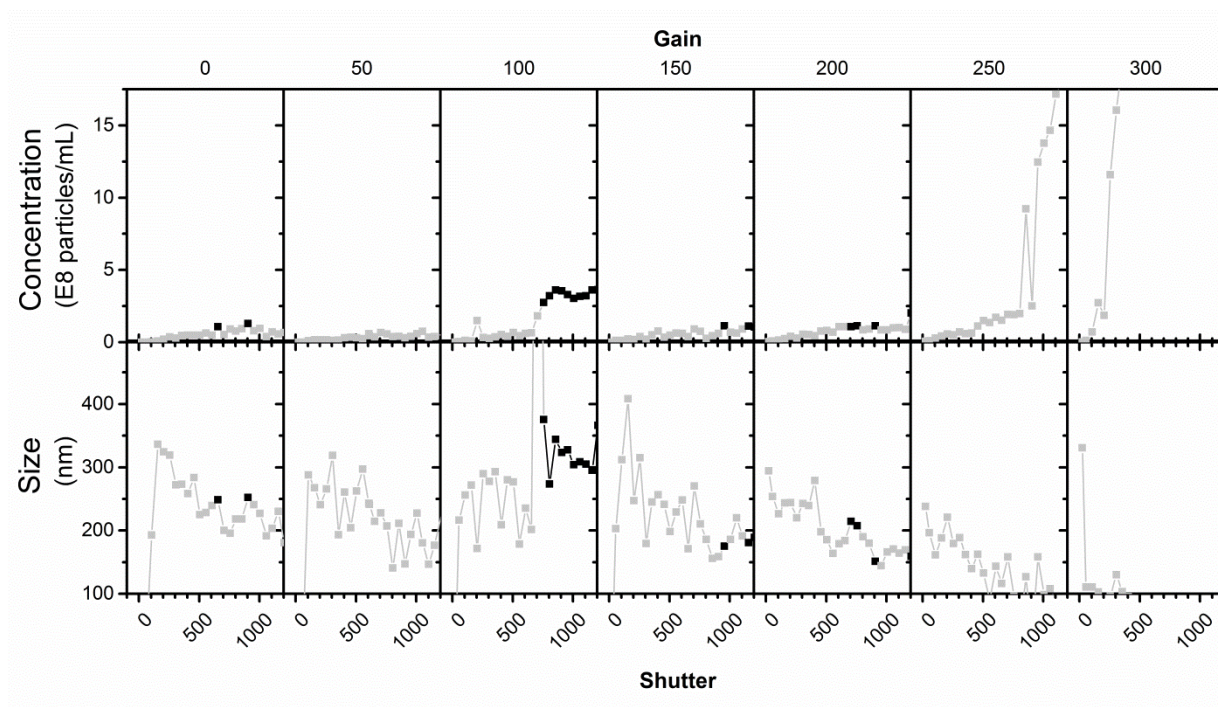
Figure S4.3 Scanning of the video recording parameters using protein particles. The same sample of artificially generated protein particles of unknown concentration and size was measured several times in NTA. Different video recording settings were applied to cover a broad combination of shutter and gain values. Each panel represents a fixed gain from 0 to 350 in steps of 50 units. The X axis represents a fixed shutter value from 0 to 1004 in steps of 50 units. The Y axis represents the concentration (upper row) and the size results (lower row). Considering limits of 20-100 centers/frame and more than 200 completed tracks, valid ■ and invalid ■ tracks are presented.

CHAPTER 4. Characterization of Sub-Visible Particles Using Nano Tracking Technology: Considerations for Method Development

143
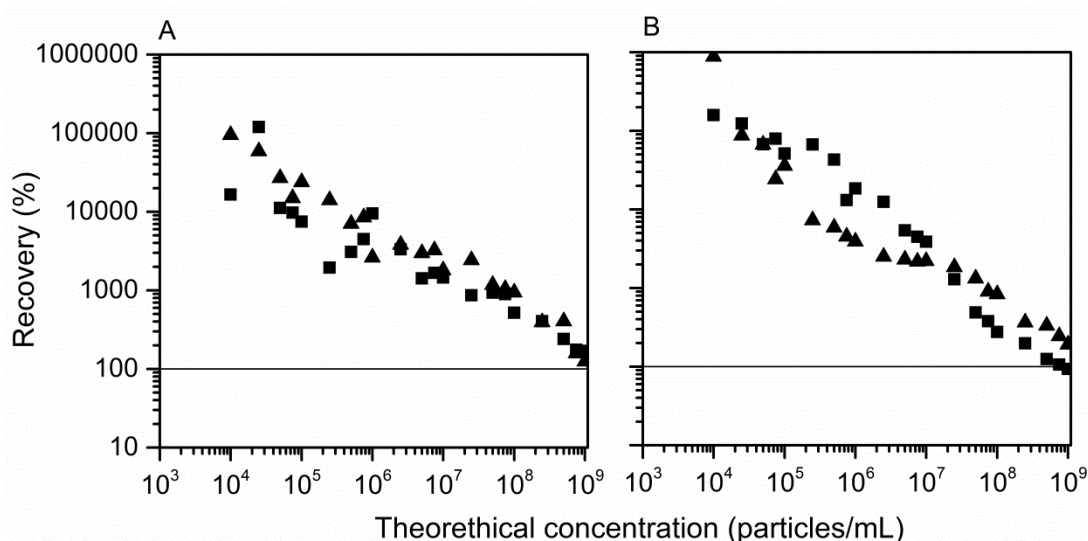
Figure S4.4 NTA performance using pump. The accuracy of NTA was studied by following the recovery of artificially generated A) Protein-3 and B) BSA particles with the dilution scheme previously reported in Chapter 2. X axes represents the theoretical particle concentration per mL of each independent sample of the dilution set. Y axes represents the calculated recovery, (theoretical concentration/experimental concentration*100). Ideal recovery of 100% is represented with the continuous horizontal line. Video duration was 60 seconds. Samples were loaded into the chamber manually (■), using a pump (▲). For the manual loading, the sample volume was limited by the chamber dimensions of 80 µm x 100 µm x 10 µm; a volume of 0.08 nL was analyzed. For the pump (Harvard apparatus catalog 98-4730, model B-57187) the loading speed was set to 20 units (1.1 x 10 $^{-3}$ mL/min); a volume of 110 nL was analyzed. Despite the increased volume that the use of the pump allows, severely overestimated counts (recoveries >>100%) were obtained regardless of the particle model and the loading method used.
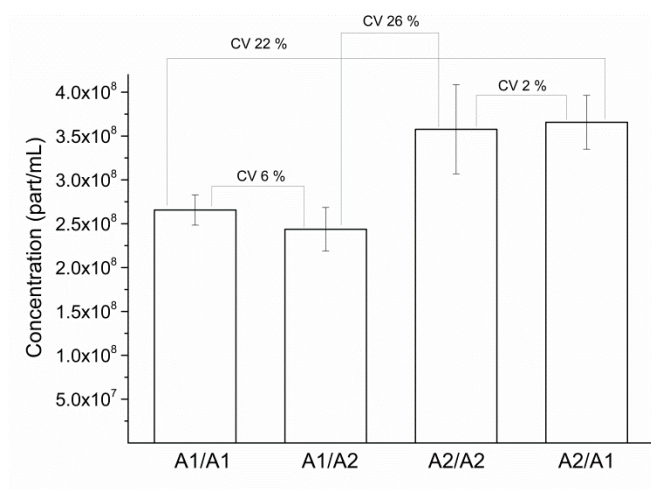
Figure S4.5 Intermediate precision-size assessment. The particle mean size of a protein sample independently assessed by two experienced analysts is presented. X axis follows the nomenclature: "Analyst who performed the video recording/Analyst who performed the video analysis". As in the case of the particle concentration assessment, the variability of the measurements when a given video was analyzed by different analysts (e.g. A1/A1 vs A1/A2) was lower than when a designated person analyzed either a self-recorded video or a video recorded by somebody else (e.g. A1/A1 vs A2/A1).

Figure S4.6 Scanning of the video recording settings using latex beads - examples of the first frame of the recorded videos. A latex solution was measured in NTA applying different video settings to cover a broad combination of shutter (from 0 to 1004 in steps of 50 units) and gain (from 0 to 350 in steps of 50 units) values. Images show the first frame of each of the collected videos.
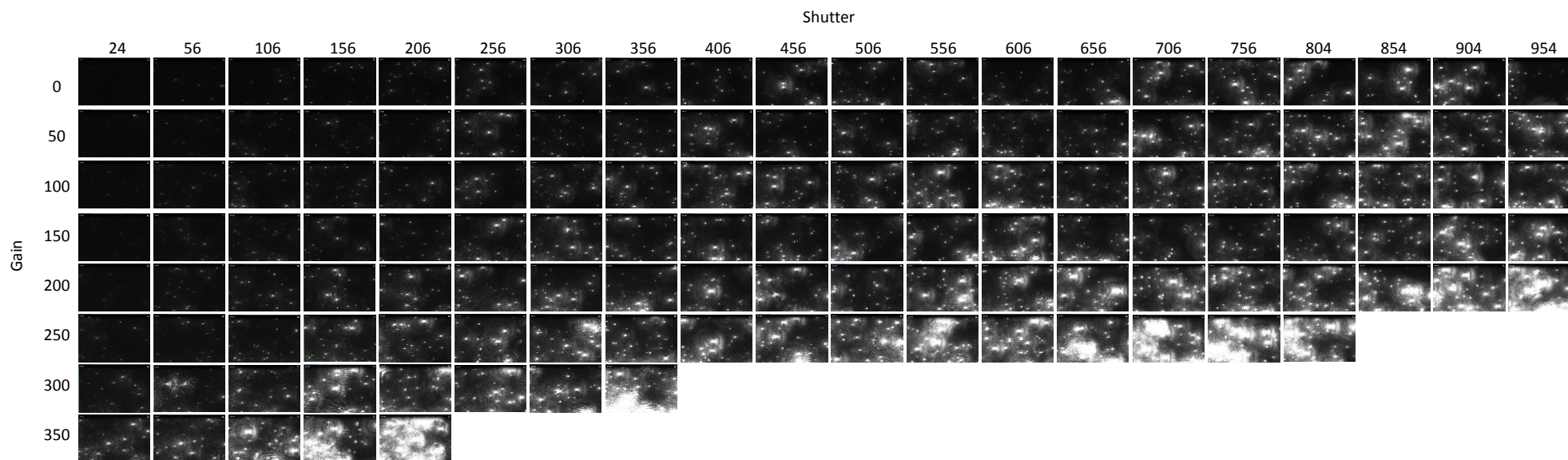
Table S4.1 The sample volume which was measured as a function of the gain and shutter video recording parameters is reported. This calculated volume is the ratio between the reported number of particles per frame and the reported particles per mL. A lower corrected concentration is obtained when a fixed measured volume of 0.08 nL is assumed.

Shutter	Gain = 0				Gain = 50				Gain = 100				Gain = 150			
	#/frame	#/mL[1]		Vol[4]	#/frame	#/mL[1]		Vol[4]	#/frame	#/mL[1]		Vol[4]	#/frame	#/mL[1]		Vol[4]
		Rep[2]	Corr[3]			Rep[2]	Corr[3]			Rep[2]	Corr[3]			Rep[2]	Corr[3]	
24	7.000	0.940	0.875	0.074	8.470	1.140	1.059	0.074	20.140	2.720	2.518	0.074	17.660	2.390	2.208	0.074
56	12.170	1.650	1.521	0.074	17.450	2.370	2.181	0.074	22.670	3.100	2.834	0.073	27.030	3.700	3.379	0.073
106	15.000	2.040	1.875	0.074	17.760	2.420	2.220	0.073	34.040	4.740	4.255	0.072	36.160	5.070	4.520	0.071
156	22.970	3.160	2.871	0.073	19.310	2.660	2.414	0.073	33.170	4.630	4.146	0.072	22.730	3.210	2.841	0.071
206	27.960	3.900	3.495	0.072	22.200	3.070	2.775	0.072	31.300	4.440	3.913	0.071	29.080	4.200	3.635	0.069
256	23.350	3.290	2.919	0.071	29.480	4.260	3.685	0.069	27.730	3.970	3.466	0.070	35.020	5.240	4.378	0.067
306	22.740	3.200	2.843	0.071	25.170	3.520	3.146	0.072	37.800	5.630	4.725	0.067	38.390	5.960	4.799	0.064
356	26.160	3.770	3.270	0.069	32.980	4.840	4.123	0.068	38.760	5.800	4.845	0.067	31.660	4.730	3.958	0.067
406	23.680	3.340	2.960	0.071	37.520	5.700	4.690	0.066	42.370	6.580	5.296	0.064	34.360	5.250	4.295	0.065
456	26.170	3.830	3.271	0.068	30.240	4.480	3.780	0.068	41.720	6.450	5.215	0.065	34.880	5.330	4.360	0.065
506	29.130	4.340	3.641	0.067	36.010	5.380	4.501	0.067	39.950	6.360	4.994	0.063	31.480	4.830	3.935	0.065
556	33.550	5.180	4.194	0.065	38.820	6.070	4.853	0.064	32.990	5.200	4.124	0.063	32.470	5.180	4.059	0.063
606	29.180	4.390	3.648	0.066	35.850	5.460	4.481	0.066	40.100	6.580	5.013	0.061	40.680	6.760	5.085	0.060
656	32.050	4.810	4.006	0.067	35.710	5.620	4.464	0.064	35.250	5.530	4.406	0.064	35.370	5.780	4.421	0.061
706	38.760	6.130	4.845	0.063	37.140	5.880	4.643	0.063	38.060	6.020	4.758	0.063	27.440	4.290	3.430	0.064
756	35.790	5.670	4.474	0.063	40.420	6.580	5.053	0.061	42.930	7.260	5.366	0.059	29.940	4.690	3.743	0.064
804	29.270	4.480	3.659	0.065	37.900	6.340	4.738	0.060	38.950	6.640	4.869	0.059	35.270	5.690	4.409	0.062
854	27.850	4.260	3.481	0.065	42.180	7.450	5.273	0.057	39.310	6.540	4.914	0.060	37.310	6.350	4.664	0.059
904	28.700	4.470	3.588	0.064	39.050	6.550	4.881	0.060	36.310	5.930	4.539	0.061	43.160	7.580	5.395	0.057
954	24.180	3.650	3.023	0.066	42.900	7.380	5.363	0.058	39.220	6.500	4.903	0.060	41.330	7.120	5.166	0.058
1004	35.430	5.490	4.429	0.065	45.620	7.860	5.703	0.058	37.730	6.470	4.716	0.058	36.050	6.370	4.506	0.057

[1] Concentration in (# of particles per mL) x 10^8
[2] Reported concentration
[3] Corrected concentration = (#/frame) / 0.08 nL
[4] Assumed volume in nL = (#/frame) / (reported concentration)

Table S4.1 *continuation*

| Shutter | Gain = 200 | | | | Gain = 253 | | | | Gain = 300 | | | | Gain = 350 | | | |
| | #/frame | #/mL[1] | | Vol[4] | #/frame | #/mL[1] | | Vol[4] | #/frame | #/mL[1] | | Vol[4] | #/frame | #/mL[1] | | Vol[4] |
		Rep[2]	Corr[3]			Rep[2]	Corr[3]			Rep[2]	Corr[3]			Rep[2]	Corr[3]	
24	17.470	2.370	2.184	0.074	21.290	2.900	2.661	0.073	37.950	5.330	4.744	0.071	7.560	5.330	0.945	0.014
56	25.570	3.520	3.196	0.073	28.470	3.950	3.559	0.072	46.580	6.930	5.823	0.067	11.310	6.930	1.414	0.016
106	29.430	4.110	3.679	0.072	40.380	5.850	5.048	0.069	50.760	8.270	6.345	0.061	14.800	8.270	1.850	0.018
156	30.100	4.270	3.763	0.070	49.130	7.660	6.141	0.064	51.720	9.150	6.465	0.057	8.850	9.150	1.106	0.010
206	38.520	5.740	4.815	0.067	46.540	7.530	5.818	0.062	55.090	9.930	6.886	0.055	4.800	9.930	0.600	0.005
256	42.620	6.640	5.328	0.064	46.390	7.530	5.799	0.062	55.120	9.900	6.890	0.056				
306	41.110	6.370	5.139	0.065	52.400	9.040	6.550	0.058	52.250	9.580	6.531	0.055				
356	39.660	6.260	4.958	0.063	48.260	8.190	6.033	0.059	47.910	9.830	5.989	0.049				
406	40.270	6.450	5.034	0.062	51.320	9.140	6.415	0.056	50.460	7.560	6.308	0.067				
456	36.320	5.950	4.540	0.061	45.340	8.320	5.668	0.055	67.500	11.310	8.438	0.060				
506	38.970	6.480	4.871	0.060	47.320	8.800	5.915	0.054								
556	45.920	7.620	5.740	0.060	50.580	9.540	6.323	0.053								
606	48.310	8.420	6.039	0.057	43.000	8.180	5.375	0.053								
656	48.660	8.580	6.083	0.057	40.360	7.910	5.045	0.051								
706	45.840	7.970	5.730	0.058	44.380	9.020	5.548	0.049								
756	52.110	9.570	6.514	0.054	36.370	7.550	4.546	0.048								
804	48.680	9.020	6.085	0.054	39.380	7.800	4.923	0.050								
854	46.010	8.330	5.751	0.055	26.840	4.790	3.355	0.056								
904	44.450	8.580	5.556	0.052												
954	38.440	7.530	4.805	0.051												
1004	35.220	6.780	4.403	0.052												

[1] Concentration in (# of particles per mL) x 10^8

[2] Reported concentration

[3] Corrected concentration = (#/frame) / 0.08 nL

[4] Assumed volume in nL = (#/frame) / (reported concentration)

III DISCUSSION

Importance of a critical evaluation of subvisible particle counting techniques

Particle profile in injections is an important quality attribute that involves a broad size range from tens of nanometers up to hundreds of micrometers (1, 2). Whilst visible particles (approx. > 100 μm) might represent a risk of capillary occlusion; subvisible particles (1 - 100 μm); submicrometer particles (100 nm - 1 μm) and even nanometer particles (< 100 nm) are thought to be possible immunogenic enhancers (3). Hence, it is of the highest importance to have analytical tools to characterize particulate matter in liquid formulations. The visible range is much more developed and instruments to detect this particle sizes as well as compendial aspects (USP regulations (4)) are well established. However, the interest in the subvisible range is rather new and expanding. The likely biological consequences previously mentioned together with the emergence of analytical tools able to characterize subvisible particles smaller than 10 μm have motivated a great interest in extending the particle characterization to smaller sizes than the currently stipulated in the USP (5, 6). This tendency is mainly driven by health authorities. In practice, however, little was known about the suitability and added value of such extended studies when analysing biotechnological products. What is more, little was known about the analytical performance of the emerging instruments. Considerable research needs to be conducted before a complete understanding of the technique is achieved.

The aforementioned necessity constituted the objective of the present dissertation. Besides the real clinical meaningfulness of proteinaceous sub visible particles, which is still to be clarified, the availability of new techniques offers interesting and challenging opportunities from the method development point of view. The present thesis was focused on increasing our understanding of basic principles and the likely applicability of the new techniques to the characterization of sub visible particles present in protein-based formulations. Over the course of this research, despite the fact that some strengths of the analytical toolbox under evaluation were confirmed, remaining challenges were also uncovered. On top of that, the collected knowledge can be applied to support better method development in the future. These aspects will be discussed in the following sections (see also Table III.a).

Analytical performance

In order to provide a sound basis for analytical evaluation, general analytical method qualification principles were applied to the study of the new methods. They were classified in micron (assessment of particles between 1-100 μm) and submicron (assessment of particles between 100-1000 nm) methods. The thesis included light obscuration, and flow imaging for the first group and electro zone sensing, resonant mass frequency measurement and nano tracking analysis for the second group. **Chapter 1** and **Chapter 2** describe the pros and coins of every technique. Unlike other analytical techniques that have a narrow range of variability, particle counting instruments have many factors had to be considered as likely contributors to artefacts (particularly when used with protein solutions). The unstable nature of protein particles itself is one example. Hence, to include a broad and complete scenario, polystyrene beads -the most frequently used standard models- were complemented with and 3 models of protein particles generated though different stress levels (therefore of different morphologies) were used. Although the experiments were designed so that the instrument response was independent of the sample handling (*i.e.* highly standardized procedures were implemented) some challenges were posed by the nature of the instruments and samples to evaluate. In the case of the precision evaluation, the small volume that some instruments required compromised the good representativeness of the sample. On the other hand, it was impossible to eliminate container to container variability, despite best sampling and pooling practices. For accuracy of sizing, although polystyrene standards are available at a broad range of sizes, they do not represent the morphological characteristics of protein particles. The generation of protein fractions sufficiently enriched to be used as size standards offers practical difficulties especially from stability aspects. The assessment of accuracy of counting and linearity offer the same difficulties with the additional issue that nano count standards made of polystyrene are not commercially available.

Precision (**Chapter 1**) as well as accuracy (**Chapter 2**) results showed a bias towards particle nature with better results for homogeneous, spherical and optically dense material. Importantly, a statistical component was found to impact both performance parameters. Better precision and accuracy was found for those particle sizes mainly represented in the sample. Poor sampling procedures explained

Table III.a Summary of the main finding of this Doctoral research

	Sizing	Counting	Linearity	Precision	Comments
HIAC		Remarkable performance at concentration bellow 100 particles/mL	Performance varied with respect to the particle type. In general acceptable at concentration higher than 1E2 particles/mL (see Figure S2.3)		**a)** Precision at lower concentrations than 3000 particles/mL not tested as such count standards are not available. **b)** Typical positive skewed particle size distributions of biotechnological samples suppose poor performance for the largest particles **c)** Improved performance when measuring the width of the signal (see Figure 3.1). Possible to lower size limit of detection (see Table S3.1) and increase accuracy of counting at concentrations as low as 10 particles/mL (see Figure 3.2 and Table S3.2)
MFI	∗ Oversizing effect for the lower size range covered by the technique. In the upper size range, an undersizing effect was found (see Figure 2.3)	Likely high method sensitivity towards small sizes (see Figure S3.2)		Acceptable for all sizes when particles are present at concentrations of at least 3000 particles/mL as verified using polystyrene standards (see Table 1.4)	**a)** For precision improvements method modifications (*e.g.* .increase of the sample volume) are possible *See also comment a) and b) for HIAC*
CC			Poorer performance as compared with micron methods. Except for polystyrene particles at the highest concentration range (see Figure S2.3)		**a)** Likely mechanical stress when measuring highly fragile particles *See also comment a) and b) for HIAC*

Table III.a *continuation*

	Sizing	Counting	Linearity	Precision	Comments
RMM	Severe undersizing effect at all size and concentration levels	Self limitant lower limit of detection (see Figure 2.1) due to probabilistic effects (see Figure S1.1) and tiny sampling volume (see Table 1.5)		** Poor performance at all sizes (see Table 1.3)	**a)** Due to the probabilistic effect described in Figure 1.2 possible to improve precision performance if sample allows for long measurement time and hence high number of events is recorded. Not nanometer counts standards are available to test hypothesis.
NTA	See *	Acceptable only for highly concentrated (particles/mL > 1E8) samples (see Figure 2.1). For accurate count assessments, video recording settings should keep constant among family of samples (see Figure 4.3C)	Poorer performance as compared with micron methods. Except for polystyrene particles at the highest concentration range (see Figure S2.3)	Video recording process is the main source of variability (see Figure 4.5) See also **	**a)** Recommended as sizing rather than counting technique (see Figure 4.3)

Table III.a *continuation*

	Sizing	Counting	Linearity	Precision	Comments
Comments		**A)** Overcounting effect at the lower concentration range of each instrument especially for highly pliable particle (see Figure 2.1) and for the smallest sizes (see Figure S2.1b). **B)** Different accuracy profiles depending on particle characteristics (see Figure 2.1) **C)** In contrast to comment *b) for HIAC* and depending on particle type (see Table 2.2), possible to obtain excellent recoveries (see Figure 2.2) **D)** Discrete agreement between instruments when comparing upper concentration ranges of overlapping size range (see Figure 2.5)	**A)** Similar to comment *A) for the counting assessment,* poor linear profiles at the lower concentration range of each instrument, especially for highly pliable particles (see Figure 2.4) **B)** For a given instrument, the linear range differ among different particle types (see Figure 2.4)	**A)** Acceptable when extrapolation factors to report counts per mililiter of sample is 20x or smaller (Figure 1.1) **B)** Remarkable improve when sample-related variability (like differences between containers (Figure 1.3)) can be cross out by appropriate sampling methodologies	

the effect – in the case of precision due to the tiny volume that the instruments measure and in the case of the accuracy due to the relative size distribution of the sample which in general is right skewed (larger sizes are poorly represented). Given that those two aspects are inherent characteristics of the instruments and samples, for the user, little is possible to do in order to improve analytical performance. As discussed in **Chapter 1**, increasing the measuring volume increases the measuring time to impractical durations. On the other hand, in **Chapter 2**, it was clearly shown that even with the use of latex beads the polydispersity of the sample will always represent a challenge for the instrument in terms of accuracy. The challenge that the typically low particle burden represents for the counting methods was also evident in terms of linearity (**Chapter 2**). Apart from the light obscuration method on which a sensor modification successfully improved the performance of the technique at concentration as low as 10 particles/mL (**Chapter 3**), all methods showed poor linearity in the respective lower concentration range. In some cases, a minimum concentration as high as 10^7 particles/mL was required (**Chapter 4**).

As single techniques cannot cover the full size range and provided that these techniques actually measure different properties, an inherent miscorrelation has to be accepted when combining different techniques. This was studied in **Chapter 2** where not only different morphologies and instruments were compared but also a concentration gradient in particles/mL was evaluated. It was already reported that the size transition from technique to technique is not smooth (7). However, this can be modified depending on the amount of particles to be analysed. In general, better correlation was found between instruments when the higher concentration ranges of each one were into comparison. Biopharmaceutical products, however will exhibit low particle burden as exemplified in **Chapter 1**.

The methodology that was applied to study the setup of specific instruments (*e.g.* the use of real products, artificially generated particle models, as well as bead standards) provides a highly integrative example on how to design such experiments and which variables to consider. However, from results in **Chapters 1 and 2** it became evident that sample-specific method development is required. The implication is that general limits of quantification cannot be provided based on instrument performance alone, we have to consider the instrument to sample compatibility. Hence, the meaningfulness of such limits should be benchmarked not only in the historical values for the specific

product, but also in the evaluation of the instrument performance in front of the specific sample setup. This would imply exhaustive method development (as demonstrated in **Chapter 4**) that in a quality control environment is difficult to implement.

Together with the number of particles, it is also important to define their nature and likely source. Particle characterization becomes a critical issue: whereas protein particles can be a trace of product instability, the presence of particles other than protein (*e.g.* silicon oil) might represent a container interaction which might or might not compromise the quality of the product when the source is well identified. That is the case of silicon oil particles that come from the inner coating layer that syringes have. The amount of silicon oil that can enter solutions depends on the speed of syringe ejection. Thus, this can represent an artefact if the speed is not kept constant throughout any particle characterization experiment (**Chapter 1**). In this frame, flow imaging technologies become highly important analytical tools. Their major strength is that these methods do not translate any particle property into a secondary signal to follow in order to provide particle counts by size. On the contrary, flow imaging technologies directly image particles. Limits of the technique are related to the optic capabilities of the camera set up. Consequently, particles smaller than 5 μm, although imaged, cannot be visually identified because the camera resolution is too low. In these cases the use of statistical filters that work with morphological descriptors are the option to improve particle identification (8-12). However, all those filters rely entirely on general particle descriptors. For example, intensity or aspect ratio values that do not take into account the effect of the media on the optical properties of the particles and hence the way they are imaged.

The lack of adequate standards

One of the main findings of this study is the description of how different the instrument performance can be depending on the type of particle to analyse. It was shown that the recovery and linear profiles appeared to be different depending on the use of polystyrene beads or the use of proteinaceous particles (**Chapter 2**). Furthermore, the artificially generated protein models that in turn showed different morphologies helped to establish that the latex beads standards can only reproduce protein profiles when the latter come from unrealistic high stress conditions. Provided that protein particles do not exist in a standard configuration, polystyrene beads represent the best option for normalized and

reproducible results when qualifying particle counting methods. However, the morphological differences existing between latex and protein particles will interfere in different degrees with the results depending on the method principle. Hence, deviations between size and count determinations of standards and proteinaceous material can be expected. The light obscuration principle is an example of this where the consequence is an undersizing effect (**Chapter 3**). Whereas the registered drop in voltage in the calibration curve comes from an optically dense and round particle (polystyrene beads), the same response in the case of a protein sample comes from an optically uneven and amorphous particle. The drop in voltage of those 2 particle types can only be equivalent when sphere morphology is assumed for the latter. Concomitantly with that assumption a "shrink" effect also occurs so that the optical density can be compared. A larger total surface area of a protein particle is required to generate a comparable voltage drop to that of a polystyrene bead with a comparable hydrodynamic radius. Another example is the coulter principle. There, not only morphology but particle pliability becomes a critical factor (**Chapter 2**). The technique is based on a pump that moves particles through an orifice. The response that is measured is the displaced volume that in turn originates resistivity changes. Whereas polystyrene standards are less affected by mechanical stress, protein particles may suffer from extended distortion. This was clearly shown when particles produced by relatively low stress level were measured in the coulter instrument. Similarly to the light obscuration principle, a discrepancy between standards and protein samples can be expected.

Estimating the error due to standards-to-sample mismatching is difficult to assess. Some of the main complications come from the fact that proteinaceous particles exhibit a broad variety of morphologies. However, in some cases like in the light obscuration method, instrument modifications could improve this situation (**Chapter 3**). In a case in which that is not possible, the present research demonstrated that a particle- and instrument-specific analysis should be conducted to expose the likely misleading effects (**Chapter 1-2**). Another tool here exemplified is the use of dilutions series to generate samples of proper and meaningful concentrations (**Chapter 2**). Although it was also shown that dilutions are not recommended due to possible particle instability, when artefacts are well understood and dilutions carefully prepared, they help to study the performance of the instruments.

Recommended use of emerging orthogonal techniques

The availability of new instruments have strongly motivated the interest in particles of sizes other (smaller) than >10 μm and >25 μm. However, over the course of this research, inherent instrument weaknesses were identified. Such characteristics will likely exclude these methods from integration into typical quality control systems. For example, some methods do not offer the possibility of performing daily suitability test or, when suitability tests are established, they may not completely reflect artefacts that are related with the nature of the sample *(see section about standards)*. In other cases, blank measurements can overlap the historical values that are reported for the sample to measure (**Chapter 1-2**). On the other hand, as some instruments overlapped, major complications appeared when different instruments reported different numbers for the same particle sizes (**Chapter 1**). Defining what the right values are is not useful as each instrument examines different characteristics of the particles that are then translated into size and counts results. Thus, outcomes will differ among each technique and assessments will not be interchangeable. The immaturity of the methods, however, was also exposed when in a stability study (**Chapter 1**) when some of them reported inconsistent trends along time and storage conditions. Some of the sources of error were identified (**Chapters 1-2 and 4**) and can be corrected. It was also possible to appreciate parallel trends between the compendial light obscuration method and *e.g.* flow imaging microscopy techniques. The real added value of implementing all the orthogonal methods then can still be topic of research. At the moment, their use constitutes an excellent tool for particle research and characterization.

Light obscuration is the method of choice as it is for the USP. Although it also has some limitations, this technique is well understood. Such sound knowledge allows for instruments modifications that directly correct for some known downsides of the technique. For example, the accuracy of the technique for particles around 1-2 μm was improved by means of changing the measuring mode from height to width of the voltage pulse (**Chapter 3**). This result shows that despite how long light obscuration has been used; some opportunity for improvement remains. Those that are described in the present Thesis build upon the already solid foundation of using and understanding this particular technique. Furthermore, as i) studies had already stated the likely transition of submicron to micron

particles and ii) a clinical relevance of submicron particles is not defined yet, the assessment of micron particles by means of the compendial light obscuration technique might be sufficient.

Future directions

Instruments for particle counting are changing on a regular base. Within the timeframe of this doctoral thesis, three generations of nano tracking analysis systems and were available. In this specific example, the newer generations correct for some operator adjustments that before increased the variability of the measurements. Flow imaging technologies have also made changes pointing towards sample automation. Those examples show the great potential that particle counting instruments have and how actively the community is using them. Scientific conferences can also confirm this as today it is more and more frequently the inclusion of particle-expert panels. However it is also possible to sense the diverging opinions about the new methodologies. Whilst academic institutions (and manufactures) are continuously finding many applications, industry is reluctant to include them as regular analytical tools. The results presented in this doctoral thesis can verify both viewpoints. The technical options and flexibility of the instruments certainly offer exciting opportunities, yet in practice they lack the automated, straightforward implementation and the functional robustness that quality control tasks require. Surely, further studies on the use of the instruments as complementary analytical techniques, more case studies more technical development from manufacturing companies, will add illuminate the field. On the other hand; even before the real added value of the assessment of < 10 µm particles is defined, *i.e.* the biological role of such particles is completely understood, interesting studies can still be implemented. For example, besides sizing and counting, particle nature is an important attribute that can be further researched and implemented to support the identification of likely degradation or stress conditions that originate in the particulate matter. One good approach can be found in the resonant mass measurements. Differences in the density values between the types of particles which are present in the sample and also with respect to the media on which they are suspended allow their discrimination due to the consequent differences in buoyancy. However, a rather large minimum density difference has to be met to achieve proper population segregation and that is only possible for no more than 2 particle types. Perhaps further technical improvements could allow a higher number of density-base sorting channels. To date, the flow imaging technologies offer a similar

possibility by means of particle morphological descriptors and actual images. Discrimination between several populations is possible *e.g.* silicon oil droplets, air bubbles protein or glass particles. However, below 5 μm the visual judgment of the images is difficult due to the actual camera pixel resolution and even morphological filters that fail for the smallest particles. Improvements in the optical system will certainly help and a better particle differentiation can be obtained in combination with mathematical models. Using morphological descriptors it is possible to define boundaries between populations of particles. Although some statistical filters have been developed, the possibility of protein particle differentiation base on the specific stress condition that generated them (instead of simply from other particle nature) is an exciting opportunity.

Another interesting area of research is the deeper understanding on the roots of instruments divergences. In the course of this dissertation it became clear that each particle counting instrument will report different concentration numbers for a given sample. Furthermore, several cases were presented suggesting that despite that fact, similar trends will be observed. Hence, finding possible correlations between the different instruments might shed light on how many and which analytical tools can characterize the particle content sufficiently. Such studies need to thoroughly examine the physical principles of each technique. That knowledge in combination with the analytical evaluation presented in this thesis will surely help the decision making process when defining strategies for particle characterization in biotechnological products.

Finally, the present status of particle counting instrumentation only allows for encouraging their careful use and data interpretation as guidance for formulation-related development activities.

References (Discussion)

1.   USP. General Requirements: <1> Injections. Foreing and particlulate matter, Pharmacopeial Forum: Volume No. 28, pp. USP32-NF27.

2.   L.O. Narhi, Schmit, J., Bechtold-Peters, K., Sharma, D. Classification of protein aggregates. Journal of Pharmaceutical Sciences. 101:493-498 (2012).

3.   A.S. Rosenberg. Immunogenicity of biological therapeutics: a hierarchy of concerns. Developments in biologicals. 112:15-21 (2003).

4.   p.U.-N. USP. General Requirements: <790> Visible Particulates in Injections. Pharmacopeial Forum: Volume No. 28.

5.   USP. General Chapters: <787> Subvisible particulate matter in therapeutic protein injections, Pharmacopeial Forum: Volume No. 28, pp. USP32-NF27.

6.   USP. General Chapters: <788> Particulate Matter in Injections, Pharmacopeial Forum: Volume No. 28, pp. USP32-NF27.

7.   V. Filipe, Hawe, A., Carpenter, J. F., Jiskoot, W. Analytical approaches to assess the degradation of therapeutic proteins. Trendsin Analytical Chemistry. 49:118-125 (2013).

8.   D.K. Sharma, P. Oma, M.J. Pollo, and M. Sukumar. Quantification and Characterization of Subvisible Proteinaceous Particles in Opalescent mAb Formulations Using Micro-Flow Imaging. Journal of Pharmaceutical Sciences. 99:2628-2642 (2010).

9.   R. Strehl, Rombach-Riegraf, V., Diez, M., Egodage, K., Bluemel, M., Jeschke, M., Koulov, A. V. Discrimination between silicone oil droplets and protein aggregates in biopharmaceuticals: a novel multiparametric image filter for sub-visible particles in microflow imaging analysis. Pharmaceutical Research. 29:594-602 (2012).

10.   N. Vandesteeg, Kilbert, C. Differentiation of subvisible silicone oil droplets from irregular standard dust particles. Journal of Pharmaceutical Sciences. 102:1696-1700 (2013).

11.   D. Weinbuch, Zolls, S., Wiggenhorn, M., Friess, W., Winter, G., Jiskoot, W., Hawe, A. Micro-flow imaging and resonant mass measurement (archimedes) - complementary methods to quantitatively differentiate protein particles and silicone oil droplets. Journal of Pharmaceutical Sciences. 102:2152-2165 (2013).

12.   J.S. Pedersenand M. Persson. Unmasking Translucent Protein Particles by Improved Micro-Flow Imaging (TM) Algorithms. Journal of Pharmaceutical Sciences. 103:107-114 (2014).

IV CONCLUSIONS

Several new techniques for the research and characterization of sub visible particulate matter in parenteral formulations have been recently developed. The present work has outlined the complications that can be faced when using the new methodologies without a deep understanding of the specific sample and instrument configuration. A systematic evaluation of the applicability of such instruments was accomplished. The analytical performance was assessed considering particle morphologies; size ranges; concentration ranges and heterogeneity aspects that are likely present in protein therapeutic samples. As a result, a highly integrative overview was explored.

Main findings pointed towards immaturity of most of the systems for inclusion as general tools for routine characterization. On the one hand they do not correlate due to their different fundaments, but on the other hand they cannot be used independently as single techniques do not cover the full size range of interest. Importantly, particle detection was found to be biased towards probabilistic aspects with better analytical performance for those particles of sizes mainly represented in the sample. Both, low sampling volumes as well as the typically left skewed size distribution of protein particles were detected as main constraints for acceptable precision and accuracy performance. Low particle burden was also found to be challenging as over-counting effects were found in the lower concentration ranges of each method.

Altogether, this research highlights the importance of exhaustive product specific method development before the implementation of any of the techniques. The analytical approach described here should serve as basis for further assessments on which the strengths and weaknesses here unveiled are considered.

Once a deeper understanding of the different techniques was achieved, it was possible to develop tools to improve the applicability of the light obscuration and nano tracking analysis techniques. Light obscuration showed the better performance in comparison with the other techniques, thus an effort to lower the size and the concentration range of the technique was tested. Successfully, a time resolved measuring mode was implemented. In contrast, nano tracking analysis, showed the highest variability as a consequence of user-defined parameters, thus experiments were designed to guide the proper method development tasks when working with this technique.

Biotechnological products will continue their incursion into the pharmaceutical market. Several studies are ongoing to understand better the alleged immunogenicity of sub visible protein particles present in this type of formulations. While this particular research comes to concise findings, it is clear that any outcome should be accompanied with a sound analytical toolbox that allows for an accurate particle characterization. The general results of this research indicate that at the moment, however, only research activities can be supported with extensive method development studies.

V REFERENCES (*Global)*

Abdul-Fattah, A. M., Oeschger, R., Roehl, H., Bauer Dauphin, I., Worgull, M., Kallmeyer, G., et al. (2013). Investigating factors leading to fogging of glass vials in lyophilized drug products. European Journal of Pharmaceutics and Biopharmaceutics, 85(2), 314-326.

Adler, M. (2012). Challenges in the development of pre-filled syringes for biologics from a formulation's scientist point of view. American Pharmaceutical Review, 15.

Ahern, T. J., Casal, J. I., Petsko, G. A., & Klibanov, A. M. (1987). Control of oligomeric enzyme thermostability by protein engineering. Proceedings of the National Academy of Sciences of the United States of America, 84(3), 675-679.

Aldrich, S. (2010). USP Workshop on particle size, particle detection and measurement. Historical perspective and current chapter review

Allmendinger, A., Fischer, S., Huwyler, J., Mahler, H.-C., Schwarb, E., Zarraga, I. E., et al. (2014). Rheological characterization and injection forces of concentrated protein formulations: An alternative predictive model for non-Newtonian solutions. European Journal of Pharmaceutics and Biopharmaceutics, 87(2), 318-328.

Arakawa, T., & Timasheff, S. N. (1982). Stabilization of protein structure by sugars. Biochemistry, 21(25), 6536-6544.

Auge, K. B., Blake-Haskins, A. W., Devine, S., Rizvi, S., Li, Y. M., Hesselberg, M., Orvisky, E., Affleck, R. P., Spitznagel, T. M., Perkins, M. D. (2011). Demonstrating the stability of albinterferon alfa-2b in the presence of silicone oil. Journal of Pharmaceutical Sciences. , 100(12), 5100-5114.

Badkar, A., Wolf, Amanda, Bohack, Leigh, Kolhe, Parag. (2011). Development of Biotechnology Products in Pre-filled Syringes: Technical Considerations and Approaches. AAPS PharmSciTech, 12(2), 564-572.

Bai, S. J., Murugesan, Y., Vlasic, M., Karpes, L. B., Brader, M. L. (2013). Effects of submicron particles on formation of micron-sized particles during long-term storage of an interferon-beta-1a solution. Journal of Pharmaceutical Sciences. 102(2), 347-351.

Barnard, J. G., Babcock, K., Carpenter, J. F. (2013). Characterization and quantitation of aggregates and particles in interferon- products: Potential links between product quality attributes and immunogenicity. Journal of Pharmaceutical Sciences. 102(3), 915-928.

Barnard, J. G., Rhyner, M. N., Carpenter, J. F. (2012). Critical evaluation and guidance for using the Coulter method for counting subvisible particles in protein solutions. Journal of Pharmaceutical Sciences. 101(1), 140-153.

Barnard, J. G., Singh, S., Randolph, T. W., Carpenter, J. F. (2011). Subvisible Particle Counting Provides a Sensitive Method of Detecting and Quantifying Aggregation of Monoclonal Antibody Caused by Freeze-Thawing: Insights Into the Roles of Particles in the Protein Aggregation Pathway. Journal of Pharmaceutical Sciences. 100(2), 492-503.

Basu, P., Krishnan, S., Thirumangalathu, R., Randolph, T. W., Carpenter, J. F. (2013). IgG1 aggregation and particle formation induced by silicone-water interfaces on siliconized borosilicate glass beads: A model for siliconized primary containers. Journal of Pharmaceutical Sciences. 102(3), 852-865.

Brekke, O. H., & Sandlie, I. (2003). Therapeutic antibodies for human diseases at the dawn of the twenty-first century. Nature Reviews Drug Discovery. 2(1), 52-62.

Britt, K. A., Schwartz, D. K., Wurth, C., Mahler, H. C., Carpenter, J. F., Randolph, T. W. (2012). Excipient effects on humanized monoclonal antibody interactions with silicone oil emulsions. Journal of Pharmaceutical Sciences. 101(12), 4419-4432.

Burg, T. P., Godin, M., Knudsen, S. M., Shen, W., Carlson, G., Foster, J. S., Babcock, K., Manalis, S. R. (2007). Weighing of biomolecules, single cells and single nanoparticles in fluid. Nature, 446(7139), 1066-1069.

Cao, S., Jiang, Y., & Narhi, L. (2010). A Light-obscuration Method Specific for Quantifying Subvisible Particles in Protein Therapeutics. Pharmacopeial Forum, 36(3), 10.

Cao, S., Jiao, N., Jiang, Y., Mire-Sluis, A., & Narhi, L. O. (2009). Sub-visible particle quantitation in protein therapeutics. Pharmeuropa Bio & Scientific Notes, 2009(1), 73-79.

Carpenter, J. F., Kendrick, B. S., Chang, B. S., Manning, M. C., & Randolph, T. W. (1999). [16] Inhibition of stress-induced aggregation of protein therapeutics. In Methods in Enzymology (Vol. Volume 309, pp. 236-255): Academic Press.

Carpenter, J. F., Randolph, T. W., Jiskoot, W., Crommelin, D. J. A., Middaugh, C. R., & Winter, G. (2010). Potential Inaccurate Quantitation and Sizing of Protein Aggregates by Size Exclusion Chromatography: Essential Need to Use Orthogonal Methods to Assure the Quality of Therapeutic Protein Products. Journal of Pharmaceutical Sciences. 99(5), 2200-2208.

Carpenter, J. F., Randolph, Theodore W., Jiskoot, Wim, Crommelin, Daan J. A., Middaugh, C. Russell, Winter, Gerhard, Fan, Ying-Xin, Kirshner, Susan, Verthelyi, Daniela, Kozlowski, Steven, Clouse, Kathleen A., Swann, Patrick G., Rosenberg, Amy, Cherney, Barry. (2009). Overlooking Subvisible Particles in Therapeutic Protein Products: Gaps That May Compromise Product Quality. Journal of Pharmaceutical Sciences. 98(4), 1201-1205.

Carr Bob, H. P., Malloy Andrew, Nelson Philip, Wright Matthew, Smith Jonathan. (2009). Applications of nanoparticle tracking analysis in nanoparticle research – a mini-review. European Journal of Parenteral & Pharmaceutical Sciences. 14(2), 45-50.

Chance, R. E., & Frank, B. H. (1993). Research, development, production, and safety of biosynthetic human insulin. Diabetes Care, 16, 133-142.

Chang, B. S., Kendrick, B. S., & Carpenter, J. F. (1996). Surface-induced denaturation of proteins during freezing and its inhibition by surfactants. Journal of Pharmaceutical Sciences. 85(12), 1325-1330.

Chantelau, E., Berger, M., Bohlken, B. (1986). Silicone oil released from disposable insulin syringes. Diabetes Care, 9(6), 672-673.

Chi, E., Krishnan, S., Randolph, T., & Carpenter, J. (2003). Physical Stability of Proteins in Aqueous Solution: Mechanism and Driving Forces in Nonnative Protein Aggregation. Pharmaceutical research, 20(9), 1325-1336.

Cicerone, M. T., Pikal, M. J., & Qian, K. K. Stabilization of proteins in solid form. Advanced Drug Delivery Reviews.

Cromwell, M. E., Hilario, E., & Jacobson, F. (2006). Protein aggregation and bioprocessing. The AAPS Journal, 8(3), E572-E579.

Das, T. K. (2012). Protein Particulate Detection Issues in Biotherapeutics Development-Current Status. AAPS PharmSciTech, 13(2), 732-746.

Demeule, B., Lawrence, M. J., Drake, A. F., Gurny, R., Arvinte, T. (2007). Characterization of protein aggregation: The case of a therapeutic immunoglobulin. Biochimica Et Biophysica Acta-Proteins and Proteomics, 1774(1), 146-153.

Demeule, B., Messick, S., Shire, S. J., Liu, J. (2010). Characterization of Particles in Protein Solutions: Reaching the Limits of Current Technologies. AAPS Journal, 12(4), 708-715.

Demeule, B., Palais, C., Machaidze, G., Gurny, R., & Arvinte, T. (2009). New methods allowing the detection of protein aggregates: A case study on trastuzumab. mAbs Journal, 1(2), 142-150.

Demeule, B., Palais, C., Machaidze, G., Gurny, R., Arvinte, T. (2009). New methods allowing the detection of protein aggregates A case study on trastuzumab. mAbs Journal, 1(2), 142-150.

den Engelsman, J., Garidel, Patrick, Smulders, Ronald, Koll, Hans, Smith, Bryan, Bassarab, Stefan, Seidl, Andreas, Hainzl, Otmar, Jiskoot, Wim. Strategies for the Assessment of Protein Aggregates in Pharmaceutical Biotech Product Development. April 2011, Volume 28, Issue 4, pp 920-933.

Dextras, P., Burg, T. P., Manalis, S. R. (2009). Integrated Measurement of the Mass and Surface Charge of Discrete Microparticles Using a Suspended Microchannel Resonator. Analytical Chemistry, 81(11), 4517-4523.

Doyle, H. A., Gee, R. J., & Mamula, M. J. (2007). Altered immunogenicity of isoaspartate containing proteins. Autoimmunity, 40(2), 131-137.

Felsovalyi, F., Janvier, S., Jouffray, S., Soukiassian, H., Mangiagalli, P. (2012). Silicone-oil-based subvisible particles: Their detection, interactions, and regulation in prefilled container closure systems for biopharmaceuticals. Journal of Pharmaceutical Sciences. 101(12), 4569-4583.

Filipe, V., Hawe, A., Carpenter, J. F., & Jiskoot, W. (2013). Analytical approaches to assess the degradation of therapeutic proteins. Trendsin Analytical Chemistry, 49, 118-125.

Filipe, V., Hawe, A., Carpenter, J. F., Jiskoot, W. (2013). Analytical approaches to assess the degradation of therapeutic proteins. Trendsin Analytical Chemistry, 49, 118-125.

Filipe, V., Hawe, Andrea, Jiskoot, Wim. (2010). Critical Evaluation of Nanoparticle Tracking Analysis (NTA) by NanoSight for the Measurement of Nanoparticles and Protein Aggregates. Pharmaceutical research, 27(5), 796-810.

Filipe, V., Jiskoot, W., Basmeleh, A. H., Halim, A., Schellekens, H., Brinks, V. (2012). Immunogenicity of different stressed IgG monoclonal antibody formulations in immune tolerant transgenic mice. mAbs Journal, 4(6), 740-752.

Filipe, V., Poole, R., Oladunjoye, O., Braeckmans, K., Jiskoot, W. (2012). Detection and Characterization of Subvisible Aggregates of Monoclonal IgG in Serum. Pharmaceutical Research, 29(8), 2202-2212.

Hamrang, Z., Rattray, N. J. W., & Pluen, A. (2013). Proteins behaving badly: emerging technologies in profiling biopharmaceutical aggregation. Trends in Biotechnology, 31(8), 448-458.

Harris, R. J., Shire, S. J., & Winter, C. (2004). Commercial manufacturing scale formulation and analytical characterization of therapeutic recombinant antibodies. Drug Development Research, 61(3), 137-154.

Hawe, A., Schaubhut, F., Geidobler, R., Wiggenhorn, M., Friess, W., Rast, M., de Muynck, C., Winter, G. (2013). Pharmaceutical feasibility of sub-visible particle analysis in parenterals with reduced

volume light obscuration methods. European Journal of Pharmaceutics and Biopharmaceutics, 85(3), 1084-1087.

Hole, P., Sillence, K., Hannell, C., Maguire, C. M., Roesslein, M., Suarez, G., et al. (2013). Interlaboratory comparison of size measurements on nanoparticles using nanoparticle tracking analysis (NTA). Journal of Nanoparticle Research, 15(12).

Janesick, J. R. (2001). Scientific Charge-coupled Devices: Society of Photo Optical.

Jiskoot, W., Randolph, T. W., Volkin, D. B., Middaugh, C. R., Schoneich, C., Winter, G., Friess, W., Crommelin, D. J. A., Carpenter, J. F. (2012). Protein instability and immunogenicity: Roadblocks to clinical application of injectable protein delivery systems for sustained release. Journal of Pharmaceutical Sciences. , 101(3), 946-954.

Johnson, I. (1983). Human insulin from recombinant DNA technology. Science, 219(4585), 632-637.

Jones, L. S., Kaufmann, A., Middaugh, C. R. (2005). Silicone oil induced aggregation of proteins. Journal of Pharmaceutical Sciences. , 94(4), 918-927.

Joubert, M. K., Luo, Q., Nashed-Samuel, Y., Wypych, J., Narhi, L. O. (2011). Classification and characterization of therapeutic antibody aggregates. The Journal of Biological Chemistry, 286(28), 25118-25133.

Kalonia, C., Kumru, O. S., Prajapati, I., Mathaes, R., Engert, J., Zhou, S., et al. (2014). Calculating the Mass of Subvisible Protein Particles with Improved Accuracy Using Microflow Imaging Data. Journal of Pharmaceutical Sciences. 2015 Feb;104(2):536-47

Kiese, S., Papppenberger, Astrid, Friess, Wolfgang, Mahler, Hanns-Christian. (2008). Shaken, not stirred: Mechanical stress testing of an IgG1 antibody. Journal of Pharmaceutical Sciences. , 97(10), 4347-4366.

Kohler, G., & Milstein, C. (1975). Continuous cultures of fused cells secreting antibody of predefined specificity. Nature, 256(5517), 495-497.

Kumru, O. S., Liu, J., Ji, J. Y. A., Cheng, W., Wang, Y. J., Wang, T. T., Joshi, S. B., Middaugh, C. R., Volkin, D. B. (2012). Compatibility, physical stability, and characterization of an IgG4 monoclonal antibody after dilution into different intravenous administration bags. Journal of Pharmaceutical Sciences. 101(10), 3636-3650.

Kusaka, Y., & Adachi, Y. (2007). Determination of hydrodynamic diameter of small flocs by means of direct movie analysis of Brownian motion. Colloids and Surfaces a-Physicochemical and Engineering Aspects, 306(1-3), 166-170.

Liu, L., Ammar, D. A., Ross, L. A., Mandava, N., Kahook, M. Y., Carpenter, J. F. (2011). Silicone Oil Microdroplets and Protein Aggregates in Repackaged Bevacizumab and Ranibizumab: Effects of Long-term Storage and Product Mishandling. Investigative Ophthalmology & Visual Science, 52(2), 1023-1034.

Liu, Y. D., van Enk, J. Z., & Flynn, G. C. (2009). Human antibody Fc deamidation in vivo. Biologicals, 37(5), 313-322.

Mach, H., Arvinte, T. (2011). Addressing new analytical challenges in protein formulation development. European Journal of Pharmaceutics and Biopharmaceutics, 78(2), 196-207.

Mahler, H.-C., Friess, W., Grauschopf, U., & Kiese, S. (2009). Protein Aggregation: Pathways, Induction Factors and Analysis. Journal of Pharmaceutical Sciences. 98(9), 2909-2934.

Mahler, H. C., Friess, W., Grauschopf, U., Kiese, S. (2009). Protein aggregation: pathways, induction factors and analysis. Journal of Pharmaceutical Sciences. 98(9), 2909-2934.

Malvern. (2015). NTA: principles and methodology. Withe paper.

Manning, M., Patel, K., & Borchardt, R. (1989). Stability of Protein Pharmaceuticals. Pharmaceutical research, 6(11), 903-918.

Manning, M. C., Chou, D. K., Murphy, B. M., Payne, R. W., & Katayama, D. S. (2010). Stability of protein pharmaceuticals: an update. Pharmaceutical Research, 27(4), 544-575.

Narhi, L. O., Jiang, Yijia, Cao, Shawn, Benedek, Kalman, Shnek, Deborah. (2009). A Critical Review of Analytical Methods for Subvisible and Visible Particles. Current Pharmaceutical Biotechnology, 10(4), 373-381.

Narhi, L. O., Schmit, J., Bechtold-Peters, K., Sharma, D. (2012). Classification of protein aggregates. Journal of Pharmaceutical Sciences. 101(2), 493-498.

Neergaard, M. S., Kalonia, D. S., Parshad, H., Nielsen, A. D., Møller, E. H., & van de Weert, M. (2013). Viscosity of high concentration protein formulations of monoclonal antibodies of the IgG1 and IgG4 subclass – Prediction of viscosity through protein–protein interaction measurements. European Journal of Pharmaceutical Sciences. 49(3), 400-410.

Nicoud, L., Cohrs, N., Arosio, P., Norrant, E., & Morbidelli, M. (2015). Effect of polyol sugars on the stabilization of monoclonal antibodies. Biophysical Chemistry, 197, 40-46.

Panchal, J., Kotarek, J., Marszal, E., & Topp, E. M. (2014). Analyzing Subvisible Particles in Protein Drug Products: a Comparison of Dynamic Light Scattering (DLS) and Resonant Mass Measurement (RMM). AAPS Journal, 16(3), 440-451.

Patel, A. R., Lau, Doris, Liu, Jun. (2012). Quantification and Characterization of Micrometer and Submicrometer Subvisible Particles in Protein Therapeutics by Use of a Suspended Microchannel Resonator. Analytical Chemistry, 84(15), 6833-6840.

Pavlou, A. K., Belsey, M. J. (2005). The therapeutic antibodies market to 2008. European Journal of Pharmaceutics and Biopharmaceutics, 59(3), 389-396.

Pedersen, J. S., Persson, Malin. Unmasking Translucent Protein Particles by Improved Micro-Flow Imaging (TM) Algorithms.

Philo, J. S. (2006). Is any measurement method optimal for all aggregate sizes and types? AAPS Journal, 8(3), E564-E571.

Rader, R. A. (2008). (Re)defining biopharmaceutical. Nature Biotechnology, 26(7), 743-751.

Reubsaet, J. L. E., Beijnen, J. H., Bult, A., van Maanen, R. J., Marchal, J. A. D., & Underberg, W. J. M. (1998). Analytical techniques used to study the degradation of proteins and peptides: chemical instability. Journal of Pharmaceutical and Biomedical Analysis, 17(6–7), 955-978.

Rhyner, M. N. (2011). The Coulter Principle for Analysis of Subvisible Particles in Protein Formulations. AAPS Journal, 13(1), 54-58.

Ríos Quiroz, A., Québatte, G., Stump, F., Finkler, C., Huwyler, J., Schmidt, R., et al. (2015). Measuring Subvisible Particles in Protein Formulations Using a Modified Light Obscuration Sensor with Improved Detection Capabilities. Analytical Chemistry. 2015 Jun 16;87(12):6119-24.

Ripple, D. C., Dimitrova, M. N. (2012). Protein particles: What we know and what we do not know. Journal of Pharmaceutical Sciences. 101(10), 3568-3579.

Ripple, D. C., Montgomery, C. B., & Hu, Z. (2014). An Interlaboratory Comparison of Sizing and Counting of Subvisible Particles Mimicking Protein Aggregates. Journal of Pharmaceutical Sciences. , n/a-n/a.

Rosenberg, A. S. (2003). Immunogenicity of biological therapeutics: a hierarchy of concerns. Developments in biologicals, 112, 15-21.

Rosenberg, A. S., Verthelyi, D., & Cherney, B. W. (2012). Managing uncertainty: A perspective on risk pertaining to product quality attributes as they bear on immunogenicity of therapeutic proteins. Journal of Pharmaceutical Sciences. 101(10), 3560-3567.

Sharma, D. K., King, D., Oma, P., & Merchant, C. (2010). Micro-Flow Imaging: Flow Microscopy Applied to Sub-visible Particulate Analysis in Protein Formulations. The AAPS Journal, 12(3), 10.

Sharma, D. K., Oma, P., Pollo, M. J., & Sukumar, M. (2010). Quantification and Characterization of Subvisible Proteinaceous Particles in Opalescent mAb Formulations Using Micro-Flow Imaging. Journal of Pharmaceutical Sciences. 99(6), 2628-2642.

Shire, S. J., Shahrokh, Z., Liu, J. (2004). Challenges in the development of high protein concentration formulations. Journal of Pharmaceutical Sciences. 93(6), 1390-1402.

Singh, S. K., Afonina, N., Awwad, M., Bechtold-Peters, K., Blue, J. T., Chou, D., et al. (2010). An industry perspective on the monitoring of subvisible particles as a quality attribute for protein therapeutics. Journal of Pharmaceutical Sciences. 99(8), 3302-3321.

Soloviev, M. E. (2012). Nanoparticles in Biology and Medicine: Methods and Protocols: Humana Press.

Southall, S., Ketkar, A., Brisbane, C., & Nesta, D. (2011). Particle analysis as a formulation development tool American Pharmaceutical Review, 5.

Strehl, R., Rombach-Riegraf, V., Diez, M., Egodage, K., Bluemel, M., Jeschke, M., Koulov, A. V. (2012). Discrimination between silicone oil droplets and protein aggregates in biopharmaceuticals: a novel multiparametric image filter for sub-visible particles in microflow imaging analysis. Pharmaceutical research, 29(2), 594-602.

Tang, X., & Pikal, M. (2004). Design of Freeze-Drying Processes for Pharmaceuticals: Practical Advice. Pharmaceutical research, 21(2), 191-200.

Torosantucci, R., Schöneich, C., & Jiskoot, W. (2014). Oxidation of Therapeutic Proteins and Peptides: Structural and Biological Consequences. Pharmaceutical research, 31(3), 541-553.

USP. General Chapters: <787> Subvisible particulate matter in therapeutic protein injections, Pharmacopeial Forum: Volume No. 28, pp. USP32-NF27.

USP. General Chapters: <788> Particulate Matter in Injections, Pharmacopeial Forum: Volume No. 28, pp. USP32-NF27.

USP. General Requirements: <1> Injections. Foreing and particlulate matter, Pharmacopeial Forum: Volume No. 28, pp. USP32-NF27.

USP. General Requirements: <790> Visible Particulates in Injections. Pharmacopeial Forum: Volume No. 28, p. U.-N.

Van der Meeren, P., Kasinos, Marios, Saveyn, Hans. (2012). Relevance of two-dimensional Brownian motion dynamics in applying nanoparticle tracking analysis. Methods in Molecular Biology (Clifton, N.J.), 906, 525-534.

Vasudev, R., Mathew, S., & Afonina, N. (2015). Characterization of Submicron (0.1-1 mum) Particles in Therapeutic Proteins by Nanoparticle Tracking Analysis. Journal of Pharmaceutical Sciences. 104(5), 1622-1631.

Walsh, G. (2014). Biopharmaceutical benchmarks 2014. Nature Biotechnology, 32(10), 992-1000.

Wang, W. (2005). Protein aggregation and its inhibition in biopharmaceutics. International Journal of Pharmaceutics, 289(1–2), 1-30.

Wang, W., Singh, S. K., Li, N., Toler, M. R., King, K. R., & Nema, S. (2012). Immunogenicity of protein aggregates-Concerns and realities. International Journal of Pharmaceutics, 431(1-2), 1-11.

Wang, W., Wang, E. Q., & Balthasar, J. P. (2008). Monoclonal Antibody Pharmacokinetics and Pharmacodynamics. Clinical Pharmacology & Therapeutics, 84(5), 548-558.

Warne, N. W. (2011). Development of high concentration protein biopharmaceuticals: The use of platform approaches in formulation development. European Journal of Pharmaceutics and Biopharmaceutics, 78(2), 208-212.

Weinbuch, D., Jiskoot, W., & Hawe, A. (2014). Light obscuration measurements of highly viscous solutions: sample pressurization overcomes underestimation of subvisible particle counts. The AAPS Journal, 16(5), 1128-1131.

Weinbuch, D., Zolls, S., Wiggenhorn, M., Friess, W., Winter, G., Jiskoot, W., Hawe, A. (2013). Micro-flow imaging and resonant mass measurement (archimedes) - complementary methods to quantitatively differentiate protein particles and silicone oil droplets. Journal of Pharmaceutical Sciences. 102(7), 2152-2165.

Werk, T., Volkin, D. B., Mahler, H. C. (2014). Effect of solution properties on the counting and sizing of subvisible particle standards as measured by light obscuration and digital imaging methods. European Journal of Pharmaceutical Sciences. 53, 95-108.

Wilson, G. A., & Manning, M. C. (2013). Flow imaging: Moving toward best practices for subvisible particle quantitation in protein products. Journal of Pharmaceutical Sciences. 102(3), 1133-1134.

Wright, M. (2012). Nanoparticle tracking analysis for the multiparameter characterization and counting of nanoparticle suspensions. Methods in Molecular Biology (Clifton, N.J.), 906, 511-524.

Wuchner, K., Buchler, J., Spycher, R., Dalmonte, P., Volkin, D. B. (2010). Development of a microflow digital imaging assay to characterize protein particulates during storage of a high concentration IgG1 monoclonal antibody formulation. Journal of Pharmaceutical Sciences. 99(8), 3343-3361.

Yoshino, K., Nakamura, K., Yamashita, A., Abe, Y., Iwasaki, K., Kanazawa, Y., et al. (2014). Functional Evaluation and Characterization of a Newly Developed Silicone Oil-Free Prefillable Syringe System. Journal of Pharmaceutical Sciences. , 103(5), 1520-1528.

Zhao, H., Diez, M., Koulov, A., Bozova, M., Bluemel, M., & Forrer, K. (2012). Characterization of aggregates and particles using emerging techniques. In H.-C. Mahler & W. Jiskoot (Eds.), Analysis of aggregates and particles in protein pharmaceuticals (pp. 133-167): Wiley & Sons, Inc.

Zhou, C., Krueger, A. B., Barnard, J. G., Qi, W., & Carpenter, J. F. (2015). Characterization of Nanoparticle Tracking Analysis for Quantification and Sizing of Submicron Particles of Therapeutic Proteins. Journal of Pharmaceutical Sciences. , n/a-n/a.

Zölls, S., Gregoritza, M., Tantipolphan, R., Wiggenhorn, M., Winter, G., Friess, W., Hawe, A. (2013). How subvisible particles become invisible-relevance of the refractive index for protein particle analysis. Journal of Pharmaceutical Sciences. 102(5), 1434-1446.

Zölls, S., Tantipolphan, R., Wiggenhorn, M., Winter, G., Jiskoot, W., Friess, W., Hawe, A. (2012). Particles in therapeutic protein formulations, Part 1: Overview of analytical methods. Journal of Pharmaceutical Sciences. 101(3), 914-935.

Zölls, S., Weinbuch, D., Wiggenhorn, M., Winter, G., Friess, W., Jiskoot, W., Hawe, A. (2013). Flow Imaging Microscopy for Protein Particle Analysis-A Comparative Evaluation of Four Different Analytical Instruments. AAPS Journal, 15(4), 1200-1211.

VI APPENDIX

LIST OF FIGURES

LIST OF TABLES